

# Thermal Management

---

Sponsored By:



The Boeing Company, David Blanding

**Authors:**

**Orlando Ardila**

**Ross Ellett**

**Calicia Johnson**

**Satira Maharaj**

Faculty Advisors

Dr. Juan Ordonez

Dr. Primal Fernando

# Table of Contents

<u>Chapter One: Project Background/Scope</u> .....	3
<u>Chapter Two: Research</u> .....	6
2.1 Secondary Research	
2.2 Primary Research: Material Testing	
2.2a Thermal Properties	
2.2b Thermal Conductivity	
2.2c Density	
2.2d Porosity	
2.2e Internal Area	
<u>Chapter Three: Project Specifications</u> .....	28
<u>Chapter Four: Concept Generation</u> .....	31
<u>Chapter Five: Concept Selection</u> .....	40
<u>Part Two Introduction</u> .....	44
<u>Chapter Six: Experiment #1: Carbon Foam vs. Aluminum</u> .....	47
6.1 Theoretical Design	
6.2a Machining Procedures	
6.2b Experiment	
<u>Chapter Seven: Experiment #2: Flow Injector System</u> .....	79
7.1 Theoretical Design	
7.2a Machining Procedures	
7.2b Experiment	
<u>Appendices</u> .....	102
Appendix A: Project Schedule	
Appendix B: Analytical Calculations	
B.1 Prototype I	
B.2 Prototype II	
<u>References</u> .....	117

# **Thermal Management**

---

---

## *Chapter One*

*Project*

*Background/Scope*

## **Project Scope**

The Boeing Company has long been a major aerospace and defense corporation. One of its recent innovations has been the development of the concept of a More Electric Aircraft (MEA). This aims to replace the mechanical systems typically found on aircraft with electric and electronic devices. These developments allow the replacement of a conventional centralized hydraulic system with a distributed electrical system. The benefits of the more electric aircraft include improved reliability, maintainability and supportability. In addition, enhancements in aircraft performance, weight and volume are expected.

Excess heat generation in electrical and electronic components severely limits the performance of aircraft systems. Many components have maximum operating temperatures above which failure results. Due to advancements in materials, the down-scaling of devices and increased switching speeds, heat flux is expected to exceed 1000 W/cm<sup>2</sup>.

Current thermal management systems and approaches include the circulation of hydraulic fluid and fuel through complex loops in different parts of the aircraft. Elimination of hydraulic systems removes the means for the transportation and rejection of waste heat. As a result, there exists a need for heat to be dissipated from electronic components, not only to improve reliability, but also to prevent premature failure.

It has become imperative to design an innovative thermal management system that will effectively meet the high demands of the twenty-first century aircraft industry. Such a system will allow the operation of electronic devices at lower temperatures for longer periods of time. Additionally, it will result in increased safety, due to the reduction in complexity caused by eliminating hydraulic fluid and fuel loops. By making use of novel technologies and materials, the mass of the aircraft system is likely to be reduced, allowing for greater net carrying capacity or payload.

An ideal thermal management system for aerospace applications must exhibit certain features beyond efficient heat removal. The design must be lightweight and should consider the volumetric constraints characteristic of the aerospace industry. It must also seek to incorporate the latest advancements in thermal materials technology. Materials with negligible deterioration are preferable. Substances with heat storage capacity can allow for heat dissipation while the vehicle is grounded.

The reliability of this system must be superb. The design must adapt to a variety of environmental conditions without compromising heat removal to a significant extent. Shock resistance and the ability to handle both extremes of temperature exposure are desirable features. A final requirement is that the system be relatively maintenance free.

# **Thermal Management**

---

---

## *Chapter Two*

### *Research*

## **Secondary Research**

Electronics are heavily used in the controlling and processing of data. Electronic components are designed to accomplish a specific function, and are generally soldered to a printed circuit board. When packaged in complex groups, they are called integrated circuits. The semiconductor devices found in integrated circuits are chiefly made of silicon. Electronics function best within a certain temperature range. It is occasionally necessary to warm up electronics to achieve satisfactory performance when surrounding conditions experience large temperature drops. Excessive temperatures can lead to decreased system performance and even failure. As a result, it often becomes crucial to implement thermal management solutions.

One of the most common methods of cooling uses heat sinks. A heat sink can be defined as any object which absorbs and dissipates heat from another body due to thermal contact. Heat sinks operate on the principle of thermal equilibrium. Thermal energy is transferred from the body at a higher temperature to the body at lower temperature until a common temperature is achieved. An efficient heat sink rapidly transfers heat from the hot body to the cooler one. This rate of thermal transfer depends on several factors, including but not limited to material, heat sink geometry and heat transfer coefficients. An increase in heat transfer can be brought about by modifying the parameters that affect heat transfer. Metals are often used since they exhibit high thermal conductivities, amplifying heat losses due to conduction. Protrusions (known as fins) serve to increase surface area, thus enhancing convective heat transfer. Air is sometimes forced over fins to increase heat loss. This is usually accomplished by means of adding a fan to the heat sink setup.

Microfluidics refers to the design, manufacture and formulation of devices and processes that deal with fluid volumes on the order of nanoliters. A microfluidic system is characterized by having at least one channel with a dimension smaller than one millimeter. This field is relatively new. Current mainstream applications do not include thermal management. However, it has been determined that this is a viable solution for

heat removal from electronic devices. A microfluidic heat exchanger makes use of an internal working fluid, and is capable of transferring heat between high and low temperature regions. Heat is transferred from a heat source to a heat sink through the circulation of a heat transfer fluid. The chief advantage of such a system is its small volume. Additionally, a microfluidic system is able to provide localized cooling at critical “hot spots” within the circuitry.

Another solution lies in the potential prevention of heat generation, as opposed to the eventual removal of heat after it has accumulated in the electronic component. Using materials of higher thermal conductivity in the circuitry itself allows heat to be dissipated from the component more rapidly, decreasing the amount of accumulated thermal energy needing to be dissipated. Silicon carbide is a ceramic compound of silicon and carbon that functions as an intrinsic semiconductor. The pure substance is a poor electrical conductor. However, its electrical conductivity can be enhanced by the addition of dopants. Silicon-carbide based parts are able to withstand high temperatures, further reducing the necessary heat removal.

As previously mentioned, heat transferred through a heat sink is generally done so via conduction. As such, metals are often chosen for use in heat sinks as they have high thermal conductivities. Copper and Aluminum alloys are common. Copper has a greater conductivity (400 W/m) as compared to aluminum (237 W/m), but aluminum has a significant advantage. It can be easily formed by extrusion, allowing for complex cross sections.

Carbon foam is an advanced porous material. It is currently being investigated for use in thermal management. Its main advantage is its porosity. Heat can be lost to the air within the channels of the foam. Because of the large surface area available for heat loss within the foam, convective heat transfer is likely to be very high. In fact, convection is predicted to be the main mode of heat transfer within carbon foam. Carbon foam has a very low thermal conductivity (approximately 50W/m), so that heat transfer due to conduction is extremely low, especially as compared to materials like aluminum and

copper. The main challenge in utilizing carbon foam becomes finding a way to effectively make use of the increased surface area within the material, to such an extent that will allow carbon foam to become a better heat transfer material than traditional metals.

Graphite foam is similar to carbon foam in that it has an open microcellular structure which makes it much lighter than other materials used in thermal management systems. Its benefits and drawbacks are extremely similar to those of carbon foam. However, its thermal properties vary somewhat. The properties of carbon foam, graphite foam, copper and aluminum are compared in the table below.

<b>Properties</b>	<b>Units</b>	<b>Carbon Foam</b>	<b>Graphite Foam</b>	<b>Copper</b>	<b>Aluminum</b>
Thermal Conductivity	W/Mk	175	149 – 181	401	237
Specific Heat Capacity	J/kgK	50 – 125	691	385	900
Density	g/cm <sup>3</sup>	0.45 - 0.59	0.57- 0.70	8.96	2.7
Porosity		0.446 - 0.806	0.69 - 0.75	0	0
Tensile Strength	MPa	2.07	0.7	270	90

*Table 2.1.1: Properties of Potential Heat Sink Materials*

## **Materials Testing (Introduction)**

Carbon foam appears to be a suitable material for use in this project. It is a relatively new material and little is known about its characteristics. These characteristics must be determined in order to make use of the beneficial properties of the material. It has become imperative to carry out tests to determine several key properties. Consequently, it has been decided that the following experiments will be carried out:

- a. Thermal Properties Experiment
- b. Thermal Conductivity Experiment
- c. Density Experiment
- d. Porosity Experiment
- e. Internal Surface Area Experiment

### **Thermal Properties Experiment**

#### Objective

To decide which of three carbon foam sample should be used for the design and manufacture of prototypes during the course of this project.

#### Theoretical Background

The main mode of heat transfer in heat sinks is conduction. Heat sinks are therefore usually made from thermally conductive materials, for instance, metals. This project aims to utilize carbon foam as a heat transfer material. However, its thermal conductivity is fairly low. Research has suggested that thermal conductivity increases with the density of the foam. This implies that it decreases as porosity rises. Since it is intended that the final design take advantage of the porous nature of the foam, it has become necessary to determine which sample would allow the use of its porosity while being sufficiently thermally conductive. This experiment will serve to eliminate the samples that will be ineffective, and will determine which sample should undergo further testing and be used for prototype design and manufacture in this project.

## Apparatus

### 1. *Carbon Foam Blocks:*

- a. Specimen 1 – Low weight, high porosity
- b. Specimen 2 – Medium weight, medium porosity
- c. Specimen 3 – High weight, low porosity

### 2. *Heat Source:* Household Stove.

### 3. *Ice cubes:* Four pieces of ice cubes per carbon foam sample.

### 4. *Stopwatch:* Timex Stopwatch.

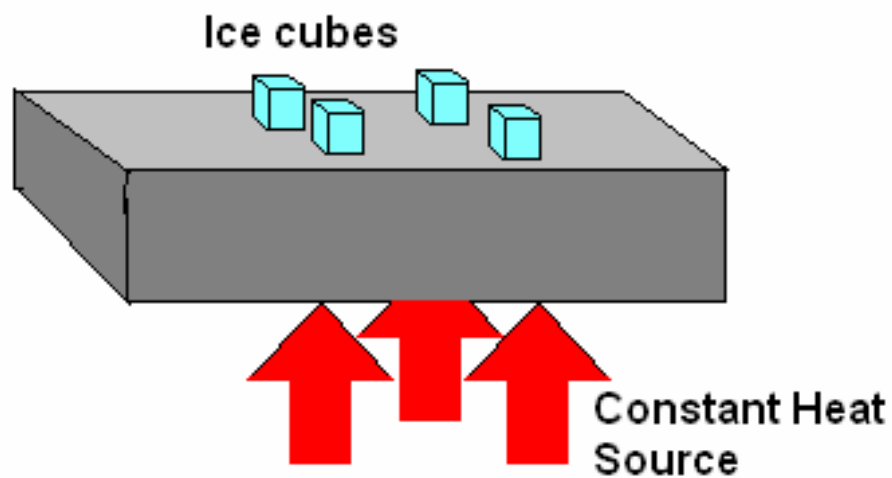


*Figure 2.2.a.1: Experimental Diagram*

### Experimental Procedure

1. Twelve ice cubes were prepared in the freezer for use in the experiment
2. The stove was set to medium and a cooking pan was placed on the burner
3. In order to achieve equilibrium between the pan and burner, the pan was allowed to sit on the burner for a time duration of approximately fifteen minutes

Specimen 1 was prepared for testing by removing it from its packaging.

1. Specimen 1 was placed on the burner, quickly followed by four ice cubes.
2. The stop watch was started as soon as the ice cubes were placed on specimen.
3. The stop watch was halted once all the ice cubes had melted.
4. The time taken for the ice cubes to melt was recorded.
5. Steps 1 through 4 were repeated for Specimen 2 and Specimen 3.

The time taken for the ice cubes on Specimens 2 and 3 were very close. The specimens were allowed to cool, while two burners were turned to high heat.

1. In order to achieve equilibrium between the pan and burner, the pan was allowed to sit on the burner for a time duration of approximately fifteen minutes
2. Specimen 2 and Specimen 3 were held with left and right hands respectively.
3. Both samples were placed on their respective burners.
4. The time taken for both samples to warm up was recorded

### Results

<b>Specimen</b>	<b>1</b>	<b>2</b>	<b>3</b>
<b>Time for Ice to Melt (s)</b>	300+	104	99
<b>Time for Specimen to Warm Up (s)</b>	N/A	15	13

*Table 2.2.a.1: Results*

### Analysis

The behavior of Specimen 1 resembled an insulator more than a thermally conductive material. Five minutes into the experiment, the ice remained solid, and time at that instant was recorded. Specimen 2 showed better performance. The ice on this sample melted within 104 seconds. The time taken for the ice on Specimen 3 (99s) to melt was not significantly different from that for Specimen 2. As a result, it was decided that Specimen 2 and Specimen 3 should be tested by hand to ensure that actually Specimen 3 took less time. When both samples were heated on High, Specimen 3 did indeed warm to the touch faster. The experiment therefore indicates that Specimen 3 possessed the best heat transfer properties.

### Conclusion

This experiment was performed in order to determine which specimen should be used for the design and prototyping of this project. Specimen 1 was quickly ruled when it failed to melt the ice even after five minutes. Specimen 2 and Specimen 3 gave similar results. To decide between them, the porosity was taken into consideration. The dense nature of Specimen 3 made it was impossible to force air through its pores (i.e. low porosity). However, Specimen 2 did allow the flow of air. The tests therefore indicated that the thermal properties of Specimen 2 did not differ greatly from those of Specimen 3, with the added benefit of increased porosity.

Specimen 2 was chosen to be used in the design and prototyping required later in this project. Before this can be done, more experiments will be carried out on Specimen to completely asses its characteristics.

## Thermal Conductivity Experiment

### Objective

To determine the thermal conductivity of a carbon foam specimen

### Theory

Fourier's Law of Heat Conduction states that the rate of heat transfer is directly proportional to temperature difference, length of travel and cross sectional area.

$$Q = k \cdot A \cdot \frac{\Delta T}{\Delta x} \quad \text{Eqn 1}$$

In the equation above, k, the constant of proportionality, represents the coefficient of thermal conductivity. By using a constant-output heat source and a constant area conduction element of uniform thickness, it is possible to measure the base and surface temperatures with thermocouples. From this data, the coefficient of thermal conductivity (k) can be determined.

This law is valid for one-dimensional heat transfer. To ensure that heat was conducted in only one direction, it is necessary for the sides of the entire system to be insulated. The top is left open to encourage heat flow in the upward direction.

### Apparatus

Conduction Element: A specimen of carbon foam measuring 6 in x 5 in x 1.5 in will be used for this experiment. This sample was chosen from among three different specimens. It was selected based on its porosity and capacity for heat transfer (See Chapter 2.2.a).



*Figure 2.2.b.1: Carbon Foam Conduction Element*

*Hot Plate:* The General Electric Single Burner Die Case Burner Plate was selected based on its ability to provide heat at a constant rate as well as the magnitude of that rate. After its initial warm up, it generates heat at a rate of 1000W. This magnitude allowed for a noticeable temperature difference between the base and top surfaces to be registered.

*Fiberglass Insulation:* In order to ensure one dimensional heat transfer, it is necessary to insulate the sides of the carbon foam specimen. For this purpose, a layer of fiberglass insulation of approximate thickness 1.5 in was used.

*Thermocouples:* Two Type J thermocouples were manufactured from thermocouple wire and used for temperature measurement. One was located at the base of the carbon foam block, while the other was situated at the top surface.

*Data Acquisition System:* The portable USB Data acquisition system NI USB-9211A consists of several components. The system can be used to collect data from four channels of 24-bit thermocouple input. This data is to be processed using LabVIEW SignalExpress data-logger software.

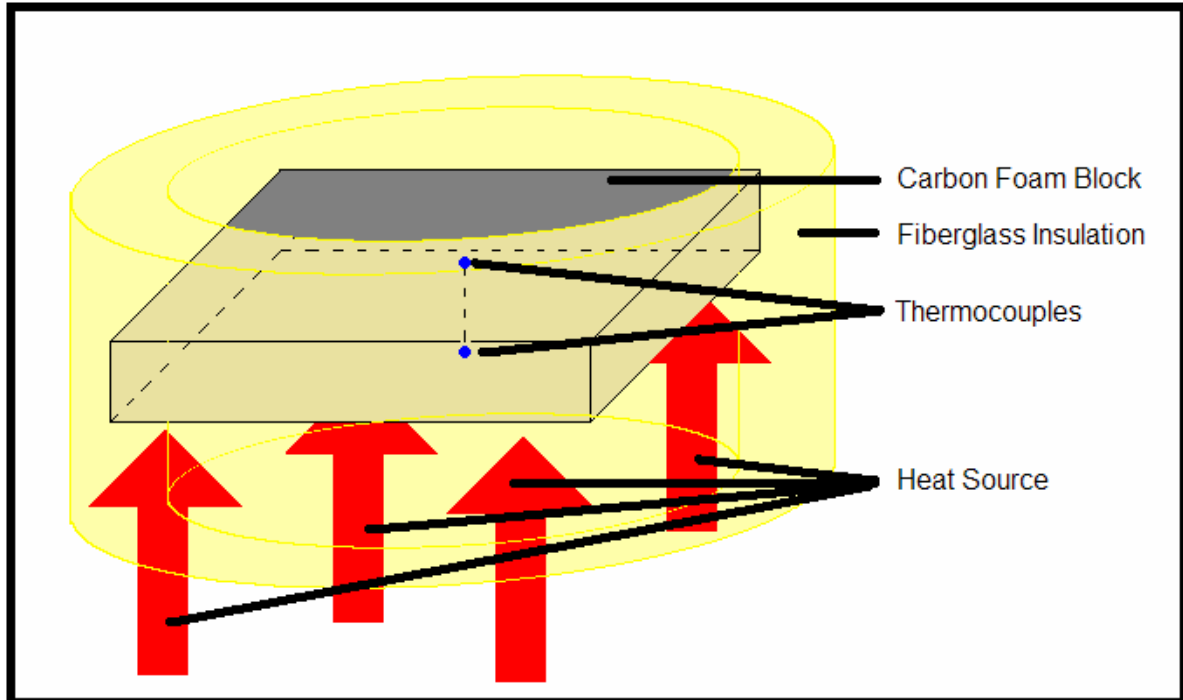


*Figure 2.2.b.2: Schematic of Experimental Setup*



*Figure 2.2.b.3: Carbon Foam on Heat Source*

## Procedure

1. Apparatus was set up as shown in Figure 2.2.b.1.
  - a. The carbon foam sample was placed directly on top of hot plate.
  - b. A hole was drilled into the carbon foam specimen so as to allow the placement of one thermocouple at the base of the specimen.
  - c. Thermocouples were placed on locations shown and connected to data acquisition system
  - d. The sides of the system were properly insulated with fiberglass.
2. Hot plate was turned on and allowed to reach steady state.
3. Temperatures on thermocouples were recorded using LabVIEW SignalExpress.
4. Thermal Conductivity was calculated.

## Results

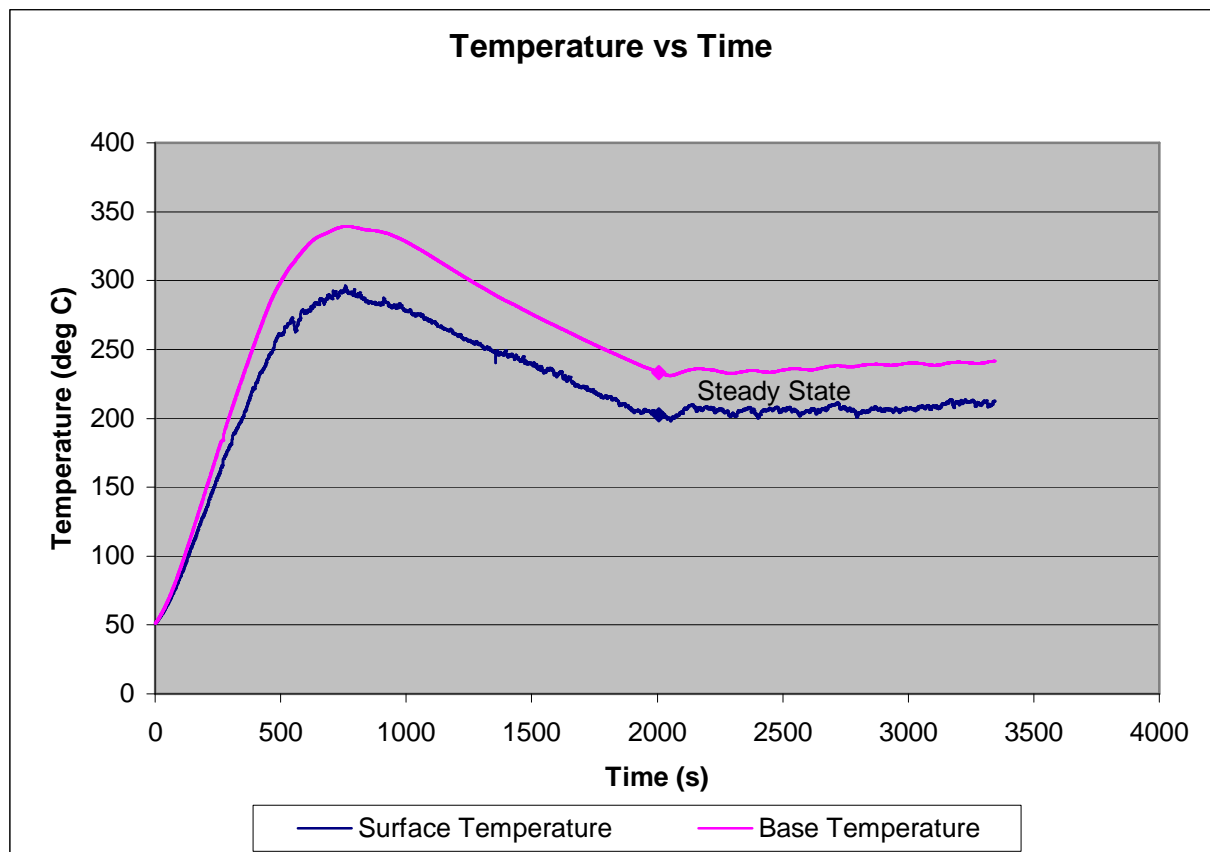


Figure 2.2.b.3: Graph of Temperature vs Time

### Analysis

$$\begin{array}{llll} Q := 1000\text{W} & l := 6\text{in} & b := 5.094\text{in} & w := 1.5\text{in} \\ A := l \cdot b & \Delta x := w & T_s := 479.72\text{K} & T_b := 509.83\text{K} \\ \Delta T := T_b - T_s & Q = k \cdot A \cdot \frac{\Delta T}{\Delta x} & k := \frac{Q \cdot \Delta x}{A \cdot \Delta T} & k = 64.171 \frac{\text{W}}{\text{m} \cdot \text{K}} \end{array}$$

### Discussion

Fourier's Law of Heat Conduction was used to calculate the thermal conductivity of the carbon foam sample. A constant heat source was used to supply heat to the specimen, and the base and surface temperatures were noted. Using these values (as well as the dimensions of the sample), the thermal conductivity of carbon foam was calculated.

Fourier's Law of Heat Conduction is applicable only for one dimensional heat transfer for a system in steady state. In order to ensure heat transfer in the upward direction, the sides of the system were heavily insulated. The top surface of the foam was left open to the atmosphere to encourage heat to travel upwards. It was also essential that the system achieve steady state. For steady state to be reached, the time duration of the experiment had to be fairly large. Previous trials determined that the approximate time taken for the system to achieve steady state was thirty minutes. As such, the experiment was allowed to run for a total duration of approximately fifty-five minutes.

The trial runs were carried out with the thermocouple held in place by human effort. It was found that placing pressure on the surface thermocouple increased the temperature on the thermocouple readout. Fluctuations on thermocouple pressure due to human error caused greater fluctuations in temperature readout. In order to eliminate this error in temperature measurement due to human error, the actual experimental run was carried out with thermocouple touching the surface but not held in place by human effort. A thermally conductive paste was used for this purpose.

### Conclusion

The thermal conductivity of the carbon foam sample was found to be 64.17 W/mK

## Density Experiment

### Objective

To determine the density of a carbon foam specimen

### Theoretical Background

The density of an object is defined as the ratio of its mass to its volume. It is used as a representation of the mass per unit volume of the object, and is given by the equation:

$$\rho = V/m$$

The quantities in the equation above are denoted as follows:

$\rho$ : Density of sample

V: Volume occupied

m: Mass of specimen

The density of carbon foam is low as compared to traditional heat transfer materials such as aluminum and copper. In aerospace applications, weight is an important consideration. Carbon foam is therefore being investigated in this project to determine whether it may be used in such applications. The specimen to be used for testing was selected based on its thermal properties (See Chapter 2.2.a).

### Equipment

Rectangular Carbon Foam Prism, Scale, Ruler

### Procedure

1. The dimensions of the carbon foam prism were measured.
2. Using these dimensions, the volume of the specimen was calculated.
3. The sample was weighed using the scale.
4. The density of the carbon foam sample was calculated using the mass and volume

## Results

Mass := 9oz

L := 6.25in

B := 6.126in

H := 1.125in

Volume:= L·B·H

Volume= 0.000706m<sup>3</sup>

$$\rho := \frac{\text{Mass}}{\text{Volume}}$$

$$\rho = 361.474 \frac{\text{kg}}{\text{m}^3}$$

Mass (kg)	Volume (m <sup>3</sup> )	Density (kg/m <sup>3</sup> )
0.255	0.000706	361.5

*Table 2.2.c.1: Summary of Results*

## Conclusion

The density of the carbon foam specimen was found to be 361.5 kg/m<sup>3</sup>

## Porosity Experiment

### Objective

To determine the porosity of a carbon foam specimen.

### Theoretical Background

Carbon foam is an example of a porous medium. It is composed of a mixture of solid carbon and air spaces. Porosity ( $\phi$ ) is defined as the ratio of the volume occupied by void space to the bulk volume of the sample. The porosity of the sample is an important characteristic for this project, as it will be needed for subsequent calculations. By measuring the volume of the solid carbon and the total volume of the sample, the porosity can be calculated as follows:

$$V_b = V_v + V_s \quad \phi = \frac{V_v}{V_b} \quad \phi = \frac{V_b - V_s}{V_b} \quad \phi = 1 - \frac{V_s}{V_b}$$

The quantities used in the equations above are denoted by:

$\phi$ : Porosity

$V_b$ : Bulk Volume

$V_s$ : Solid Volume

$V_v$ : Void Volume

### Experimental Setup

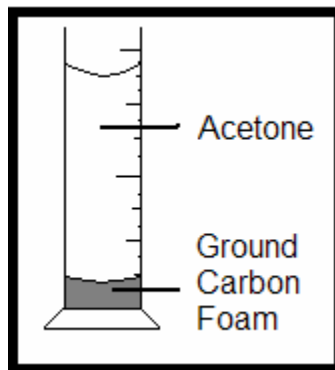


*Figure 2.2.d.1: Schematic of Experimental Setup*

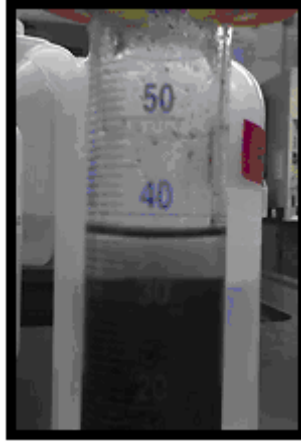


*Figure 2.2.d.2: Experimental Setup*

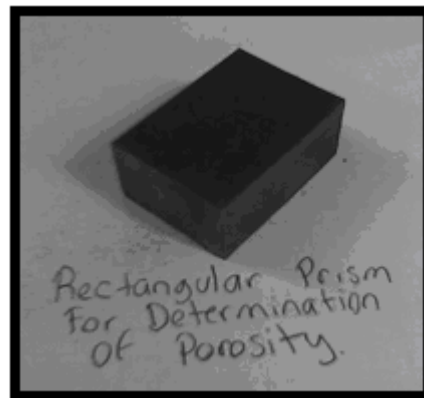


*Figure 2.2.d.3: Rectangular Carbon Foam Prism*

### Procedure

1. A rectangular prism was cut from the carbon foam specimen.
2. The dimensions of the prism were noted and the bulk volume calculated.
3. The prism was ground into powder.
4. 30 ml of acetone was poured into a graduated cylinder.
5. The ground carbon foam powder was submerged in the acetone.
6. The increase in volume due to the addition of the powder was noted.
7. Using the values for bulk volume and solid volume, the porosity of the carbon foam specimen was calculated.

### Analysis

$$\begin{array}{llll} l := 1.9\text{cm} & b := 4.8\text{cm} & w := 3.4\text{cm} & V_b := l \cdot b \cdot w \\ V_s := 7.5\text{mL} & V_b = 31.008\text{mL} & \phi := 1 - \frac{V_s}{V_b} & \phi = 0.758 \end{array}$$

Bulk Volume (ml)	Solid Volume (ml)	Porosity (%)
31	7.5	75.8

*Table 2.2.d.1: Summary of Results*

### Discussion

The typical method for determining volume by displacement involves the immersion of the entire sample into a liquid, usually water. However, this method could not be used for two reasons. The surface tension of water would not allow the liquid to seep into the small pores of the carbon foam. As such, the change in volume measured by such a method would be inaccurate. This situation was rectified by grinding the carbon foam so as to allow immersion. However, carbon foam is less dense than water, making it difficult for it to sink (and so create a noticeable volume change) even when ground. For this reason, this experiment uses acetone as the liquid of immersion.

### Conclusion

The porosity of the carbon foam specimen is 75.8 %

## **Internal Surface Area Experiment**

### Objective

To approximate the internal surface area available for heat transfer within a carbon foam sample due to its porosity

### Theoretical Background

Carbon foam is composed of a mixture of carbon and air. Heat is able to travel through the foam by conduction (due to the solid region) as well as by convection (within the pores of the foam). Convection depends on the surface area from which heat can be transferred (i.e. the internal surface area of the pores) In characterizing the thermal properties of carbon foam, it is therefore important to consider this internal area available for heat transfer.

The most accurate method of determining this internal surface area involves statistical analysis. This method described in “A Method for Estimating Volume-Surface Ratios,” by Harold W. Chalkley, Jerome Cornfield, and Helen Park, is based on probability theory. An enlarged photomicrograph is used. If a needle of length “l” is repeatedly allowed to fall on the picture from a distance, the following quantities are counted: the number of time that the ends of the needle fall into the pores and the number of times the needle intersects the circumference of the pores. The equation below can be used to obtain an estimate for the internal surface area per unit volume.

$$\Sigma := \frac{0.4\phi c}{l \cdot h} \cdot m_1 \quad \text{Equation 1}$$

In the equation above, the nomenclature used is as follows:

$\Sigma$ : Internal surface area per unit volume

$\phi$ : Porosity

c: Number of circumference intersections

l: Length of needle

h: Number of times needle ends fall within pores

$m_1$ : Photomicrograph Magnification

## Equipment

Microscope, Rod

## Procedure

1. A series of photomicrographs from a section of the carbon foam specimen were taken in an overlapping fashion, with a final magnification of 180X.
2. The pictures were arranged next to each other by identifying defining features (see Figure 2.2.e.1).
3. The rod was allowed to fall onto the photomicrograph a total of 450 times.
4. The number of times that the ends of the rod fell into the pores was counted, as well as the number of times the rod intersected the circumference of the pores.
5. The internal surface area per unit volume was calculated from Equation 1.

## Results

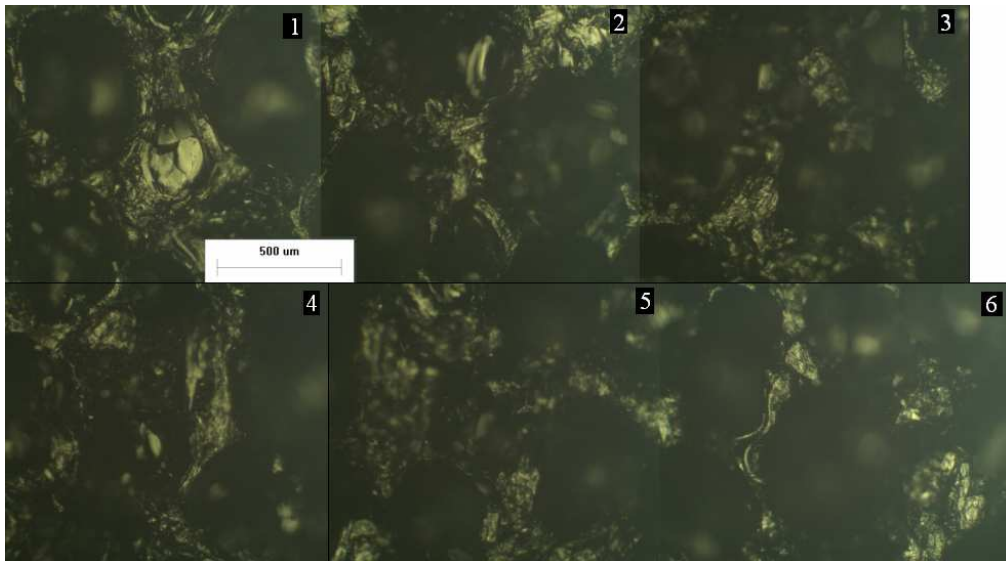


*Figure 2.2.e.1: Photomicrograph of Carbon Foam*

Analysis

$$m_1 := \frac{9\text{cm}}{500\mu\text{m}}$$

$$m_1 = 180$$

$$c := 1163$$

$$l := 11.4\text{cm}$$

$$h := 540$$

$$\phi := 0.758$$

$$\Sigma := \frac{.4\phi \cdot c}{l \cdot h} m_1$$

$$\Sigma = 1.031 \times 10^3 \frac{\text{m}^2}{\text{m}^3}$$

Needle Length (cm)	11.4
Magnification	180
Porosity	0.758
Total Repetitions	450
Circumference Intersections	1163
Drops Within Pores	540
<b>Internal Surface Area per Unit Volume (m<sup>-1</sup>)</b>	<b>1031</b>

Table 2.2.e.1: Summary of Results

Discussion

The internal surface area per unit volume was determined by the method previously described. For a sample of a certain volume, the internal surface area corresponding to that volume can be therefore obtained.

The research paper from which this method was obtained provides error values with respect to the number of repetitions carried out. Using this data, a curve was plotted, and the approximate error for 450 drops was determined to be approximately 22%.

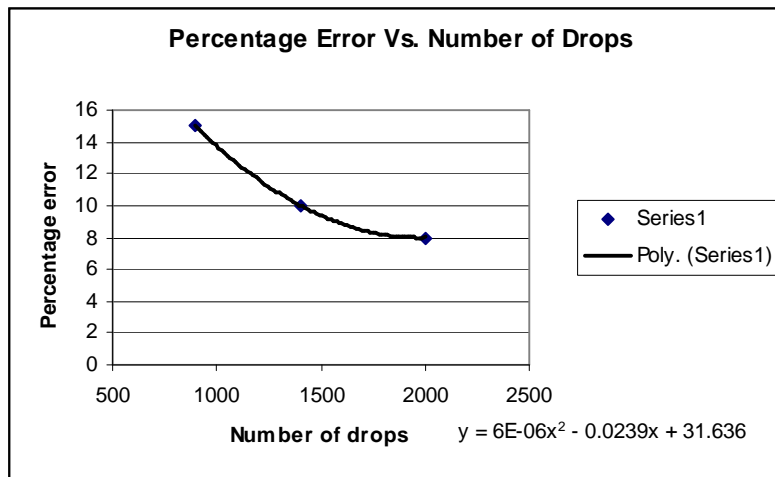


Figure 2.2.e.2: Graph of Error vs. Number of Repetitions

From the graph above, it was possible to determine an equation for the curve, and so estimate a value for the percentage error when 450 repetitions are carried out.

$$y(x) := 6 \cdot 10^{-6} \left( \frac{1}{x^2} \right) - 0.0239 \cdot (x) + 31.636$$

$$y(450) = 22.096$$

### Conclusion

The internal surface area per unit volume due of the carbon foam sample due to its porosity was found to be  $1031\text{m}^{-1}$ .

# **Thermal Management**

---

---

## *Chapter Three*

### *Project Specifications*

## Product Specifications

- Design must remove heat from a processor at a rate of 60 W.
- Prototype must have a maximum volume of 0.005 m<sup>3</sup>
- Product must have a maximum mass of 1 kg.
- The use of advanced materials is desirable
- A passive system is preferable
- The primary cooling source should not be water or air
- System must be fully operational at an altitude of 40,000ft (i.e. at a temperature of 220K and a pressure of 20kPa)

For this project, an electronic processor will be used to simulate an electronic component typical of those found on aircraft. However, it is impractical to simulate the extreme temperatures actually achieved (250°C to 300°C). Consequently, our project will focus on removing heat generated by a typical processor (approximately 60 W), at temperatures that can be withstood by it.

Weight is an important factor in any component meant for use on an airplane. Larger airplane masses require more lift, causing fuel consumption to rise. Minimizing the weight of the system requires less power, decreasing the fuel cost.

A compact design is also desirable. Drag increases with surface area. A compact aircraft design minimizes this area, thus reducing drag. Compact design of all aircraft systems allow for all necessary components to be included without significantly increasing the drag.

Customary means of thermal management for aircraft electronics have already been investigated. Our project aims to explore unconventional methods. As such, it is desired that the primary cooling source be a substance other than water or air.

A superior system would require no additional power for startup or continued operation. Additional power sources add complexity and weight to the operating systems of the aircraft. For this reason, a passive system is recommended. However, any system that requires minimal power input is satisfactory.

Cruising occurs at an altitude of approximately 40,000 ft. At this height, conditions differ from those at sea level. The system must be designed not only to withstand these conditions, but to be fully functional at the pressures and temperatures that usually occur at cruising altitude.

# **Thermal Management**

---

---

## *Chapter Four*

### *Concept Generation*

## Concept Generation

This project requires the design of a heat exchanger capable of removing the heat produced by the operation of electrical devices. Heat transfer from an electrical component encompasses all modes of heat transfer. Although radiation will occur as long as temperature of the component is above absolute zero, conduction and convection are the key modes of heat transfer in this project.

The process of heat conduction is mathematically described by the following equation:

$$Q = kA (T_1 - T_2) / \Delta x. \quad \text{Eqn 4.1}$$

The equation for convective heat transfer is given below:

$$Q = hA_s(T_2 - T_1) \quad \text{Eqn 4.2}$$

Taking the above information into consideration, the following designs were generated.

### Concept 1: Carbon Foam Finned Heat Sink

One idea involves replacing current aluminum or copper heat sinks with similar ones made of carbon foam, or another thermally conductive lightweight material. Heat travels upward from the base towards the pores by conduction. It is then transferred by convection to the air trapped within the pores of the carbon foam.

The thermal conductivity of the carbon foam has been measured as 64W/m-K, which is significantly below that of traditional heat sink materials. However, it is expected that the heat lost due to conduction will be overshadowed by the heat lost as a result of convection through the pores of the material. Consequently, convective heat transfer is the chief mode of heat removal for this design.

The porous nature of carbon foam may prove to be potentially problematic during the transfer of thermal energy from the electronic component to the heat sink. Thermally conductive grease will therefore be applied between the base of the heat sink and the top

of the electronic component. This will allow for maximum heat transfer from the component to the heat sink.

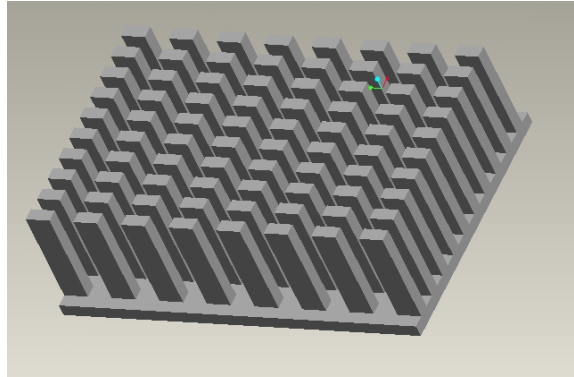


*Figure 4.1.1: Carbon Foam Rectangular Fin Configuration  
Model Constructed on Pro-Engineer*

#### Concept 2: Carbon Foam Heat Sink: Honeycomb Design

This design was inspired by vehicle heat exchangers built to resemble honeycombs. Wilhelm Maybach introduced the first honeycomb radiator for “Mercedes” in the late 1800s. Its benefits included improved efficiency and a coolant reservoir tank of decreased volume.

This design requires a number of hexagonally shaped holes to be machined in the heat exchanger. Increasing the number of holes increases the surface area, thus allowing a greater amount of heat to be taken away from the system. This design complements the porous nature of carbon foam. It further increases the area available for convective heat transfer. In addition, this system allows for future modification. A fluid may be run through the holes, should the need for improved heat removal become apparent.

#### System Description

Carbon foam is cut and shaped into a rectangular honeycomb pattern as shown in Figure 4.2.1. The processor is attached to the heat sink by means of a highly thermally conductive paste.

This design is based on the premise that heat will be transferred from the processor chip through the carbon foam toward the holes by conduction. A fan or another form of air circulation (possibly provided by the airplane) can be utilized to remove heat from the holes. A concept design is shown in Figure 4.2.1. The green (bottom) layer represents the processor, while the red layer (middle) serves as a thermally conductive adhesive. The large piece is made of carbon foam and contains cylindrical holes (in place of conventional hexagonal ones) designed to mimic a honeycomb pattern.

### System Components

- Processor Chip (AMD Athlon 64 3500)
- Carbon Foam Machined into Honeycomb (Figure 4.2.1)
- Thermally Conductive Solution

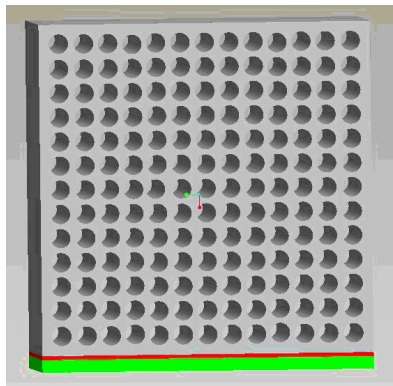


*Figure 4.2.1: Carbon Foam Heat Sink (Honeycomb Design)*

*Model Constructed on Pro-Engineer*

### Concept 3: Microfluidic Cooling System

The processor chip to be cooled has dimensions 17mm x 17mm x 1.4mm. In order to cool a component this small, it becomes necessary to design a system of dimensions comparable to the chip itself. A microfluidic system can be defined as having at least one channel with dimensions less than a millimeter (1mm).

The microscopic properties of a fluid differ from its macroscopic properties. In microfluidics, the particles of the fluid become comparable in size to the apparatus itself. As a result of a very low Reynold's number (often less than 1), the flow remains laminar throughout. However, this means that flows will not mix easily by turbulence, so diffusion will be needed.

### System Description

Fluid motion through the channels will be achieved by pressure driven flow. A syringe pump drives the flow through ten microchannels in a parallel arrangement across the surface of the processor chip (Figure 4.3.1). The chip acts as an evaporator, converting the saturated liquid to vapor. The heat transferred to the working fluid from the chip is then transported to a condenser. The condenser is responsible for removing the heat from the working fluid, which is then re-circulated through the system. In summary, the fluid undergoes a closed loop thermodynamic cycle. (Figure 4.3.2)

### System Components

Processor Chip (AMD Athlon 64 3500) (Figure 4.3.3)

- Syringe Pump (Figure 4.3.4)
- Condenser
- Microchannel Tubing

Limitations for this system will include viscous effects and boiling limitations of the working fluid. The continuum assumption is not valid when the mean free path of the molecules becomes comparable to the smallest significant dimension. However, it is still applicable away from solid boundaries. Another issue deals with the tubing material.

Currently, most microfluidics channels are made from silicon, which exhibits a low thermal conductivity. This can be potentially problematic at the evaporator stage, during heat transfer from the processor chip to the working fluid.

The analysis of this system involves the First Law of Thermodynamics, Fourier's Law of Heat Conduction, as well as Newton's Law of Cooling. The governing equations will include the conservation of mass, energy and momentum.



*Figure 4.3.1: Processor Chip  
AMD Athlon 64 3500*

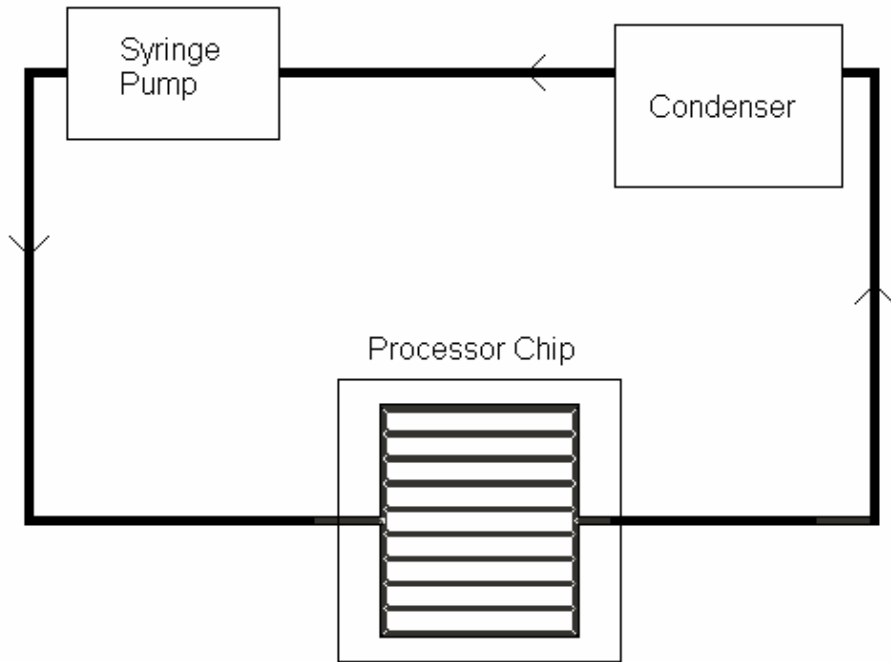


*Figure 4.3.2: Schematic of Microfluidics Cooling System*

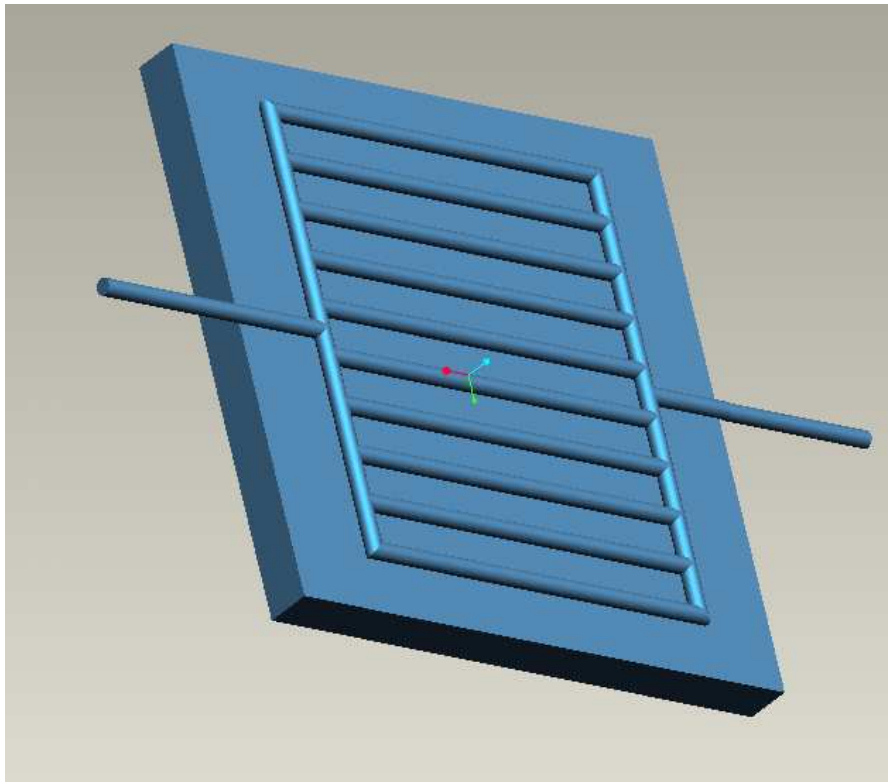


*Figure 4.3.3 Microchannel System on Processor Chip  
Model Constructed on Pro-Engineer*

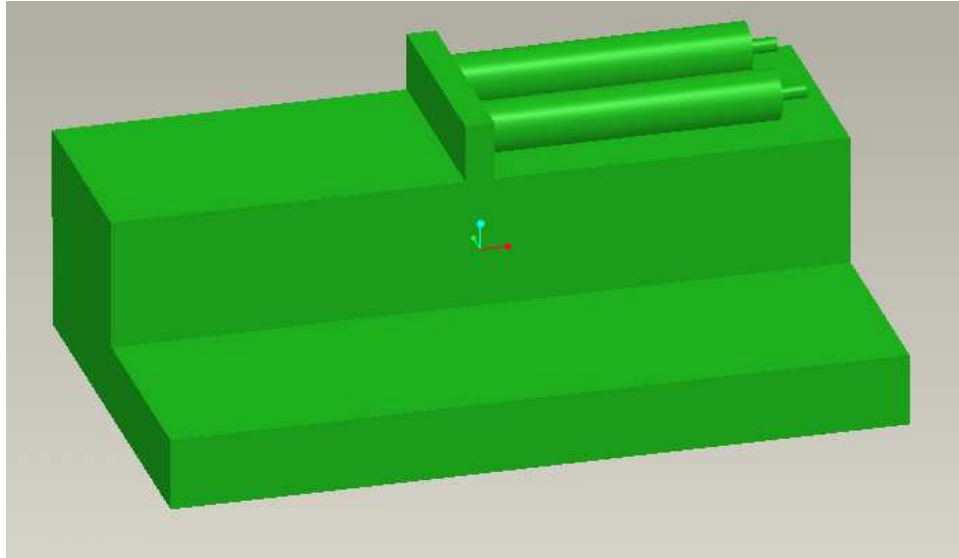


*Figure 4.3.4: Syringe Pump  
Model Constructed on Pro-Engineer*

#### Concept 4: Carbon Foam Fluid Injection System

This concept involves a carbon foam heat sink in the form of a cylinder. The bottom of the cylinder is in contact with the electronic component. A tube is run from the outside of the aircraft through the center of the cylinder. Several small holes exist in the portion of the tube immersed in the cylinder. These allow air at high pressure to force a path through the porous cylinder from the center in a radial direction. This concept is illustrated in Figure 4.4.1.

Heat travels from the electronic component upwards through the heat sink, towards the pores by conduction. Forcing air through the pores causes this heat to be carried away by convection. This design makes use of the increased area available for convective heat transfer due to the porosity of the foam.

A feature common to all carbon foam heat sinks deals with the thermal transfer between the electronic component and the base of the heat sink. This design is no exception. This problem will be solved as before; by applying a thermally conductive paste between the base of the heat sink and the electronic component.

### System Components

- Carbon Foam Cylindrical Heat Sink
- Perforated Tubing
- Thermally Conductive Paste

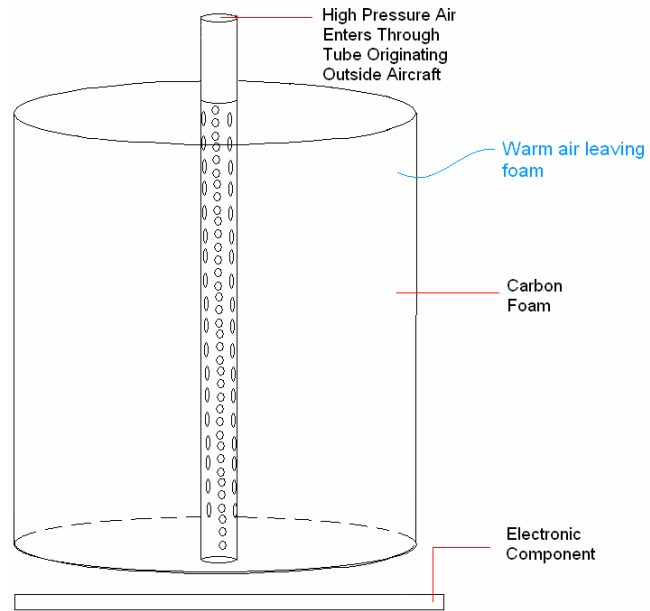


*Figure 4.4.1: Schematic of Carbon Foam Fuel Injection System*

# **Thermal Management**

---

---

## *Chapter Five*

### *Concept Selection*

## Concept Selection

It was desired that advanced materials be used in this project, and carbon foam has been the obvious choice. Of the four designs presented, three make use of this material. Its main advantage is that it allows for two modes of heat transfer: conduction and convection.

The process of conduction is mathematically described by the following equation:

$$Q = kA (T_1 - T_2) / \Delta x. \quad \text{Eqn 5.1}$$

The equation for convective heat transfer is given below:

$$Q = hA_s(T_2 - T_1) \quad \text{Eqn 5.2}$$

It can be seen that conduction depends on the thermal conductivity ( $k$ ) of the material. As previously indicated, the thermal conductivity of carbon foam does not compare well with those of traditional heat transfer materials. It can, however, be increased. Thermal conductivity rises as density rises. This can be cause for potential problems. As density increases, porosity decreases, thus reducing the area available for convective heat transfer within the foam. In addition, the circulation of air or fluid within the foam becomes increasingly difficult as density is increased.

From equation 5.2, it is evident that surface area is directly proportional to heat transfer by convection. Due to the high porosity of carbon foam, the area available for convective heat transfer within the foam is quite large. Because of its morphology, carbon foam has an area much greater than that of traditional heat exchanger materials. Consequently, carbon foam is well suited for use in convective heat transfer.

The first design incorporates two modes of heat transfer. Heat travels through the fins via conduction, after which it is dissipated to the environment by convection. The finned surface increases the area available for convective heat transfer to the environment. However, heat transfer away from the processor and through the carbon foam fin may not occur as rapidly as is necessary, due to the relatively low thermal conductivity of carbon

foam. It is therefore expected that the heat removed from this finned heat sink design may not be sufficient to keep the processor at its desired operating temperature. One major advantage of this design is that it can be easily used as a basis for the comparison of carbon foam and traditional heat transfer materials. If two identical models were used, one each of carbon foam and a metal, the performance of the two materials can be compared.

The honeycomb heat sink design also allows heat removal by conduction and convection. Like the previous design, heat travels upward through the heat sink by conduction. Another feature they share is an increased area for convection. In the previous heat sink, this increase in area is due to the finned configuration. However, in the honeycomb design, the increase in area results from the holes that have been drilled into the heat sink. The increase in area for the second design is less than the increase in area for the first design. It is therefore expected that the first design will exhibit a higher heat removal rate. The second design is not without its benefits though. If it becomes necessary to improve the rate of heat removal, a working fluid can be pumped through the holes. Thus, the honeycomb design allows for future modifications should improvements to the design become necessary.

The microfluidic cooling system is the only concept that does not incorporate the use of carbon foam. The microfluidic tubing occupies a very small volume and has a very low mass. This is highly beneficial, since the design is to be used on aircraft, where strict volumetric constraints are enforced. However, although the microfluidic portion meets weight and volume constraints, the system requires cumbersome external components, namely a pump and the power source needed for its operation. Unless some other means can be found to drive the working fluid through the system, this concept is not feasible. In addition, leakages within the system are unsafe, as this would allow fluid to come into contact with electronic devices. As such, high maintenance is required for the safe continued operation of the microfluidic cooling concept.

The final concept involves running air (originating from the outside of the aircraft) through a carbon foam cylinder in a radial direction from its center. Although this design allows heat loss both by conduction and convection, it does so in a different manner from the first two designs. This concept is the only one that fully takes advantage of the porous nature of carbon foam. Heat travels from the base of the cylinder upward through conduction. As previously discussed, this conduction is limited by the thermal properties of the material, namely, the thermal conductivity. However, when air is passed through the pores of the material, a large amount of heat is lost as a result of convection. This is due to the increased area within the material available for convective heat transfer. Heat is not only lost via the flow rate of air. Some is also removed from the top and outside walls of the cylinder, much like a typical fin. However, it is expected that the heat lost due to the flow rate of air will dominate the total heat loss.

Selection Matrix

	<b>Design #1</b> Finned Heat Exchanger	<b>Design #2</b> Honeycomb Heat Exchanger	<b>Design #3</b> Microfluidic Cooling System	<b>Design #4</b> Fluid Injection System
<b>Lightweight (15%)</b>	12	12	5	13
<b>Cost (5%)</b>	4	4	3	5
<b>Feasibility (15%)</b>	12	12	5	12
<b>Aesthetics (5%)</b>	5	3	4	4
<b>Performance (20%)</b>	15	10	15	18
<b>Material Availability (10%)</b>	5	5	7	5
<b>Safety (10%)</b>	8	8	5	8
<b>Durability (10%)</b>	9	8	6	9
<b>Ease of Use (10%)</b>	10	9	7	8
<b>FINAL SCORE</b>	<b>80</b>	<b>71</b>	<b>57</b>	<b>82</b>
<b>RANKING</b>	<b>2</b>	<b>3</b>	<b>4</b>	<b>1</b>

*Table 5.1: Selection Matrix*

# **Thermal Management**

---

---

## *Part Two*

## **PART TWO**

### **Introduction**

For this project, carbon foam will be used to build two heat removal systems for use with electronic components on an aircraft. As a result of prior testing, it was decided that Carbon Foam Sample 2 will be used in these systems.

Prototype I is intended to be a replica of an existing aluminum finned heat sink design. Testing both heat sinks will provide a sound basis for the comparison of carbon foam against aluminum as a heat transfer material. Heat travels upward from the base towards the pores by conduction. It is then transferred by convection to the air trapped within the pores of the carbon foam.

It is expected that the heat removal rate of the carbon foam heat sink will be less than that of the aluminum heat sink. However, it is also anticipated that a major benefit of this design will be a significant decrease in mass. It is believed that the advantage of decreased mass will outweigh the disadvantage of decreased heat removal.

Prototype I is designed to focus on the comparison of carbon foam to a conventional heat transfer metal, Aluminum. Prototype II aims to go a step further by using a concept that will take advantage of the intrinsic properties of the foam, thus enhancing its heat removal abilities.

Prototype II is a fluid injection heat removal system. Air is run via a tube through the center of a cylindrical carbon foam heat sink. Holes in the tube allow air to be forced through the porous foam. Heat travels from the electronic component upwards through the heat sink, towards the pores by conduction. Forcing air through the pores causes this heat to be carried away by convection.

This system is expected to remove heat from the processor at a high rate. The magnitude of its dimensions is comparable to that of a conventional heat sink. Like Prototype I, an

important feature is its low density. Therefore, it is anticipated that this system will demonstrate improved heat removal while conforming to the necessary volumetric constraints, with the added benefit of exhibiting a low system mass.

# **Thermal Management**

---

---

## *Chapter Six*

*Experiment 1:*

*Carbon Foam vs.*

*Aluminum*

## **Chapter 6.1: Theoretical Design**

### Introduction

In order to investigate the use of carbon foam as a thermally conductive material, it was decided that a finned heat sink machined from carbon foam would be tested against an aluminum heat sink of identical configuration. Heat sinks absorb heat from electronic components by thermal conduction. The heat travels through the fins of the sink, and is dissipated to the environment by convection.

Rather than machining two heat sinks, the carbon foam sample will be machined into a replica of an existing aluminum heat sink. The heat sink will contain seventy-eight (78) rectangular fins on a rectangular base. The fins will be arranged into ten rows with eight fins each, except for the back row. In the original aluminum heat sink, the two middle fins were absent from this row in order to provide sufficient room to clamp the sink onto the processor. The two front-most rows consist of short fins, while the other rows contain longer fins. These features will be duplicated in the carbon foam heat sink, to ensure that the geometries of both fins are the same.

Once the carbon foam heat sink has been machined, it will be mounted onto a AMD Athlon 64 3500 processor chip. Because of the porous nature of carbon foam, it is likely that a thermally conductive paste will be necessary to attach the heat sink to the processor. The processor with the attached heat sink will then be installed into a barebone computer from Tiger Direct (Item Number P459-1236C). Another computer containing another AMD Athlon 64 3500 processor with the original aluminum heat sink will be used for comparison. Applications will be run on both computers to cause a constant heat generation in both processors. Theoretically, the heat sinks will dissipate heat from their respective processors. Thermocouples mounted at the same locations on each heat sink will be used to determine the temperatures at those locations, from which heat loss, fin efficiency and heat sink effectiveness can be calculated.

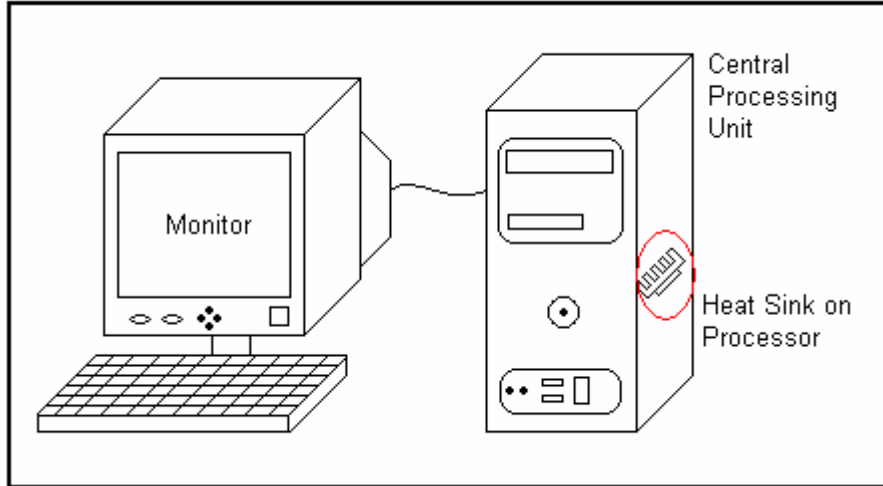


*Figure 6.1.1: System Diagram*

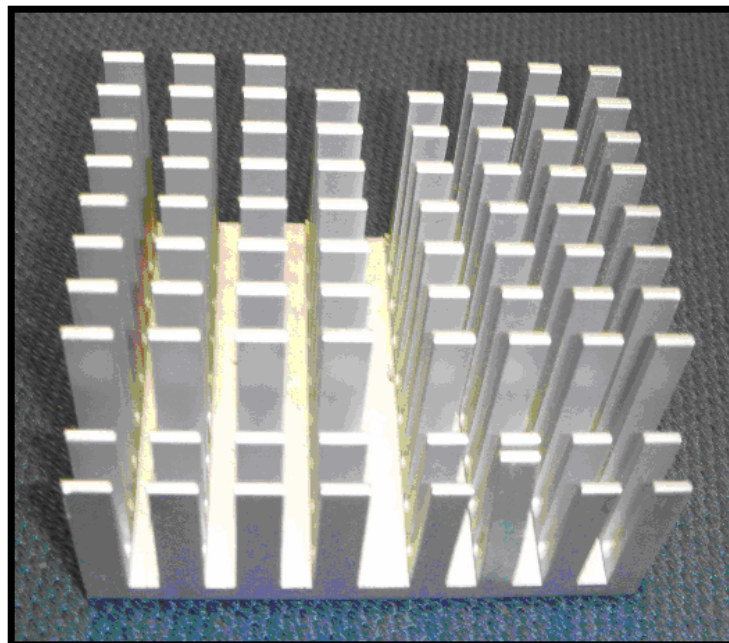


*Figure 6.1.2: Aluminum Heat Sink*

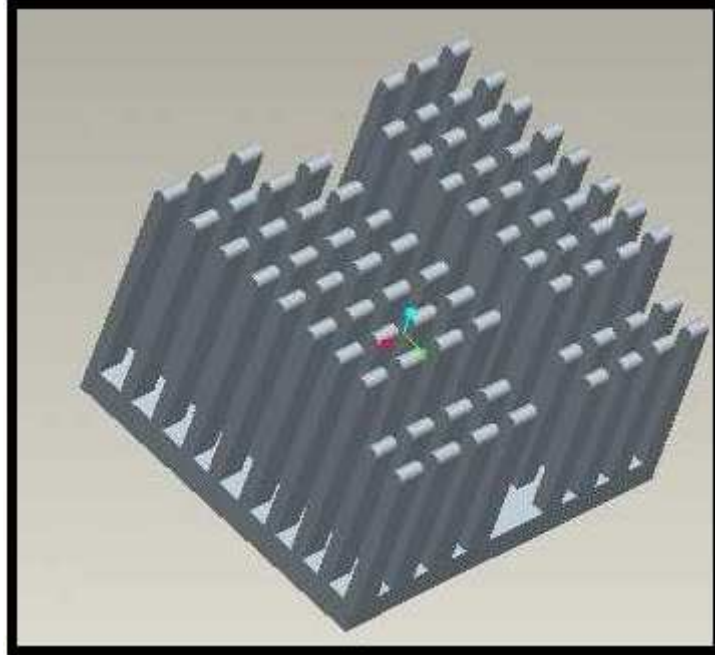


*Figure 6.1.3: Carbon Foam Finned Heat Sink Model*

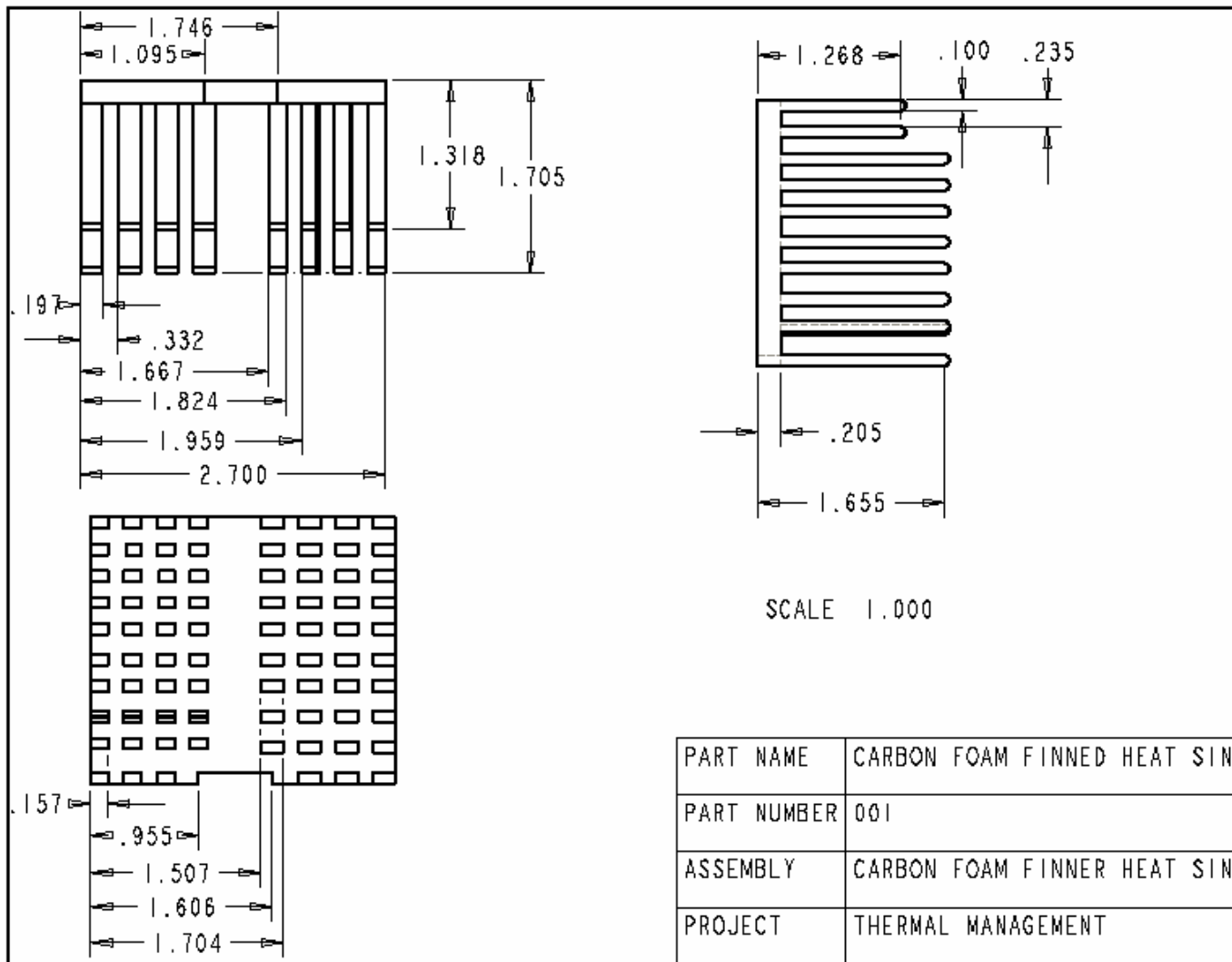


Figure 6.1.4: Engineering Drawing of Prototype II

### Bill of Materials: Ordered Parts

For our selected designs, several items had to be ordered. Below is a list of the parts that were ordered, as well as a detailed description of them.

#### Two Computers

Supplier: Tiger Direct

Item Number: P459-1236C

Specs:

- PCChips A13G+ V3.0 Motherboard
- AMD Athlon 64 3500+ 2.20GHz OEM
- Ultra 1024MB PC4200 DDR2
- Cooler Master Elite Mid-T Case
- 350W Power Supply

Barebone kits were ordered and put together. A monitor, keyboard, mouse hard drive and CD-Rom drive were bought separately and installed. Selected programs will be run in order for the processor to reach its maximum temperature. The heat sink from one computer will be replicated carbon foam and the heat transfer from the two will be compared.

#### Thermocouples

Supplier: Omega Engineering

Item Number: TT-J-20-SLE-25

Specs:

- J Type
- Temperature Range: 0°C to 750°C (32°F to 1382°F)
- Special Limits of Error:  $\pm 1.1^{\circ}\text{C}$  or 0.4%
- Wire Diameter: 0.81mm or 0.032inches
- Total Length: 25ft

Thermocouple wire was ordered, from which thermocouples will be manufactured. They will be used to measure the temperature profile of the fins on the heat sink. They will be connected to a data acquisition card.

### Data Acquisition System

Supplier: National Instruments Corp.

Item Number: 779436-01

Specs:

- 4 channels of 24-bit thermocouples input
- Maximum sampling rate: 12

The Data Acquisition System will be used to monitor and record the temperatures from the thermocouples.

### Theoretical Analysis

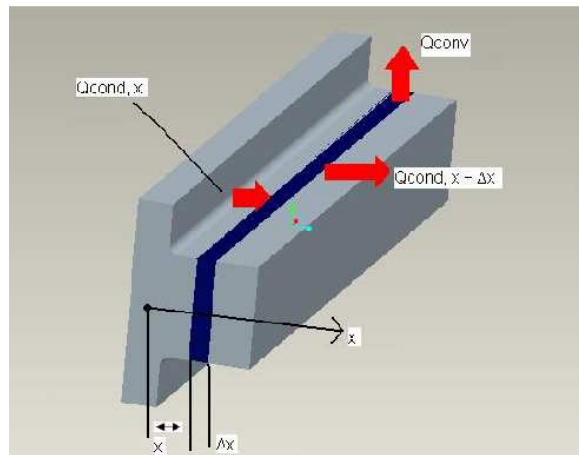


*Figure 6.1.5: Thermodynamic Model for Fin Analysis*

Assumptions:

1. Steady state conditions apply to the system
2. Fin geometry has constant cross section
3. Material has constant thermal conductivity
4. Heat is lost from fin tip by convection

Thermodynamic Analysis was carried out based on the following:

1. Conservation of Energy Principle: Energy can neither be created nor destroyed; it can only change forms. This law provides a sound basis for studying the relationships among various forms of energy and energy interactions.
2. Energy Balance:

$$\sum_{\text{in}} E = \sum_{\text{out}} E$$

3. First law of Thermodynamics:

$$Q_{\text{dot}} - W_{\text{dot}} + \sum_{\text{in}} (m_{\text{dot}} \cdot \theta) - \sum_{\text{out}} (m_{\text{dot}} \cdot \theta) = 0$$

4. Fourier's Law of Heat Conduction:

$$Q_{\text{cond}} = -k \cdot A_c \cdot \frac{dT}{dx}$$

Based on the thermodynamic model shown in Figure 6.1.5, the assumptions above and the laws and principles used, the following equations were derived. (*Details can be found in Appendix B.1*)

Heat loss from a rectangular fin (taking into consideration convection at the fin tip):

$$Q_{\text{fin}} = \sqrt{h \cdot p \cdot k \cdot A_c} \cdot (T_b - T_{\text{inf}}) \cdot \tanh\left(a \left(L + \frac{t}{2}\right)\right)$$

Total heat loss from heat sink:

$$Q_{\text{total}} = n \cdot \left[ \sqrt{h \cdot p \cdot k \cdot A_c} \cdot (T_b - T_{\text{inf}}) \cdot \tanh\left(a \left(L + \frac{t}{2}\right)\right) \right] + h \cdot A_{\text{unfin}} \cdot (T_b - T_{\text{inf}})$$

Fin Efficiency:

$$\eta_{\text{fin}} = \frac{Q_{\text{fin}}}{Q_{\text{fin.maz}}} = \frac{Q_{\text{fin}}}{h \cdot A_{\text{fin}} \cdot (T_b - T_{\text{inf}})}$$

Overall heat sink effectiveness:

$$\epsilon_{\text{overall}} = \frac{Q_{\text{total}}}{Q_{\text{no.fin}}} = \frac{Q_{\text{total}}}{h \cdot A_b \cdot (T_b - T_{\text{inf}})}$$

The calculated values for the Aluminum and Carbon Foam heat sinks are stated below:

<b>Heat Sink Material</b>	<b>Total Heat Loss <math>Q_{\text{total}}</math> (W)</b>	<b>Fin Efficiency <math>\eta_{\text{fin}}</math></b>	<b>Heat Sink Effectiveness <math>\epsilon_{\text{overall}}</math></b>
<b>Aluminum</b>	22	98 %	27
<b>Carbon Foam</b>	21	95 %	26

*Table 6.1.1: Calculated Values for Aluminum and Carbon Foam Finned Heat Sinks*

The total heat lost from the aluminum heat sink is greater than the total heat lost from the carbon foam heat sink of identical dimensions. This is due to the higher thermal conductivity of aluminum. In addition, the efficiency and effectiveness of the aluminum heat sink exceeds that of the carbon foam heat sink, for the same reason.

From the calculations above, it can be observed that parameters affecting the performance of the fin design are as follows:

- Thermal Conductivity (k)
- Geometry: perimeter to cross-sectional area ratio (p/A<sub>c</sub>)
- Convection heat transfer coefficient (h)

## Chapter 6.2a: Machining Procedures

### Prototype I

The carbon foam finned heat sink was manufactured at the FAMU-FSU College of Engineering Industrial Engineering Composites Laboratory using a tile saw (see Figure 6.2.a.1). A replica of an existing finned aluminum heat sink was machined by making a series of vertical and horizontal cuts at the appropriate locations. It was not possible to manufacture an exact copy. The fins of the aluminum heat sink were very thin. Carbon foam is very fragile, and attempting to machine such thin fins would have resulted in damage to the material. As a result, the carbon foam heat sink was a close, but not exact replica of the existing aluminum heat sink.



*Figure 6.2.a.1: Machining of Prototype I*

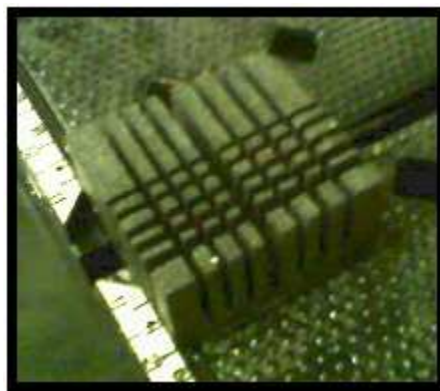


*Figure 6.2.a.2: Prototype I During Machining*

## **Chapter 6.2b Experiment**

### Objective

This experiment aims to compare the effectiveness of carbon foam and aluminum as materials for use in thermal management. This will be accomplished by comparing heat sinks of identical configurations made from both materials.

### Theoretical Background

Traditional heat sinks are made of metals such as Aluminum. A new material under investigation for use in heat sinks is carbon foam. This material is porous and thus has an increased surface area within the material that is available for use in convective heat transfer.

In order to adequately compare the performance of the two materials, identical heat sinks made from each material will be used to cool two identical processors being used for the same applications. Temperature measurements will be taken at the same locations on both heat sinks using thermocouples. From this, the total heat lost, as well as the efficiency and effectiveness of each thermocouple will be calculated.

The following factors will be held constant: heat sink geometry, environmental conditions, processor, computer system, thermocouple placement and heat generated by the processor. The heat generated by the processor will be kept constant by using running the same application program on both computers for the same time duration. The variable to be manipulated is the type of heat sink material. The responding or dependent variable is the temperature at various locations along the heat sinks.

Temperature readings will be taken at the base and tip of selected thermocouples. These readings will allow for the calculation of heat loss, efficiency and effectiveness. The heat sink was divided into four regions, based on distance away from the site of heat generation (processor). This is demonstrated in Figure 6.2.b.8. The fins in each region lose approximately the same amount of heat (i.e. all fins in Region 1 lose the same amount of heat). Because of the symmetry of the heat sink, it is unnecessary to take

readings from all nine regions. As such, the placement of the thermocouples was determined as shown in Figure 6.2.b.8.

### Equipment

*Heat Sinks:* Two identical heat sinks made of carbon foam and aluminum will be used. It is necessary to machine the carbon foam heat sink based on the dimensions of the conventional aluminum heat sink that will be tested. (See Chapter 6.2.a for machining procedures)

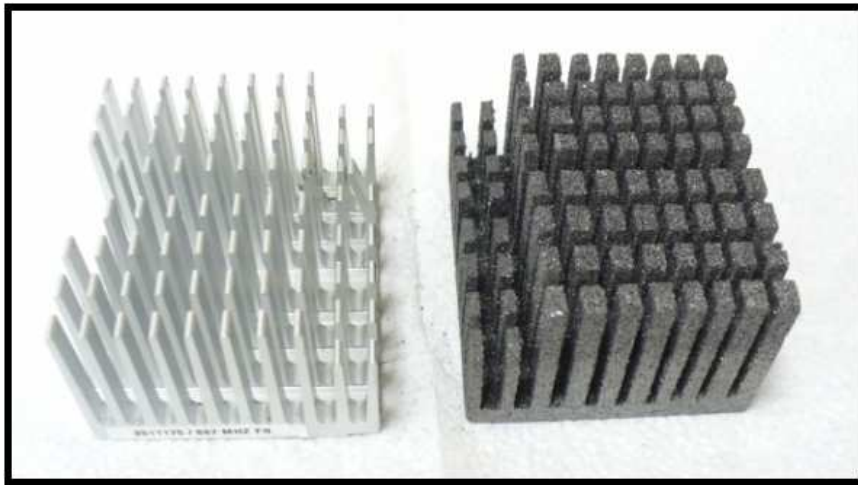


*Figure 6.2.b.1: Aluminum and Carbon Foam Heat Sinks*

*Thermocouples:* Four type J thermocouples were used at various locations. These thermocouples were manufactured from thermocouple wire.



*Figure 6.2.b.2: Thermocouple Wire Used to Manufacture Thermocouples*



*Figure 6.2.b.3: Thermocouples*

*Data Acquisition System:* The portable USB Data acquisition system NI USB-9211A can be used to collect data from four channels of 24-bit thermocouple input. This data will be processed using LabVIEW SignalExpress data-logger software.



*Figure 6.2.b.4: Data Acquisition System*

*Computer System:* The computer system consists of a barebone kit obtained from Tiger Direct (Item Number P459-1236C), hard drive (4 GB), CD-Rom Drive, monitor, keyboard and mouse. The processor with attached heat sink will be installed into the barebone component of the system. This will be set to run selected applications during the following experiment, while temperature measurements are taken.



*Figure 6.2.b.5: Computer System*

*Processor Chip:* Two AMD Athlon 64 3500 chips will be used to generate heat at a constant rate by means of running the same applications on both computers. The heat sinks will be attached to the processor chips by means of a thermally conductive paste if necessary.



*Figure 6.2.b.6: AMD Athlon 64 3500 Processor Chip*

*Application Software:* The ideal application causes heat to be generated at a constant rate by the processor chip. Additionally, the amount of heat generated per unit time should be high enough to provide a challenging test for the heat sinks. The application should operate for an adequate time period with little to no human input. Norton Antivirus 7.0

was selected. This repetitive program ensures a constant heat generation of a sufficiently high magnitude. Once begun, no human input is required. In addition, once sufficient data has been collected, the application can merely be stopped. For these reasons, it was decided that the Norton Virus Scan 7.0 is to be used as the application software for the generation of a large, constant heat flux.

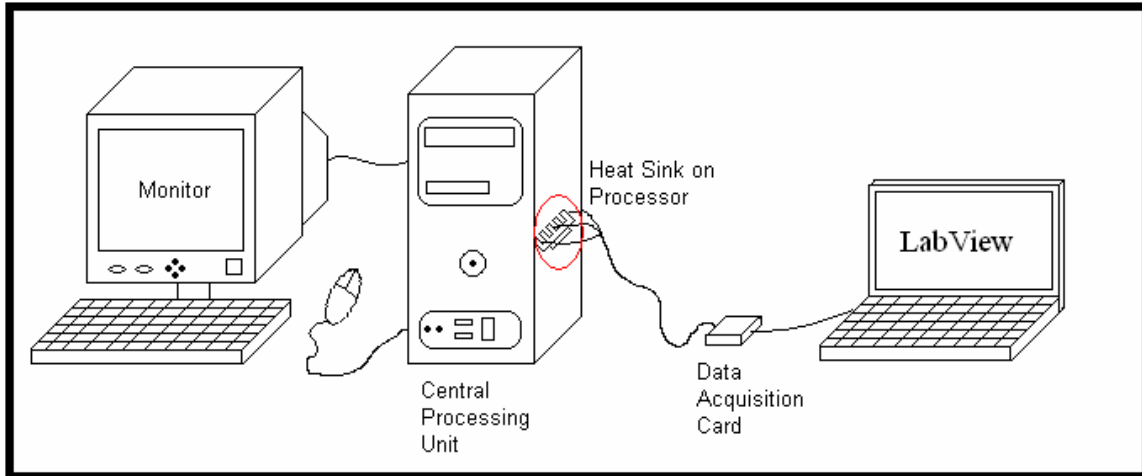


*Figure 6.2.b.7: Experimental Setup*

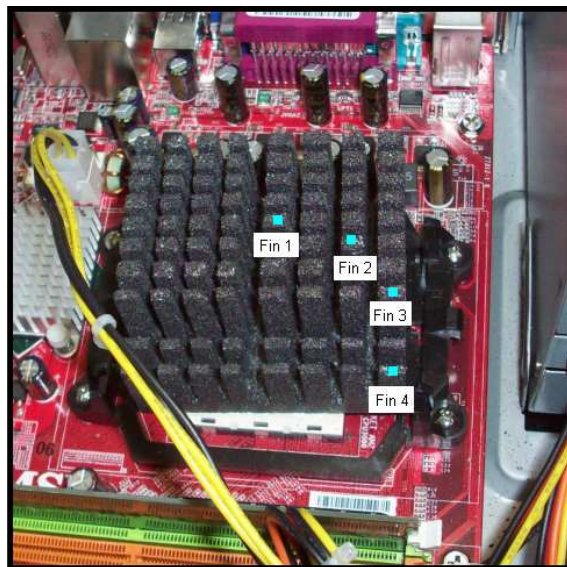


*Figure 6.2.b.8: Fins Selected for Thermocouple Placement*

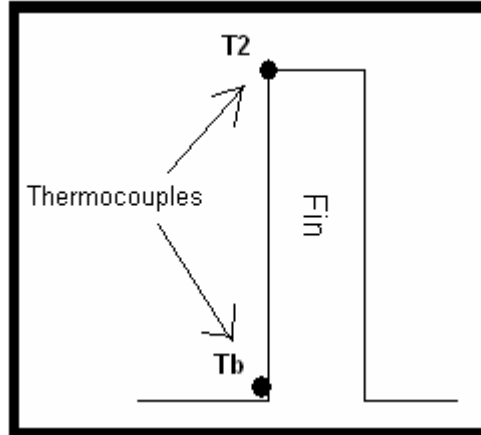


Figure 6.2.b.9: Location of Thermocouples along Fin

## Procedure

### Preparation

1. Manufacture of Thermocouples
  - a. Four sections of thermocouple wire were cut.
  - b. Both ends of all four sections were stripped of all insulation
  - c. For each thermocouple, the two wires protruding from one end were soldered together.
  - d. The wires protruding from the other end of the thermocouple were connected to the data acquisition system.
2. Thermocouple Calibration
  - a. Water was brought to a boil using a hot plate
  - b. An ice bath was created by filling a styrofoam cup with ice blocks.
  - c. The four thermocouples were connected to the data acquisition system, which was in turn connected to a laptop computer via a USB cable.
  - d. The LabVIEW SignalExpress program was started on the laptop.
  - e. At the prompt, one thermocouple was immersed in the ice bath. The temperature registered by the thermocouple was recorded using LabView.
  - f. The same thermocouple was then immersed in boiling water the temperature registered by the thermocouple was again recorded.
  - g. The software was allowed to plot the thermocouple calibration curve.
  - h. Steps a-g were repeated for the remaining thermocouples.

3. Computer System Assembly
  - a. The barebone kit was put together and the processor was fixed in place.
  - b. With the Aluminum heat sink and fan in place (so as to prevent overheating), the hard drive and CD-Rom drive were installed.
4. Norton Antivirus 7.0 was installed, again using the Aluminum heat sink and fan.

#### Methodology

1. The thermocouples were positioned along the Aluminum heat sink on fins 1 and 2 as shown in Figure 6.2.b.8 and Figure 6.2.b.9.
2. The heat sink was secured to processor chip using the thermally conductive paste.
3. The thermocouples were connected to the Data Acquisition System.
4. The Data Acquisition System was turned on and LabVIEW SignalExpress started.
5. The computer was turned on and allowed to boot up.
6. Norton Virus Scan 7.0 was started, and LabVIEW was set to record the temperatures measured by the thermocouples.
7. The virus scan was run for approximately five minutes in order to ensure steady state heat generation in the processor chip was achieved.
8. Norton Virus Scan 7.0 was exited.
9. Data Acquisition System was stopped
10. The virus scan was run again to measure the temperatures on fins 3 and 4.
11. Steps 1 through 9 were repeated, replacing the Aluminum heat sink with the carbon foam heat sink.
12. The entire procedure was repeated with a fan placed on top of both heat sinks.

Analysis

The following graphs show the temperatures obtained for Fins 1 through 4 as a function of time for the aluminum heat sink without a fan.

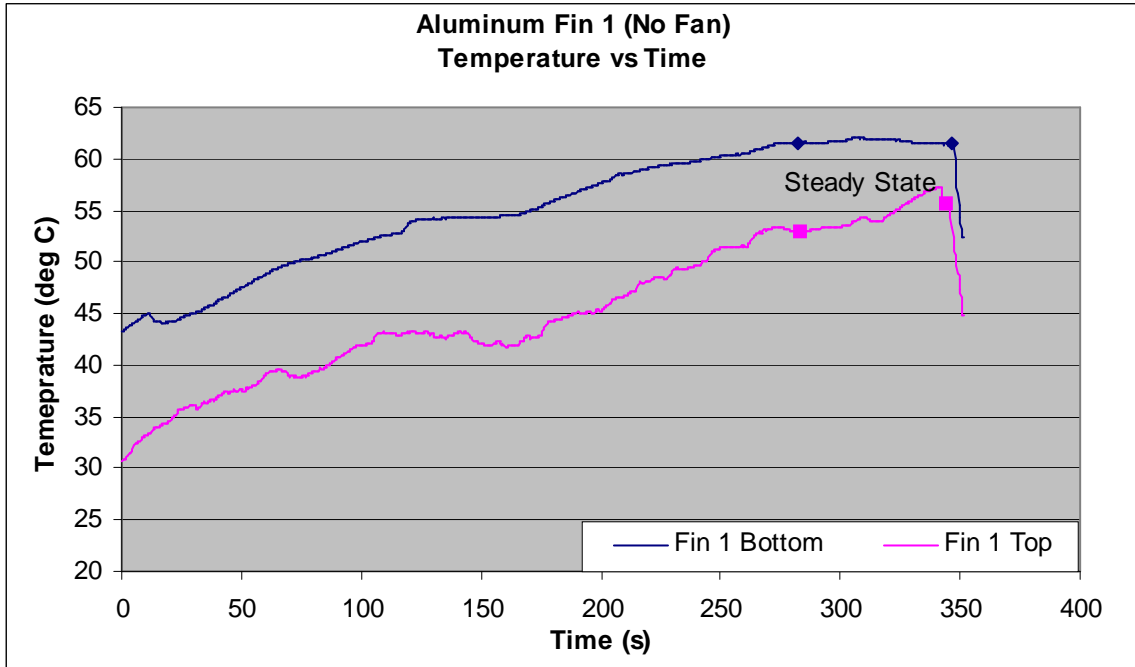


Figure 6.2.b.10: Temperature with Time along Fin 1 of Aluminum Heat Sink Without Fan

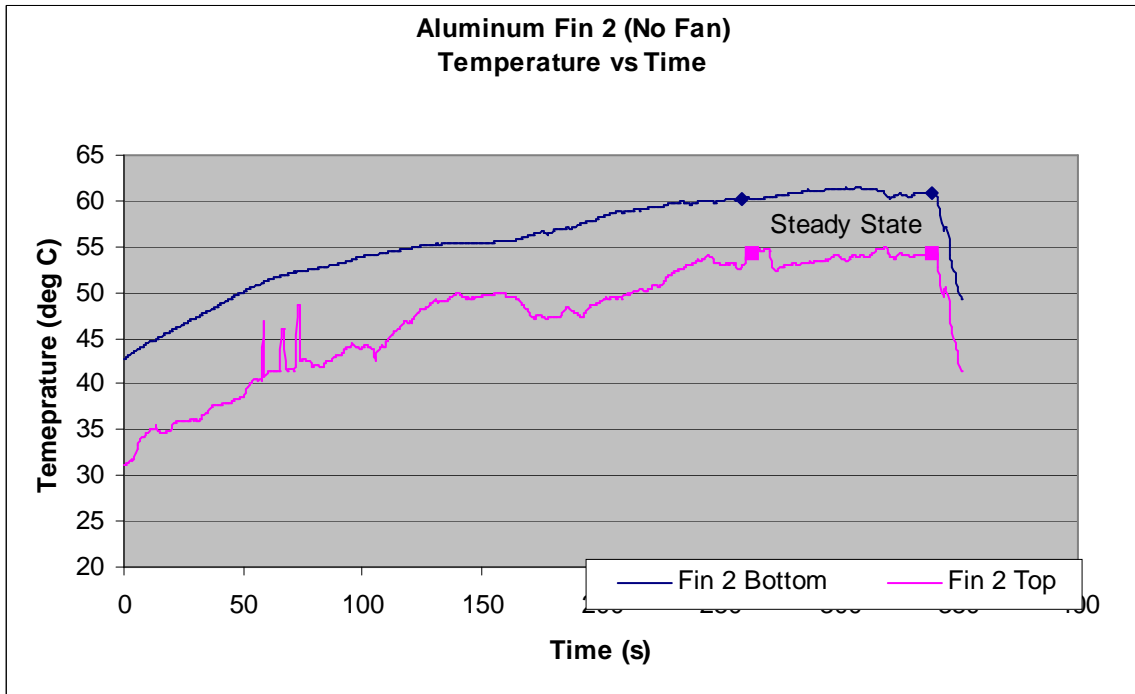


Figure 6.2.b.11: Temperature with Time along Fin 2 of Aluminum Heat Sink Without Fan

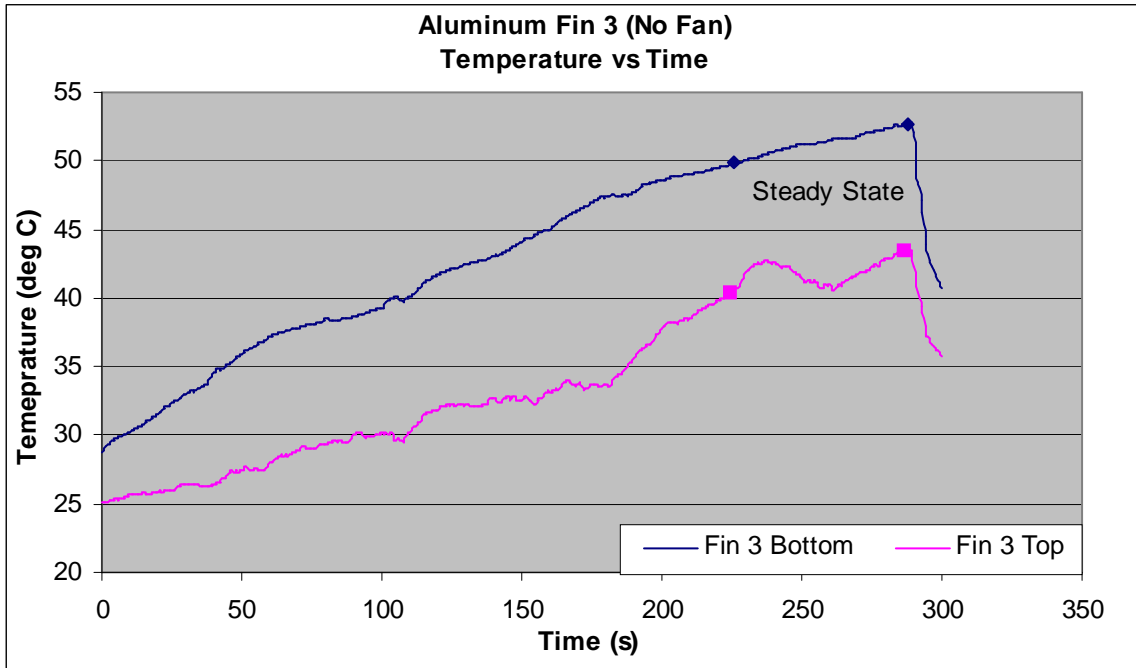


Figure 6.2.b.12: Temperature with Time along Fin 1 of Aluminum Heat Sink Without Fan

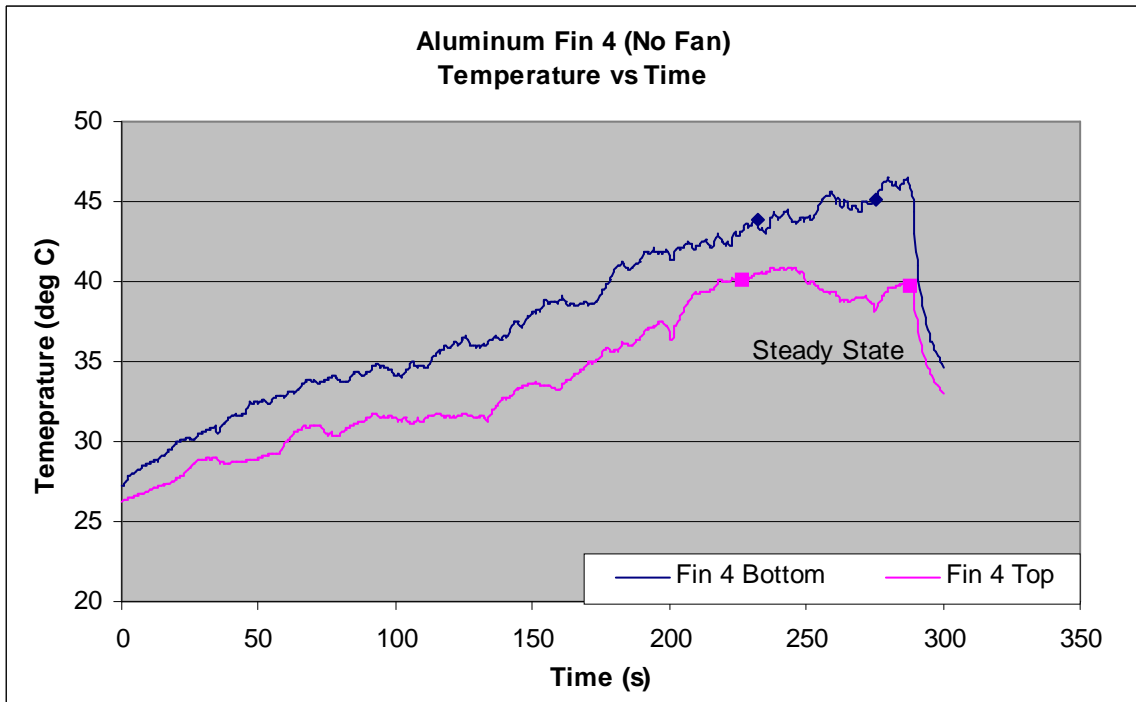


Figure 6.2.b.13: Temperature with Time along Fin 4 of Aluminum Heat Sink Without Fan

$$T_{b1} := 334.67\text{K} \quad T_{b2} := 333.77\text{K} \quad T_{b3} := 324.06\text{K} \quad T_{b4} := 317.26\text{K}$$

$$T_{t1} := 326.72\text{K} \quad T_{t2} := 326.72\text{K} \quad T_{t3} := 314.65\text{K} \quad T_{t4} := 312.75\text{K}$$

$$l := 0.04\text{m} \quad w := 0.0075\text{m} \quad t := 0.005\text{m} \quad n := 78$$

$$h := 8 \frac{\text{W}}{\text{m}^2 \cdot \text{K}} \quad k := 237 \frac{\text{W}}{\text{m} \cdot \text{K}} \quad p := 2(w + t) \quad T_{\text{inf}} := 300\text{K}$$

$$A_c := w \cdot t \quad L_c := l + \frac{A_c}{p} \quad a := \sqrt{\frac{h \cdot p}{k \cdot A_c}} \quad H := 0.04\text{m}$$

$$B := 0.075\text{m} \quad A_b := H \cdot B \quad T_b := 0.25(T_{b1} + T_{b2} + T_{b3} + T_{b4})$$

$$A_{\text{fin}} := 2(l \cdot w + l \cdot t) + w \cdot t \quad A_{\text{unfin}} := A_b - n \cdot A_c$$

$$Q_{\text{fin}} := \sqrt{h \cdot p \cdot k \cdot A_c} \cdot (T_b - T_{\text{inf}}) \cdot \tanh(a \cdot L_c)$$

$$Q_{\text{fin,max}} := h \cdot A_{\text{fin}} \cdot (T_b - T_{\text{inf}}) \quad Q_{\text{no,fin}} := h \cdot A_b \cdot (T_b - T_{\text{inf}})$$

$$Q_{\text{n,fin}} := n \cdot \sqrt{h \cdot p \cdot k \cdot A_c} \cdot (T_b - T_{\text{inf}}) \cdot \tanh(a \cdot L_c)$$

$$Q_{\text{unfin}} := h \cdot A_{\text{unfin}} \cdot (T_b - T_{\text{inf}})$$

$$Q_{\text{total}} := Q_{\text{n,fin}} + Q_{\text{unfin}}$$

$$\eta_{\text{fin}} := \frac{Q_{\text{fin}}}{Q_{\text{fin,max}}} \quad \varepsilon_{\text{fin}} := \frac{Q_{\text{fin}}}{Q_{\text{no,fin}}} \quad \varepsilon_{\text{overall}} := \frac{Q_{\text{total}}}{Q_{\text{no,fin}}}$$

$$Q_{\text{fin}} = 0.225 \text{ W}$$

$$Q_{\text{n,fin}} = 17.539 \text{ W}$$

$$Q_{\text{unfin}} = 0.016 \text{ W}$$

$$\varepsilon_{\text{fin}} = 0.341$$

$$Q_{\text{fin,max}} = 0.228 \text{ W}$$

$$Q_{\text{total}} = 17.555 \text{ W}$$

$$\eta_{\text{fin}} = 0.987$$

$$\varepsilon_{\text{overall}} = 26.657$$

The following graphs show the temperatures obtained for Fins 1 through 4 as a function of time for the aluminum heat sink without a fan.

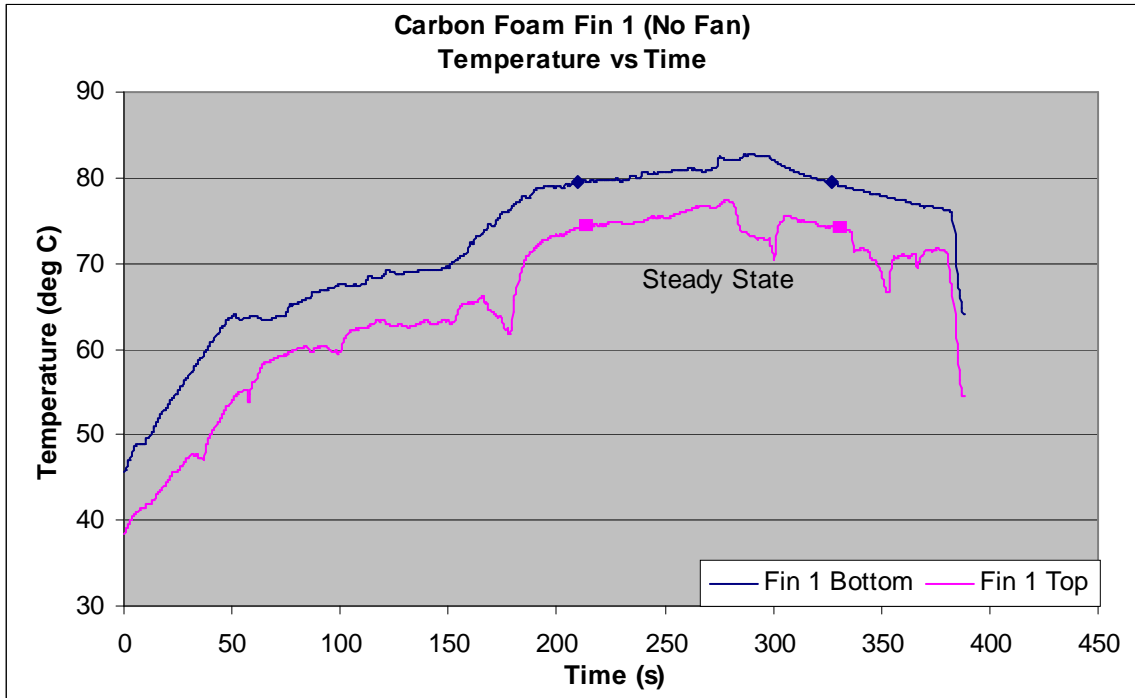


Figure 6.2.b.14: Temperature with Time of Fin 1 of Carbon Foam Heat Sink Without Fan

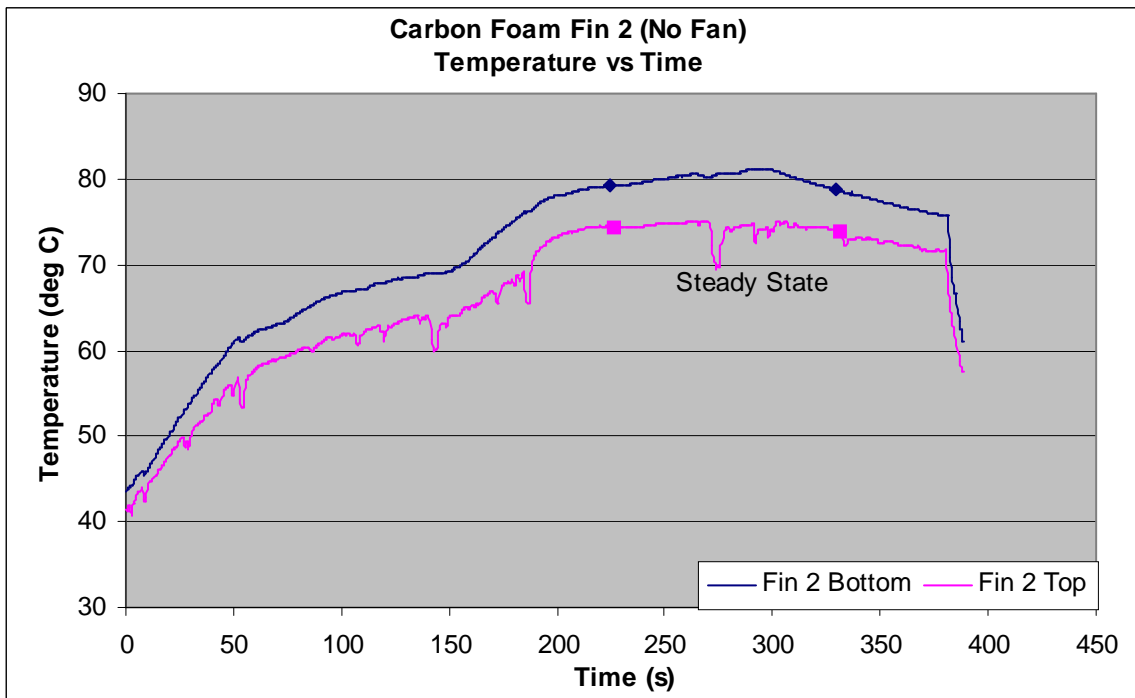


Figure 6.2.b.15: Temperature with Time of Fin 2 of Carbon Foam Heat Sink Without Fan

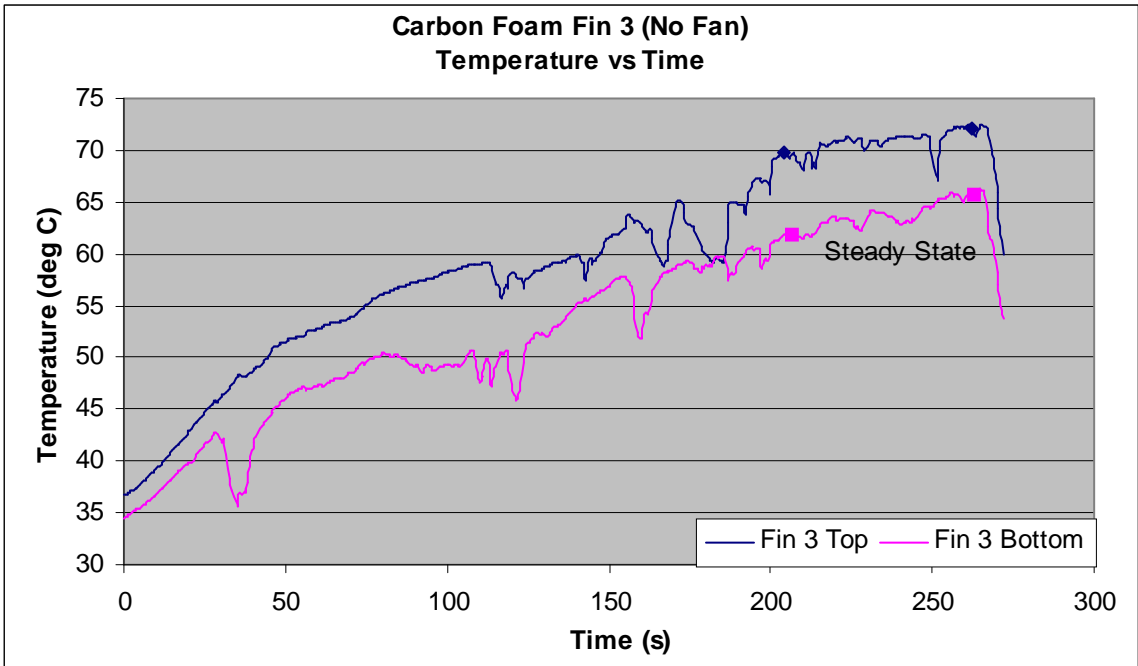


Figure 6.2.b.16: Temperature with Time of Fin 3 of Carbon Foam Heat Sink Without Fan

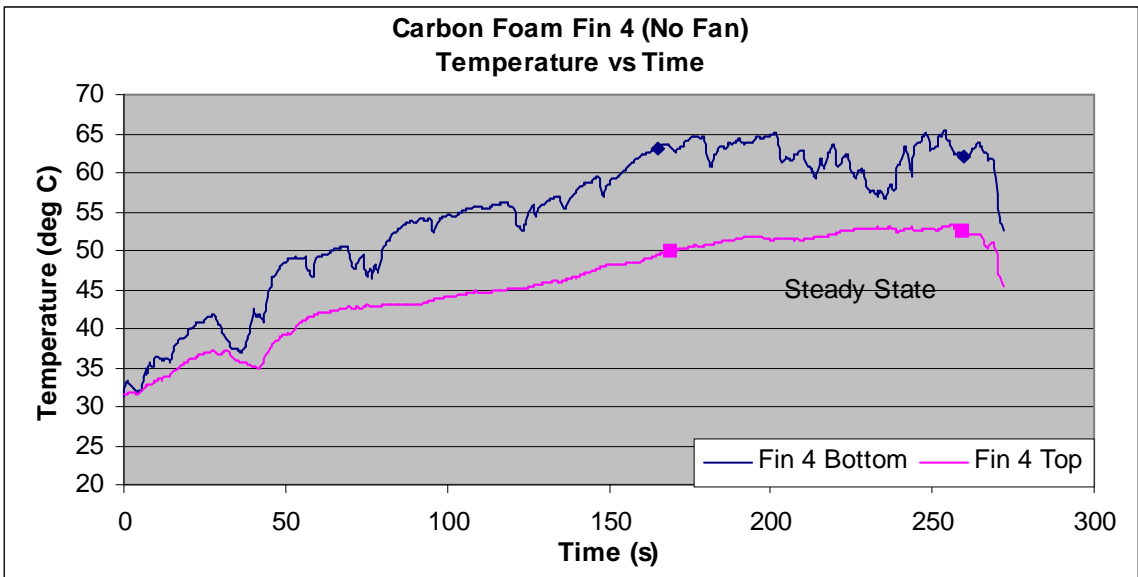


Figure 6.2.b.17: Temperature with Time of Fin 4 of Carbon Foam Heat Sink Without Fan

$$T_{b1} := 354.02\text{K} \quad T_{b2} := 353.20\text{K} \quad T_{b3} := 343.77\text{K} \quad T_{b4} := 335.34\text{K}$$

$$T_{t1} := 348.05\text{K} \quad T_{t2} := 347.3\text{K} \quad T_{t3} := 336.71\text{K} \quad T_{t4} := 324.68\text{K}$$

$$l := 0.04\text{m} \quad w := 0.0075\text{m} \quad t := 0.005\text{m} \quad n := 78$$

$$h := 8 \frac{\text{W}}{\text{m}^2 \cdot \text{K}} \quad k := 64 \frac{\text{W}}{\text{m} \cdot \text{K}} \quad p := 2(w + t) \quad T_{\text{inf}} := 300\text{K}$$

$$A_c := w \cdot t \quad L_c := l + \frac{A_c}{p} \quad a := \sqrt{\frac{h \cdot p}{k \cdot A_c}} \quad H := 0.04\text{m}$$

$$B := 0.075\text{m} \quad A_b := H \cdot B \quad T_b := 0.25(T_{b1} + T_{b2} + T_{b3} + T_{b4})$$

$$A_{\text{fin}} := 2(l \cdot w + l \cdot t) + w \cdot t \quad A_{\text{unfin}} := A_b - n \cdot A_c$$

$$Q_{\text{fin}} := \sqrt{h \cdot p \cdot k \cdot A_c} \cdot (T_b - T_{\text{inf}}) \cdot \tanh(a \cdot L_c)$$

$$Q_{\text{fin,max}} := h \cdot A_{\text{fin}} \cdot (T_b - T_{\text{inf}}) \quad Q_{\text{no,fin}} := h \cdot A_b \cdot (T_b - T_{\text{inf}})$$

$$Q_{\text{n,fin}} := n \cdot \sqrt{h \cdot p \cdot k \cdot A_c} \cdot (T_b - T_{\text{inf}}) \cdot \tanh\left[a \cdot \left(1 + \frac{t}{2}\right)\right]$$

$$Q_{\text{unfin}} := h \cdot A_{\text{unfin}} \cdot (T_b - T_{\text{inf}})$$

$$Q_{\text{total}} := Q_{\text{n,fin}} + Q_{\text{unfin}}$$

$$\eta_{\text{fin}} := \frac{Q_{\text{fin}}}{Q_{\text{fin,max}}} \quad \varepsilon_{\text{fin}} := \frac{Q_{\text{fin}}}{Q_{\text{no,fin}}} \quad \varepsilon_{\text{overall}} := \frac{Q_{\text{total}}}{Q_{\text{no,fin}}}$$

$$Q_{\text{fin}} = 0.369 \text{ W} \quad Q_{\text{n,fin}} = 29.423 \text{ W} \quad Q_{\text{unfin}} = 0.028 \text{ W}$$

$$\varepsilon_{\text{fin}} = 0.33 \quad Q_{\text{fin,max}} = 0.387 \text{ W}$$

$$Q_{\text{total}} = 29.451 \text{ W}$$

$$\eta_{\text{fin}} = 0.955$$

$$\varepsilon_{\text{overall}} = 26.343$$

The following graphs show the temperatures obtained for Fins 1 through 4 as a function of time for the aluminum heat sink with a fan.

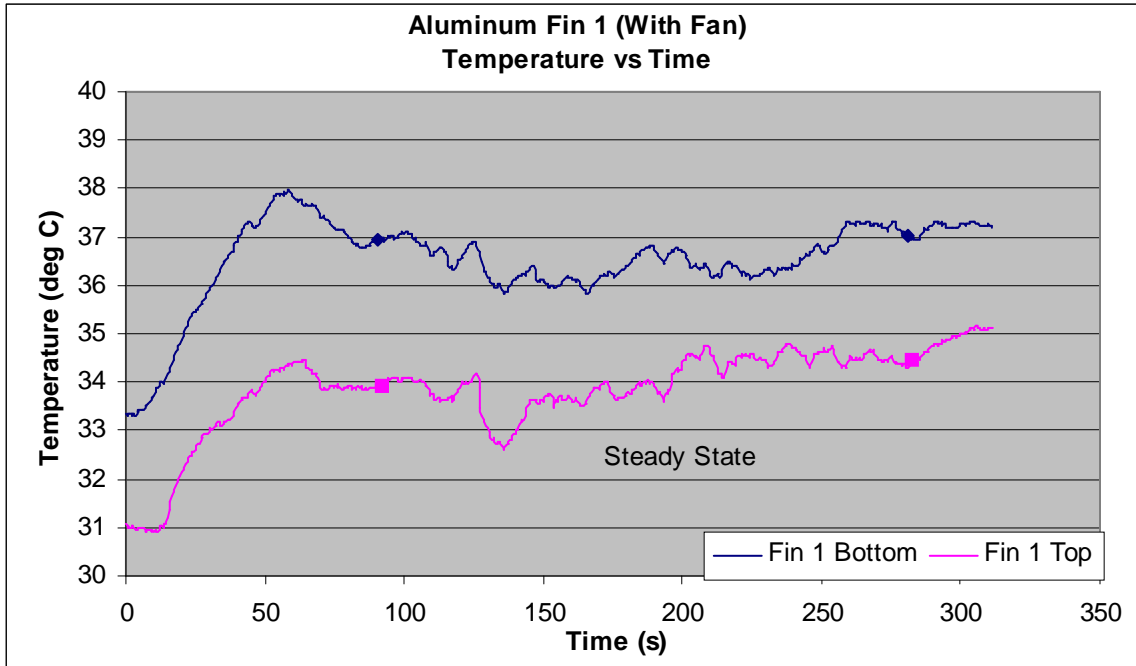


Figure 6.2.b.18: Temperature with Time of Fin 1 of Aluminum Heat Sink With Fan

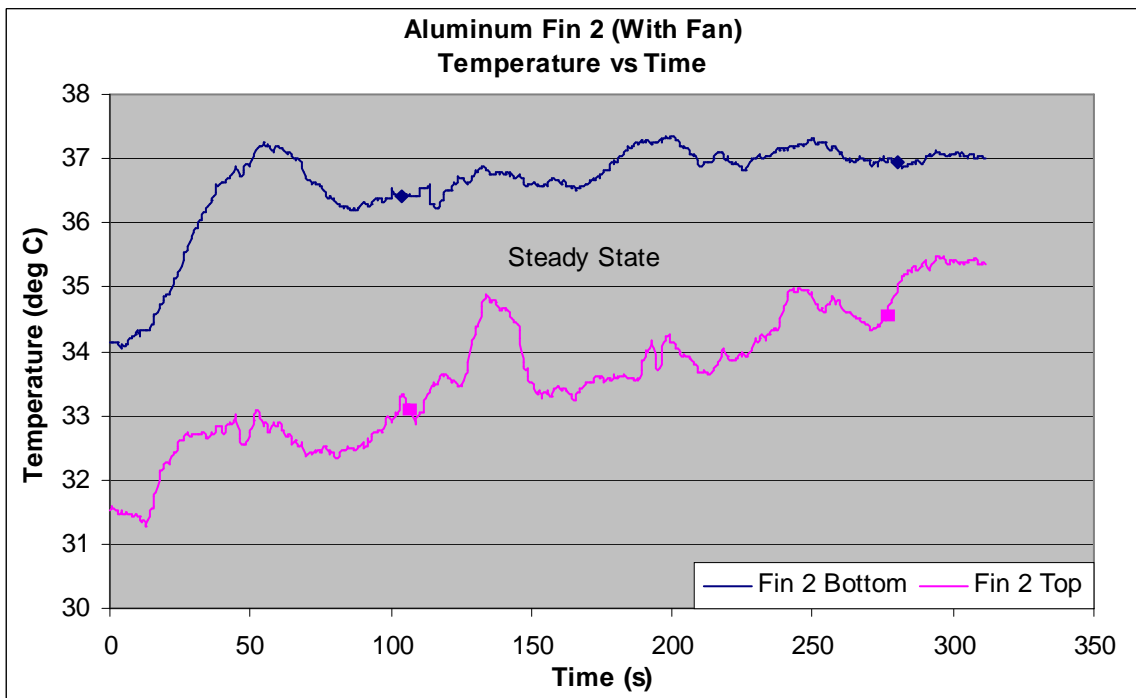


Figure 6.2.b.19: Temperature with Time of Fin 2 of Aluminum Heat Sink With Fan

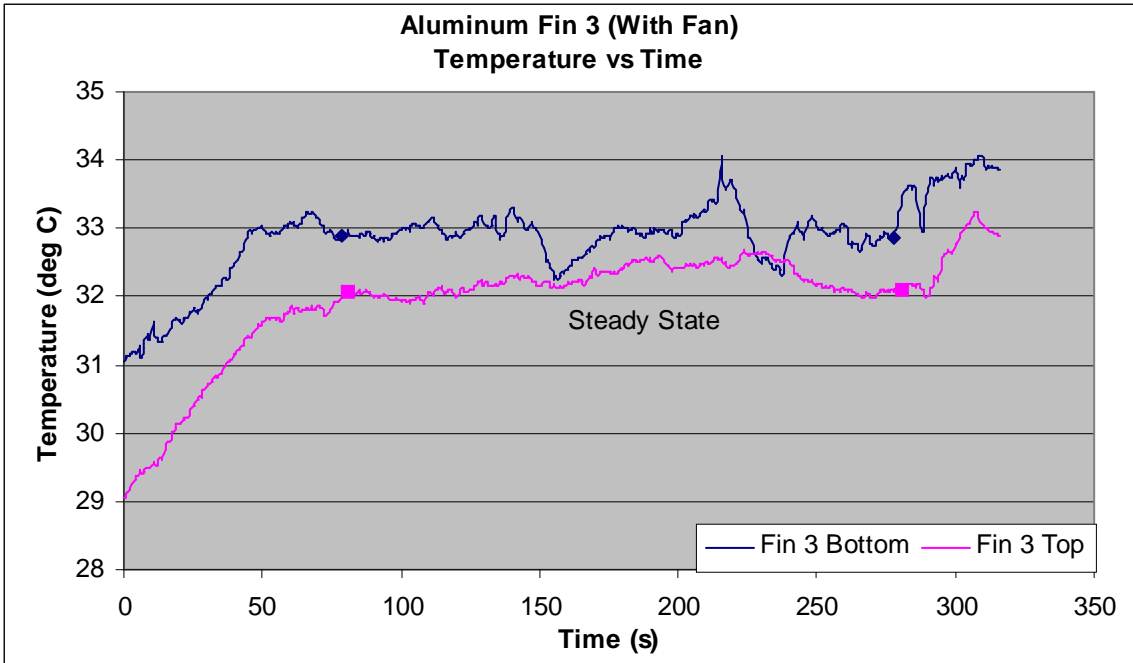


Figure 6.2.b.20: Temperature with Time of Fin 3 of Aluminum Heat Sink With Fan

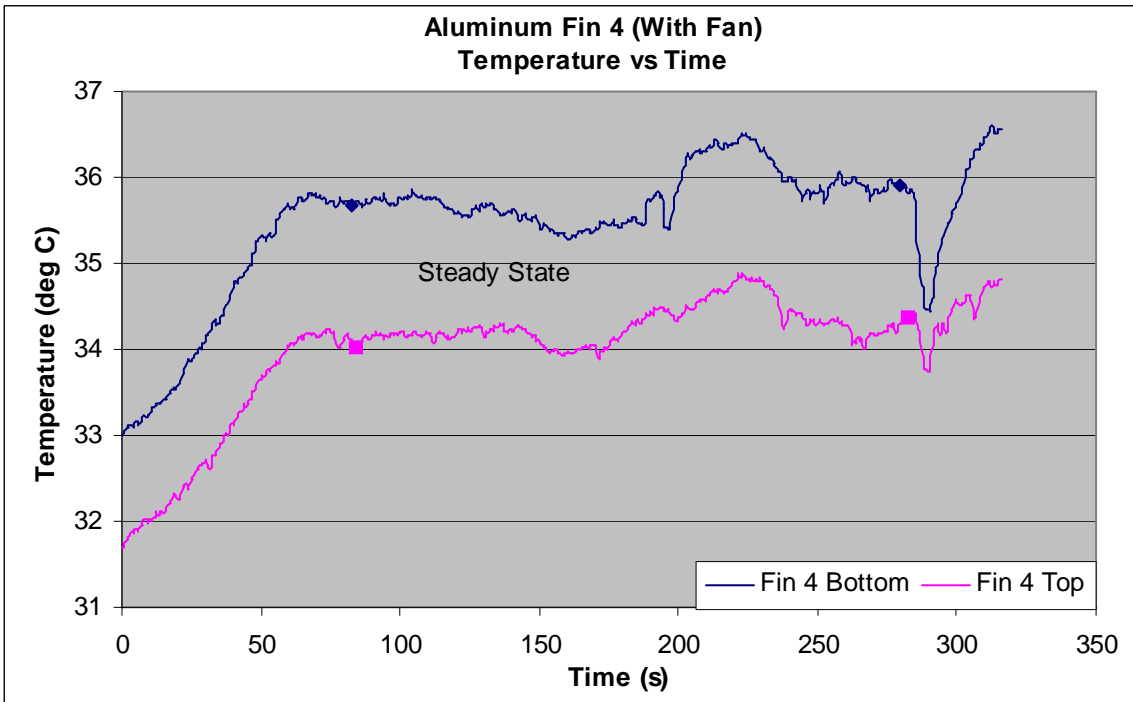


Figure 6.2.b.21: Temperature with Time along Fin 4 of Aluminum Heat Sink With Fan

$$\begin{aligned}
T_{b1} &:= 309.64\text{K} & T_{b2} &:= 309.84\text{K} & T_{b3} &:= 306.05\text{K} & T_{b4} &:= 308.77\text{K} \\
T_{t1} &:= 307.14\text{K} & T_{t2} &:= 306.86\text{K} & T_{t3} &:= 305.31\text{K} & T_{t4} &:= 307.30\text{K} \\
n_1 &:= 12 & n_2 &:= 16 & n_3 &:= 20 & n_4 &:= 30 \\
l &:= 0.04\text{m} & w &:= 0.0075\text{m} & t &:= 0.005\text{m} & A_c &:= w \cdot t \\
n &:= 78 & p &:= 2(w + t) & H &:= 0.04\text{m} & B &:= 0.075\text{m} \\
A_b &:= H \cdot B & A_{\text{fin}} &:= 2(l \cdot w + l \cdot t) + w \cdot t & A_{\text{unfin}} &:= A_b - n \cdot A_c \\
k &:= 237 \frac{\text{W}}{\text{m} \cdot \text{K}} & L_c &:= 1 + \frac{A_c}{p} & T_{\text{inf}} &:= 295\text{K}
\end{aligned}$$

$$T_{b\_avg} := (n_1 \cdot T_{b1} + n_2 \cdot T_{b2} + n_3 \cdot T_{b3} + n_4 \cdot T_{b4}) \cdot n^{-1}$$

Properties of air at 25 deg. C and  $V := 2\text{m} \cdot \text{s}^{-1}$

$$\begin{aligned}
Pr &:= 0.7296 & k_a &:= 0.02551\text{W} \cdot \text{m}^{-1} \cdot \text{K}^{-1} & \nu &:= 1.562 \cdot 10^{-5} \text{m}^2 \cdot \text{s}^{-1} \\
Re &:= V \cdot l \cdot \nu^{-1} & Nu &:= 0.664 \cdot Re^{0.5} \cdot Pr^{0.33} & h &:= Nu \cdot k_a \cdot l^{-1} \\
Re &= 5121.639 & Nu &= 42.824 & h &= 27.311\text{W} \cdot \text{m}^{-2} \cdot \text{K}^{-1}
\end{aligned}$$

$$a := \sqrt{\frac{h \cdot p}{k \cdot A_c}} \quad Q_{\text{fin}} := \sqrt{h \cdot p \cdot k \cdot A_c} \cdot (T_{b\_avg} - T_{\text{inf}}) \cdot \tanh(a \cdot L_c)$$

$$Q_{\text{fin,max}} := h \cdot A_{\text{fin}} \cdot (T_{b\_avg} - T_{\text{inf}}) \quad Q_{\text{no,fin}} := h \cdot A_b \cdot (T_{b\_avg} - T_{\text{inf}})$$

$$Q_{\text{n,fin}} := n \cdot \sqrt{h \cdot p \cdot k \cdot A_c} \cdot (T_{b\_avg} - T_{\text{inf}}) \cdot \tanh\left[a \cdot \left(1 + \frac{t}{2}\right)\right]$$

$$Q_{\text{unfin}} := h \cdot A_{\text{unfin}} \cdot (T_{b\_avg} - T_{\text{inf}}) \quad Q_{\text{total}} := Q_{\text{n,fin}} + Q_{\text{unfin}}$$

$$\eta_{\text{fin}} := \frac{Q_{\text{fin}}}{Q_{\text{fin,max}}} \quad \varepsilon_{\text{fin}} := \frac{Q_{\text{fin}}}{Q_{\text{no,fin}}} \quad \varepsilon_{\text{overall}} := \frac{Q_{\text{total}}}{Q_{\text{no,fin}}}$$

$$Q_{\text{fin}} = 0.364\text{W}$$

$$Q_{\text{n,fin}} = 29.057\text{W}$$

$$Q_{\text{unfin}} = 0.028\text{W}$$

$$Q_{\text{total}} = 29.084\text{W}$$

$$\eta_{\text{fin}} = 0.958$$

$$\varepsilon_{\text{overall}} = 26.439$$

The following graphs show the temperatures obtained for Fins 1 through 4 as a function of time for the carbon foam heat sink with a fan.

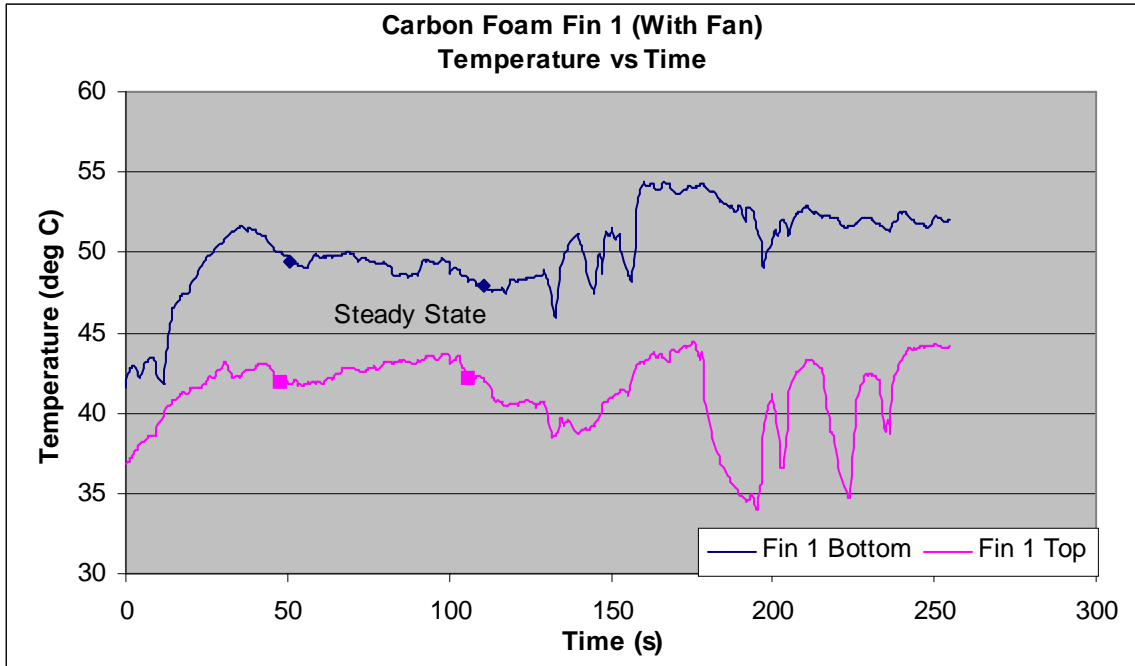


Figure 6.2.b.22: Temperature with Time of Fin 1 of Carbon Foam Heat Sink With Fan

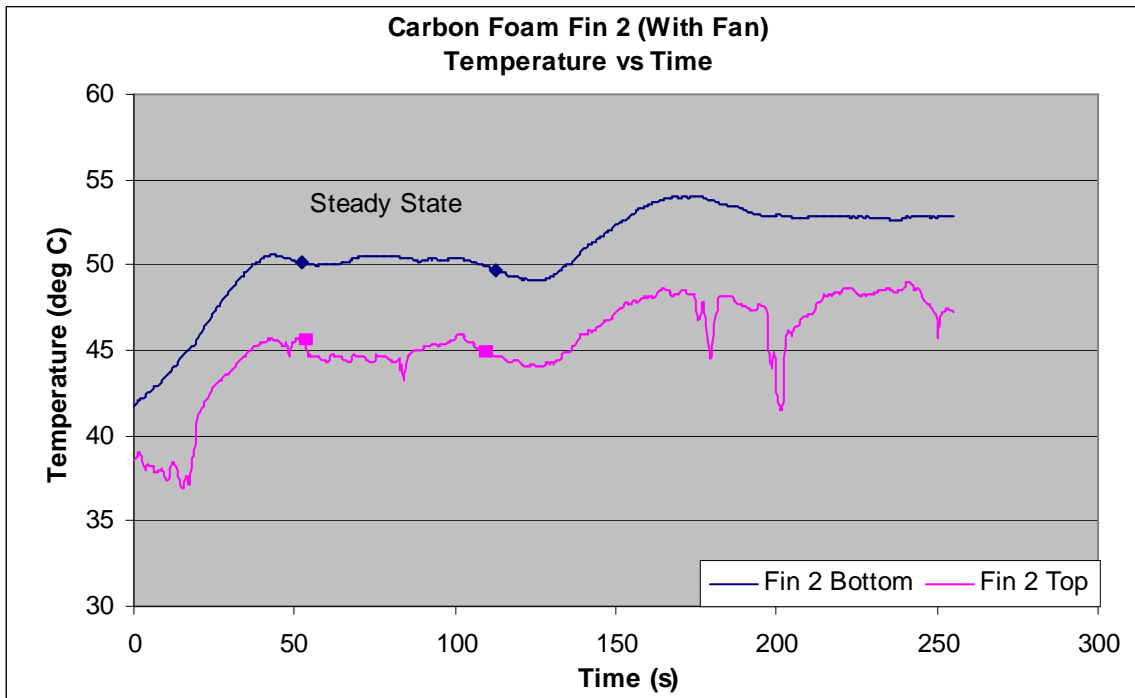


Figure 6.2.b.23: Temperature with Time of Fin 2 of Carbon Foam Heat Sink With Fan

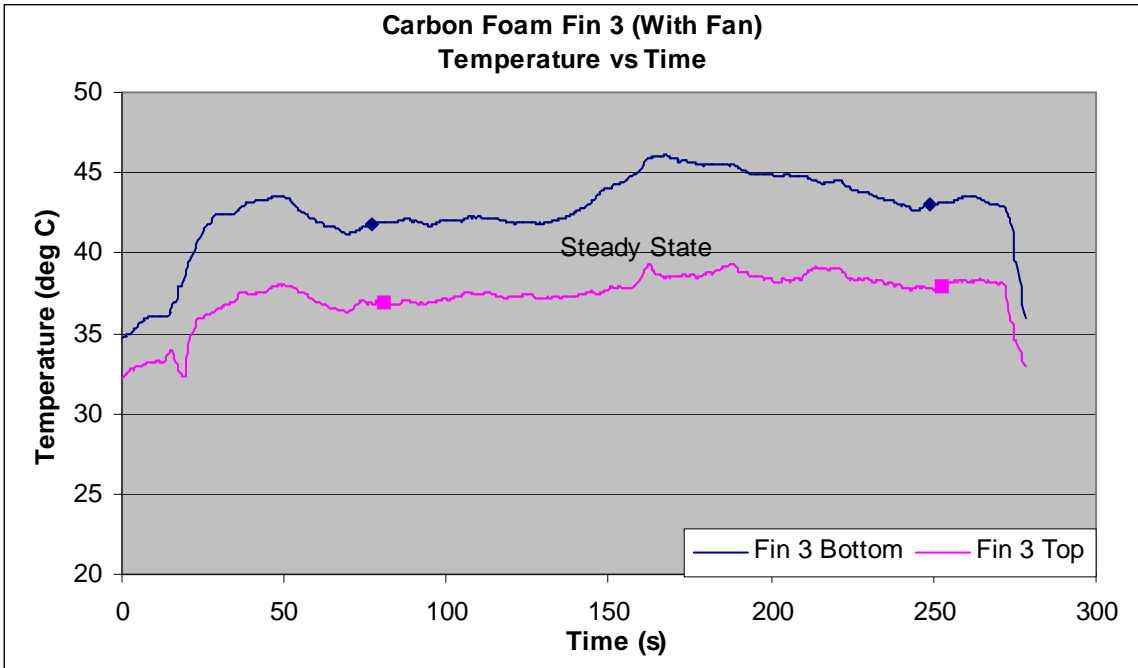


Figure 6.2.b.24: Temperature with Time of Fin 3 of Carbon Foam Heat Sink With Fan

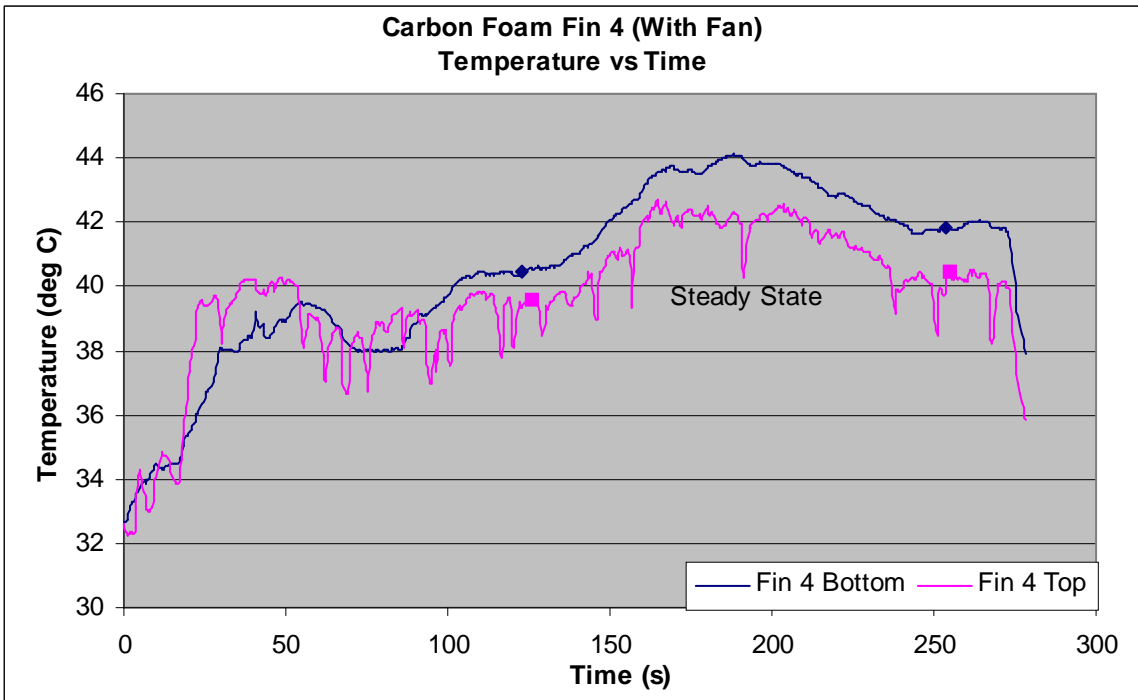


Figure 6.2.b.25: Temperature with Time of Fin 4 of Carbon Foam Heat Sink With Fan

$$\begin{aligned}
T_{b1} &:= 322.36\text{K} & T_{b2} &:= 323.28\text{K} & T_{b3} &:= 316.56\text{K} & T_{b4} &:= 315.65\text{K} \\
T_{t1} &:= 315.73\text{K} & T_{t2} &:= 317.80\text{K} & T_{t3} &:= 310.93\text{K} & T_{t4} &:= 314.17\text{K} \\
n_1 &:= 12 & n_2 &:= 16 & n_3 &:= 20 & n_4 &:= 30 \\
l &:= 0.04\text{m} & w &:= 0.0075\text{m} & t &:= 0.005\text{m} & A_c &:= w \cdot t \\
n &:= 78 & p &:= 2(w + t) & H &:= 0.04\text{m} & B &:= 0.075\text{m} \\
A_b &:= H \cdot B & A_{\text{fin}} &:= 2(l \cdot w + l \cdot t) + w \cdot t & A_{\text{unfin}} &:= A_b - n \cdot A_c \\
k &:= 64 \frac{\text{W}}{\text{m} \cdot \text{K}} & L_c &:= 1 + \frac{A_c}{p} & T_{\text{inf}} &:= 295\text{K} \\
T_{b\_avg} &:= (n_1 \cdot T_{b1} + n_2 \cdot T_{b2} + n_3 \cdot T_{b3} + n_4 \cdot T_{b4}) \cdot n^{-1} & T_{b\_avg} &= 318.481\text{K}
\end{aligned}$$

Properties of air at 45 deg. C and  $V := 0.5 \text{m} \cdot \text{s}^{-1}$

$$\begin{aligned}
Pr &:= 0.7241 & k_a &:= 0.02699 \text{W} \cdot \text{m}^{-1} \cdot \text{K}^{-1} & \nu &:= 1.75 \cdot 10^{-5} \text{m}^2 \cdot \text{s}^{-1} \\
Re &:= V \cdot l \cdot \nu^{-1} & Nu &:= 0.664 \cdot Re^{0.5} \cdot Pr^{0.33} & h &:= Nu \cdot k_a \cdot l^{-1} \\
Re &= 1142.857 & Nu &= 20.179 & h &= 13.616 \text{W} \cdot \text{m}^{-2} \cdot \text{K}^{-1}
\end{aligned}$$

$$a := \sqrt{\frac{h \cdot p}{k \cdot A_c}} \quad Q_{\text{fin}} := \sqrt{h \cdot p \cdot k \cdot A_c} \cdot (T_{b\_avg} - T_{\text{inf}}) \cdot \tanh(a \cdot L_c)$$

$$Q_{\text{fin,max}} := h \cdot A_{\text{fin}} \cdot (T_{b\_avg} - T_{\text{inf}}) \quad Q_{\text{no.fin}} := h \cdot A_b \cdot (T_{b\_avg} - T_{\text{inf}})$$

$$Q_{\text{n.fin}} := n \cdot \sqrt{h \cdot p \cdot k \cdot A_c} \cdot (T_{b\_avg} - T_{\text{inf}}) \cdot \tanh\left[a \cdot \left(1 + \frac{t}{2}\right)\right]$$

$$Q_{\text{unfin}} := h \cdot A_{\text{unfin}} \cdot (T_{b\_avg} - T_{\text{inf}}) \quad Q_{\text{total}} := Q_{\text{n.fin}} + Q_{\text{unfin}}$$

$$\eta_{\text{fin}} := \frac{Q_{\text{fin}}}{Q_{\text{fin,max}}} \quad \varepsilon_{\text{fin}} := \frac{Q_{\text{fin}}}{Q_{\text{no.fin}}} \quad \varepsilon_{\text{overall}} := \frac{Q_{\text{total}}}{Q_{\text{no.fin}}}$$

$$Q_{\text{fin}} = 0.307 \text{W} \quad Q_{\text{n.fin}} = 24.443 \text{W} \quad Q_{\text{unfin}} = 0.024 \text{W}$$

$$\boxed{Q_{\text{total}} = 24.467 \text{W}}$$

$$\boxed{\eta_{\text{fin}} = 0.926}$$

$$\boxed{\varepsilon_{\text{overall}} = 25.51}$$

	NO FAN		WITH FAN	
	Al	CF	AL	CF
<b>Heat Loss (W)</b>	17.6	29.5	29.1	24.5
<b>Fin Efficiency</b>	98.7	95.5	95.8	92.6
<b>Heat Sink Effectiveness</b>	26.7	26.3	26.4	25.5

*Table 6.2.b.1: Summary of Results for Experiment 1*

	NO FAN	
	Al	CF
<b>Heat Loss (W)</b>	21.5	20.6
<b>Fin Efficiency</b>	98.3	94.3
<b>Heat Sink Effectiveness</b>	27.2	26.0

*Table 6.2.b.2: Expected Results for Experiment 1*

### Discussion

Steady heat generation from the processor does not occur immediately. For this reason, sufficient time is allotted after the beginning the application to ensure that steady state is achieved. Plotting graphs of temperature with respect to time is helpful in determining when steady state has been reached. From this, an average temperature was calculated for each thermocouple in steady state.

It was originally intended for this experiment to be carried out without the use of a fan. However, temperatures over 80 degrees Celsius were reached. This is unacceptable for the uses to which the heat sink will later be put. As a result, it was decided that the experiment would be repeated with the use of a fan. For this reason, expected values for heat loss, fin efficiency and heat sink effectiveness were not calculated for aluminum and carbon foam heat sinks aided by a fan.

The experimental results corresponded well to the expected results, with the exception of heat loss by the carbon foam heat sink. It was anticipated that the aluminum heat sink would remove heat from the processor at a higher rate than the carbon foam heat sink (see Appendix B.1 for calculation details). These results were expected because heat removal from finned heat sinks was thought to occur chiefly by conduction. Aluminum exhibits a higher thermal conductivity than carbon foam. It was therefore expected that

the Aluminum heat sink would yield higher values for heat lost per fin and total heat lost by, as well as for fin efficiency and effectiveness of the heat sink. This trend holds true for values of fin efficiency and heat sink effectiveness. However, theoretical calculations assumed carbon foam to be a solid. In actuality, it is porous, and heat is transferred through the foam by conduction as well as convection within the pores. The actual heat loss therefore was greater than the expected heat loss, surpassing even that of the aluminum heat sink.

The addition of a fan resulted in increased airflow around the heat sink. Calculations were modified to account for this additional forced convection. The convective heat transfer coefficient is increased, and this new value is calculated based on the velocity of the airflow caused by the fan. Effectiveness ( $\epsilon$ ) and heat transfer coefficient ( $h$ ) have an inverse relationship. Consequently, as the coefficient increases, effectiveness is decreased. This is evident with both the aluminum and carbon foam heat sinks. The amount by which effectiveness decreases, however, is negligible (1.5% for Aluminum and 3% for Carbon Foam). Upon the addition of the cooling element (fan), efficiency, like effectiveness, is expected to decrease. This is validated by the data obtained.

Effectiveness increases as thermal conductivity increases. Therefore, the anticipated effectiveness of the Aluminum heat sink is always greater than that of the Carbon Foam replica. This is supported by the data in Table 6.2.b.2.

Overall, the greatest amount of heat was removed by the Carbon Foam heat sink without the use of a fan. The efficiency and effectiveness for this prototype was surpassed by the Aluminum heat sink (without a fan). However, the determining factor of this heat sink is its capacity for heat removal. This is the most important feature for the applications to which the heat sink can be put. As such, the Carbon Foam heat sink (without a fan) gave the best performance. This concurs with the performance specifications, which required a passive system.

### Conclusion

Contrary to the expected results, the Carbon Foam heat sink showed a better overall performance than its Aluminum counterpart. Although the thermal conductivity of Aluminum is greater than that of carbon foam, the porous nature of the foam allowed for heat to be transferred not only by conduction, but also by convection.

The Aluminum heat sink had the following values. The total heat loss was found to be 18 W. The fin efficiency was calculated to be 99%, while the effectiveness of the heat sink was approximately 27. The Carbon Foam heat sink had the following values. The total heat loss was found to be 30 W. The fin efficiency was calculated to be 96%, while the effectiveness of the heat sink was approximately 26.

The numbers above demonstrate that the Carbon Foam heat sink showed better performance, removing almost twice as much heat as the Aluminum heat sink. The effect of the lesser value of the thermal conductivity of carbon foam was outweighed by the effect of convection due to its porous nature. In addition, Carbon Foam is significantly lighter than Aluminum. Therefore, it can be said that the Carbon Foam heat sink demonstrated a heat removal rate higher than that of the Aluminum heat sink, with the additional benefit of reduced system mass.

# **Thermal Management**

---

---

## *Chapter Seven*

### *Experiment 2:*

### *Flow Injection System*

## **Chapter 7.1 Theoretical Design**

### Introduction

Prototype I allowed the evaluation of carbon foam vs. aluminum as a heat transfer material. Now, the design will be taken one step further by coming up with an innovative design to see if it will be able to remove even more heat.

Prototype II will make use of the carbon foam as a cylindrical piece with a flow injection tube in the middle, which will be used to take advantage of the high porosity of carbon foam. The air flowing into the flow injection tube will be a simulation of outside air of an aircraft flying at an altitude of 40,000ft. A compressed air tank will be used to pressurize the air. The mode of heat transfer for this design is conduction from the processor to the carbon foam and convection from the carbon foam to the ambient air. Heat transfer by convection is directly proportional to the surface area, which will take advantage of the high porosity of the carbon foam.

Once the cylindrical carbon foam heat sink has been machined, it will be mounted onto a AMD Athlon 64 3500 processor chip. Because of the porous nature of carbon foam, it is likely that a thermally conductive paste will be necessary to attach the heat sink to the processor. The processor with the attached heat sink will then be installed into a barebone computer from Tiger Direct (Item Number P459-1236C). Applications will be run on the computer to cause a constant heat generation in the processor. Theoretically, the heat sink will dissipate heat from the processor due to the mass flow rate of the air coming from the air tank. Thermocouples mounted at various locations on the heat sink will be used to determine the temperatures at those locations, from which heat loss can be calculated.

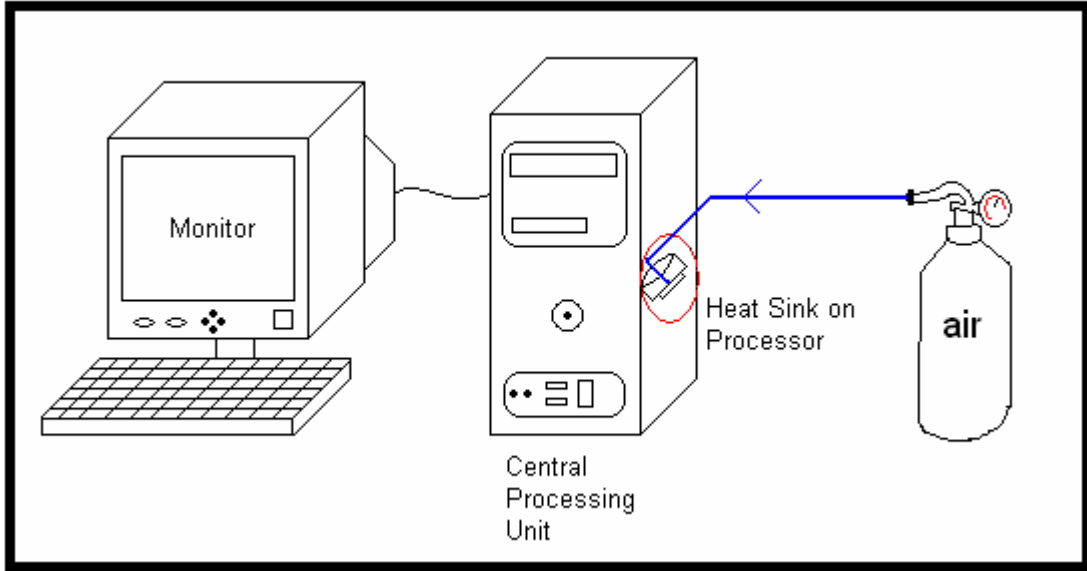


Figure 7.1.1: System Diagram

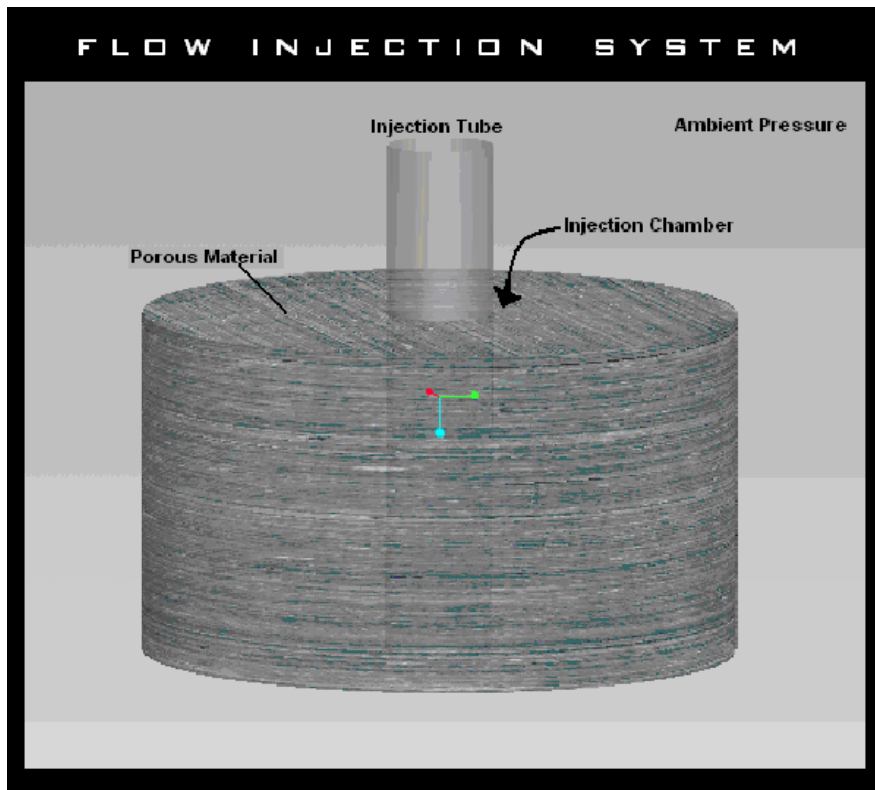
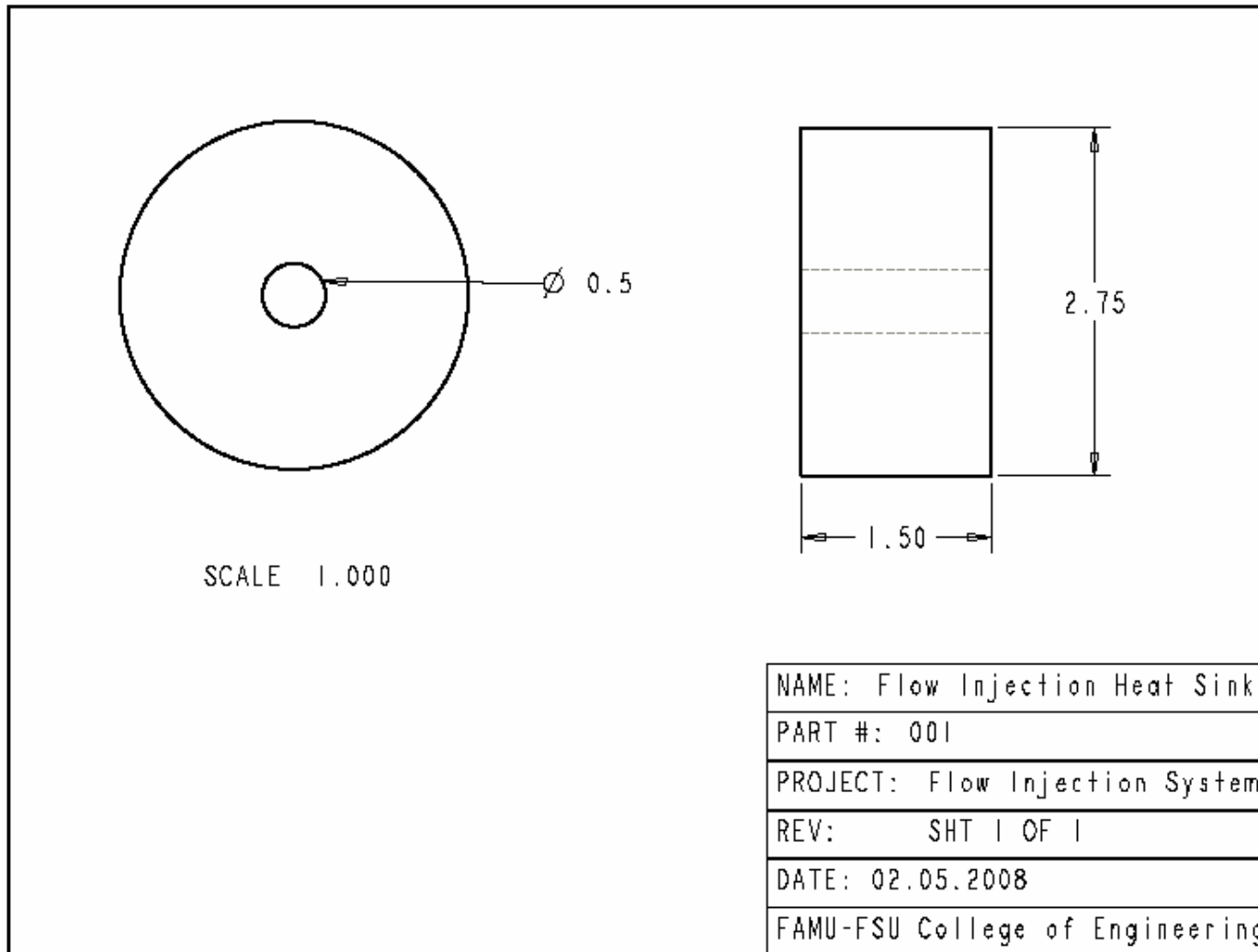
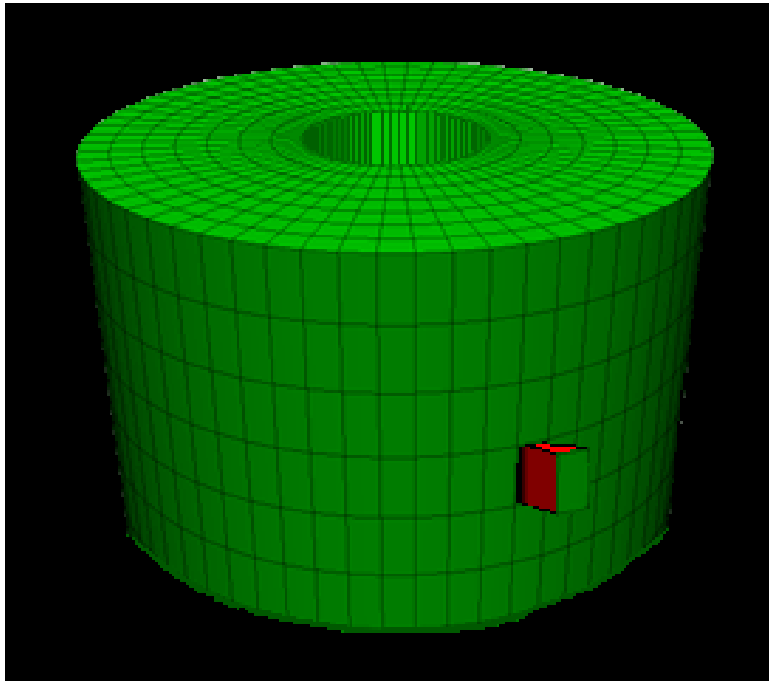


Figure 7.1.2: Carbon Foam Cylinder Model



*Figure 7.1.3: Part Drawing of Carbon Foam Cylinder*

Analysis



*Figure 7.1.4*

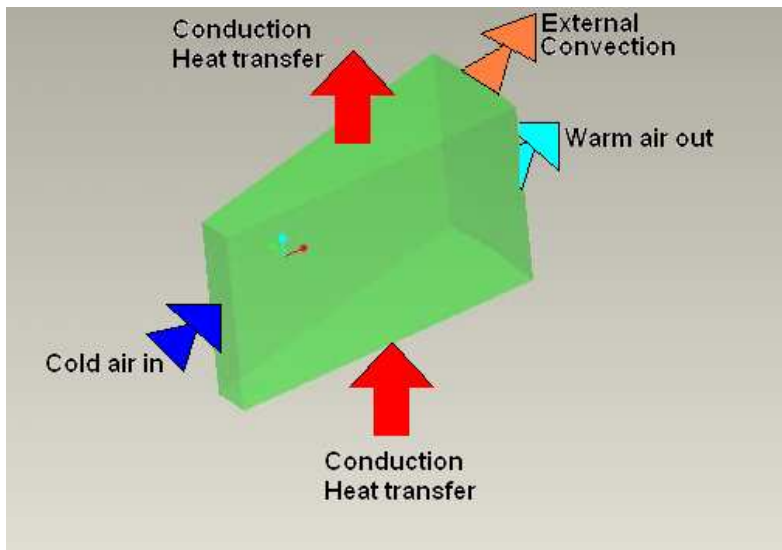


*Figure 7.1.5*

Analyzing a system of such characteristics can prove complex, given that no equations for the heat transfer of devices of similar properties exist.

For this analysis, the fundamental laws of heat transfer were used in conjunction with assumptions for values that will be measured during the latter phase of this project. An equation relating the heat transfer as a function of initial conditions (air inlet pressure, air inlet temperature and contact surface temperature) was obtained. The efficiency and effectiveness were also calculated. A detailed description of these calculations can be found in Appendix B.2. The table below summarizes the findings from the calculations. Graphs of the heat transfer as a function of initial conditions are provided, in addition to supporting mathematical expressions.

<b>Base Temperature (K)</b>	<b>Inlet Temperature (K)</b>	<b>Inlet Pressure (psi)</b>	<b>Heat Dissipation (W)</b>	<b>Efficiency (%)</b>
343	295	21.5	89	89

*Table 7.1.1: Theoretical Values for Prototype II*

The flow through a porous material can be characterized by using the Darcy's law of permeability. It is possible to obtain the pressure difference necessary to create a desired flow rate through the material.

$$V_{fr} = \frac{\kappa \cdot A_{ave} \cdot (P_{in} - P_{out})}{\mu \cdot (R_{tot} - R_{tube})}$$

A Reynolds number is also available for porous media.

$$Re_{porous}(P_{in}) = \frac{V_{fr}(P_{in}) \cdot \rho \cdot d_{pore}}{\mu \cdot A_{ave} \cdot \phi}$$

The Nusselt Number selected for this heat transfer analysis depends on inlet pressure since the Reynolds number term is expressed as a function of this pressure.

$$Nu = 0.037Re(P_{in})^{0.8} Pr^{\frac{1}{3}}$$

By obtaining this Nusselt number expression, it was possible to determine the convective coefficient for this form of heat transfer as a function of inlet pressure.

$$Nu(P_{in}) = \frac{h \cdot L_c}{K_{air}}$$

Solving for the convective coefficient gives:

$$h(P_{in}) := \left( \frac{K_{air}}{L_c} \right) \cdot \left[ 0.037 \left[ \frac{\kappa \cdot A_{ave} \cdot |P_{in} - P_{out}| \cdot \rho \cdot d_{pore}}{\mu \cdot (R_{total} - R_{tube})} \right]^{0.8} \cdot Pr^{\frac{1}{3}} \right]$$

With this expression, the modeling of heat transfer through a fin may be used to model heat transfer through our flow injection system if properly altered to account for the parameters that change due to the special properties of this particular material. The fin equation is therefore altered to account for internal surface area of the carbon foam heat exchanger.

$$Q_{conv} = h \cdot A_s \cdot (T - T_{inf})$$

$$Q = \sqrt{h \cdot \psi \cdot k_{foam} \cdot A_c} (T_{z0} - T_{flow\_in}) \cdot \tanh(\beta \cdot 4 \cdot h_{layer})$$

Q	Total heat lost	h	Convective coefficient
k <sub>foam</sub>	Thermal Conductivity	A <sub>c</sub>	Cross-sectional area of part
T <sub>z0</sub>	Base Temperature	T <sub>flow_in</sub>	Temperature of cooling fluid
h <sub>layer</sub>	Length of heat exchanger	ψ	Rate of change of surface area with displacement

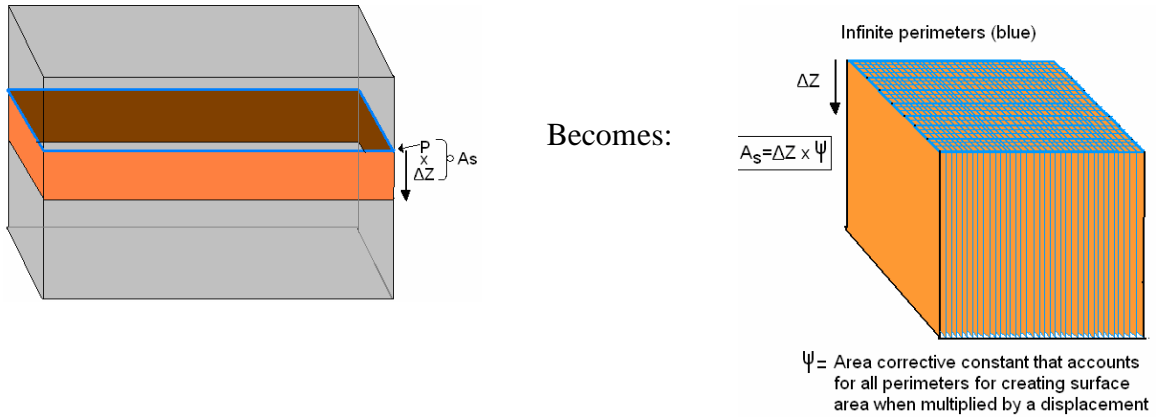
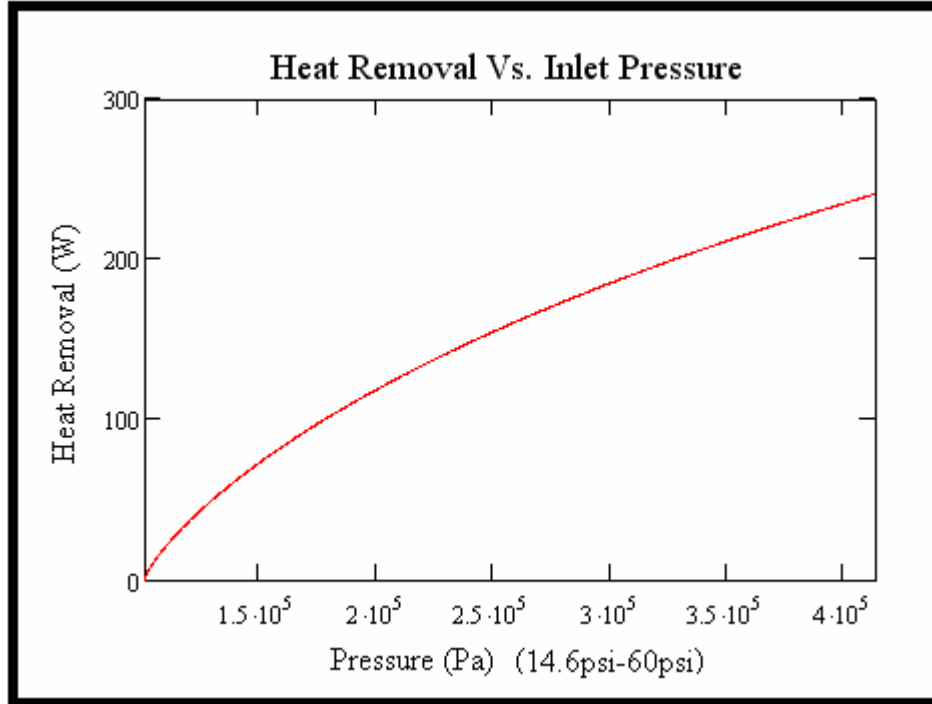


Figure 7.1.6

Heat dissipation as a function of inlet pressure:

$$Q(P_{in}) = \sqrt{h(P_{in}) \cdot \Psi \cdot k_{foam} \cdot A_c} (T_{z0} - T_{flow\_in}) \cdot \tanh(\beta(P_{in}) \cdot 4 \cdot h_{layer})$$

$$\beta = \frac{\left( \frac{K_{air}}{L_c} \right) \cdot 0.037 \cdot \left[ \frac{\kappa \cdot A_{ave} \cdot (P_{in} - P_{out})}{\mu \cdot (R_{total} - R_{tube})} \cdot \rho \cdot d_{pore} \right]^{0.8} \cdot \frac{1}{Pr^3} \cdot \Psi}{k_{foam} \cdot A_c}$$



*Figure 7.1.7: Graph of Heat Removal vs. Inlet Pressure*

Most of the parameters used in this analysis were calculated in Chapter 2.2. However, it was necessary to make some assumptions. A strong effort was made to assume reasonable values for these initial calculations. The results obtained imply that the heat transfer is greatly enhanced by the implementation of the device. However, although the heat transfer appears to have been an improvement over Prototype I, the efficiency has been decreased. This decrease is not excessively large, and the trade-off in terms of increased heat transfer makes Prototype II a viable option.

## **Chapter 7.2a: Machining Procedures**

The carbon foam cylinder was machined with an OMAX JetMachining Center (See Figure 7.2.1). The appropriate cuts are made using a stream of high-speed water mixed with titanium abrasive. The machine allows the parts to be manufactured based on a CAD drawing input by the user. For this part, the dimensioning included the inner and outer diameters, as well as the cylinder height. This method was selected because water jet cutting does not cause dust to be released into the air. Typical machining methods cause a large amount of dust to be released, and an accumulation of this dust in the lungs over a prolonged duration can lead to respiratory disease. There is also weak evidence to suggest that prolonged exposure to carbon dust may be related to lung cancer. One typical problem with water jet cutting is that the pressure of the water stream may decrease between the top and bottom of the part, resulting in a slight difference between the sizes of the top and bottom surfaces. However, this difference is negligible, and will not affect the performance of the carbon foam flow injection system.



*Figure 7.2.1: OMAX JetMachining Center*

## Chapter 7.2b: Experiment

### Objective

To investigate the performance of a carbon-foam based Fluid Injection Heat Removal System

### Theoretical Background

Air is run via a tube through the center of a cylindrical carbon foam heat sink. Holes in the tube allow air to be forced through the porous foam. Heat travels from the electronic component upwards through the heat sink, towards the pores by conduction. Forcing air through the pores causes this heat to be carried away by convection.

### Equipment

*Heat Sink:* A cylindrical heat sink with sufficient room for a tube to be run through its center will be machined from carbon foam. (See Chapter 7.2.a for machining procedures)

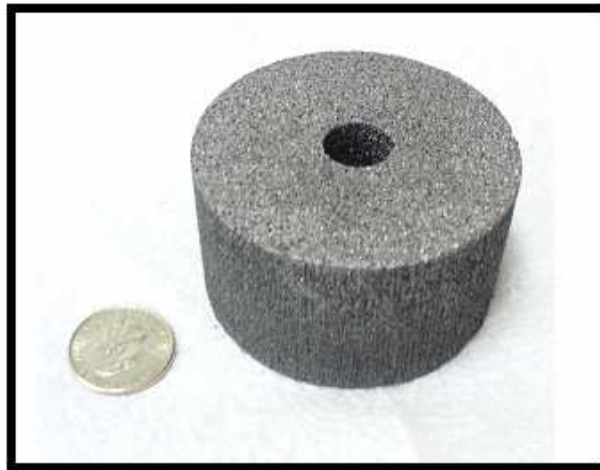


*Figure 7.2.b.1: Carbon Foam Cylindrical Heat Sink*

*Thermocouples:* Four type J thermocouples were used at various locations. These thermocouples were manufactured from thermocouple wire.



*Figure 7.2.b.2: Thermocouple Wire*



*Figure 7.2.b.3: Thermocouples*

*Data Acquisition System:* The portable USB Data acquisition system NI USB-9211A consists of several components. The system can be used to collect data from four channels of 24-bit thermocouple input. This data will be processed using LabVIEW SignalExpress data-logger software.



*Figure 7.2.b.4: Data Acquisition System*

*Computer System:* The computer system consists of a barebone kit obtained from Tiger Direct (Item Number P459-1236C), hard drive (4 GB), CD-Rom Drive, monitor, keyboard and mouse. The processor with attached heat sink will be installed into the barebone component of the system. This will be set to run applications identical to those used in the preceding experiment, while temperature measurements are taken.



*Figure 7.2.b.5: Computer System*

*Processor Chip:* A AMD Athlon 64 3500 chip will be used to generate heat at a constant rate by running an application. The carbon foam cylinder will be attached to the processor chip by means of a thermally conductive past if necessary



*Figure 7.2.b.6: AMD Athlon 64 3500 Processor Chip*

*Application Software:* The ideal application causes heat to be generated at a constant rate by the processor chip. Additionally, the amount of heat generated per unit time should be high enough to provide a challenging test for the heat sinks. The application should operate for an adequate time period with little to no human input. For these reasons, it was decided that the Norton Virus Scan Version 7.0 will be used as the application software for the generation of a large, constant heat flux.

*Compressed Air Tank:* For this experiment, the air originating outside the airplane will be simulated by using a compressed air tank, which forces air through the system at the same rate as would occur for an airplane during flight.



*Figure 7.2.b.9: Compressed Air Tank*

Experimental Setup

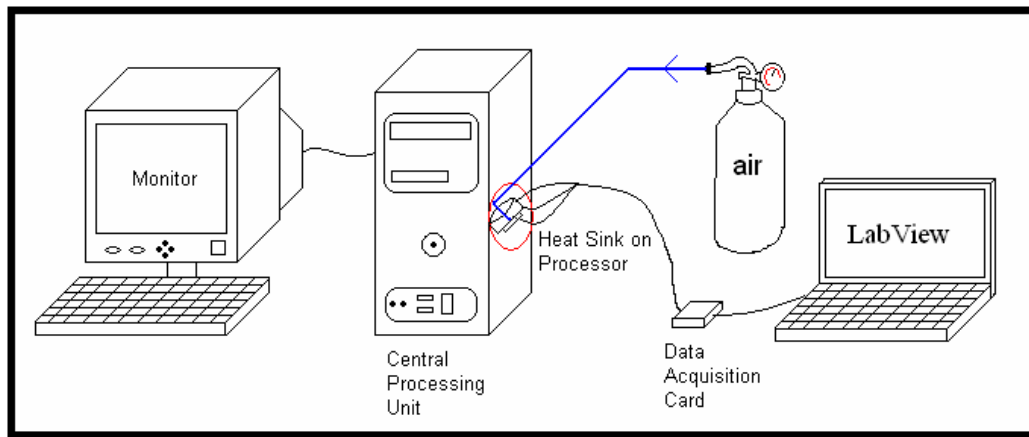


*Figure 7.2.b.8: Experimental Setup*



*Figure 7.2.b.9: Heat Sink on Processor*

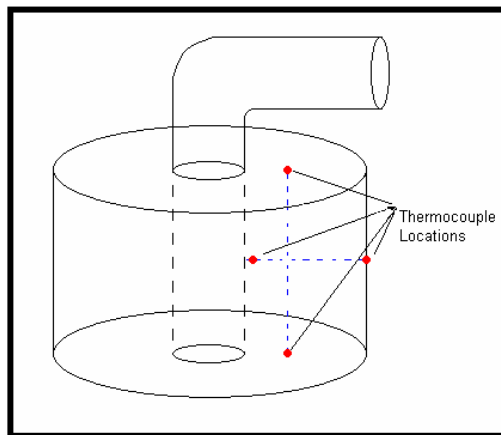


*Figure 7.2.b.10: Schematic of Thermocouple Placement within Heat Sink*

## **Procedure**

### Preparation

#### 5. Manufacture of Thermocouples

- a. Four sections of thermocouple wire were cut.
- b. Both ends of all four sections were stripped of all insulation
- c. For each thermocouple, the two wires protruding from one end were soldered together.

- d. The wires protruding from the other end of the thermocouple were connected to the data acquisition system.
6. Thermocouple Calibration
    - i. Water was brought to a boil using a hot plate
    - j. An ice bath was created by filling a styrofoam cup with ice blocks.
    - k. The four thermocouples were connected to the data acquisition system, which was in turn connected to a laptop computer via a USB cable.
    - l. The LabVIEW SignalExpress program was started on the laptop.
    - m. At the prompt, one thermocouple was immersed in the ice bath. The temperature registered by the thermocouple was recorded using LabView.
    - n. The same thermocouple was then immersed in boiling water the temperature registered by the thermocouple was again recorded.
    - o. The software was allowed to plot the thermocouple calibration curve.
    - p. Steps a-g were repeated for the remaining thermocouples.
  7. Computer System Assembly
    - a. The barebone kit was put together and the processor was fixed in place.
    - b. With an aluminum heat sink and fan in place (so as to prevent overheating), the hard drive and CD-Rom drive were installed.
  8. Norton Antivirus 7.0 was installed, again using the aluminum heat sink and fan.

## Methodology

13. The thermocouples were positioned along the carbon foam cylindrical heat sink as shown in Figure 6.2.b.10.
14. The heat sink was secured to processor chip using the thermally conductive paste.
15. The thermocouples were connected to the Data Acquisition System.
16. The Data Acquisition System was turned on and LabVIEW SignalExpress started.
17. The computer was turned on and allowed to boot up.
18. Norton Virus Scan 7.0 was started, and LabVIEW was set to record the temperatures measured by the thermocouples.
19. The virus scan was run for approximately five minutes in order to ensure steady state heat generation in the processor chip was achieved.

20. Norton Virus Scan 7.0 was exited.

21. Data Acquisition System was stopped.

### Analysis

It was concluded that the flow injection system is an excellent alternative when the necessity of cooling high thermal output devices arises.

The theoretical calculation of heat transfer as a function of inlet pressure was determined to follow the following trend:

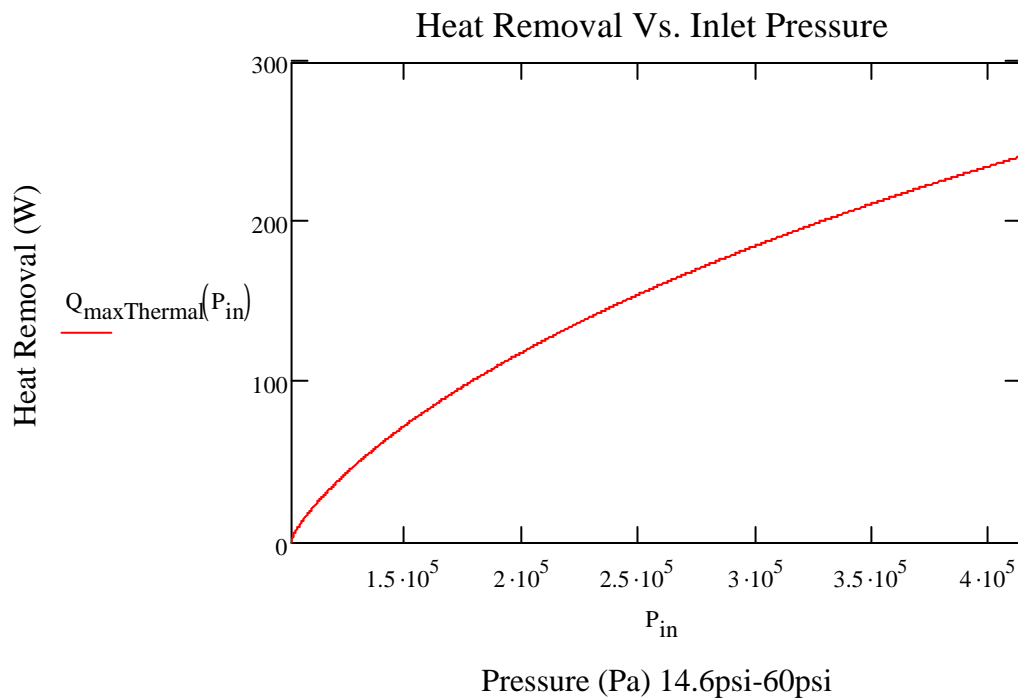


*Figure 7.2.b.11: Graph of Heat Removal vs. Inlet Pressure*

This will be limited by two parameters:

- 1) Size of the heat exchanger
- 2) Strength of carbon foam to hold high pressure.

Initial calculations indicated that the flow injection system was capable of removing the maximum heat output of 89W at the maximum operating temperature of 70C if held at 21.5psi.

After numerous experimental runs, it was determined, that the heat output of this particular processor was on average 68.3W, and the operating temperature was maintained at an average value of 59C when the flow injection system was fed with 21.5psi of air.

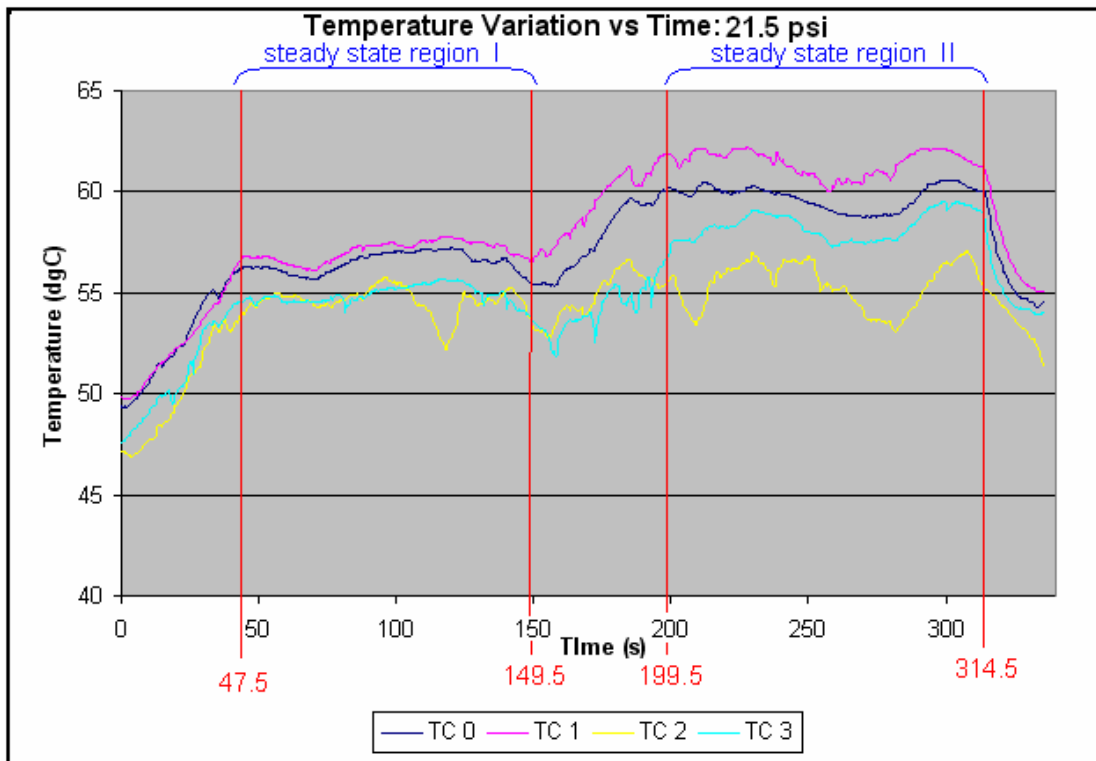


Figure 7.2.b.12: Temperature Variation vs. Time

Actual/Ideal	Heat Dissipation	Maximum Operating Temp	Inlet Pressure
Calculated	89W	70C	21.5 psi
Experimental	68.6W	59C	21.5 psi
Error	22%	15.7%	

Table 7.2.b.1: Calculated Values

The expected operating temperature of the electronic component as a function of inlet pressure is as follows:

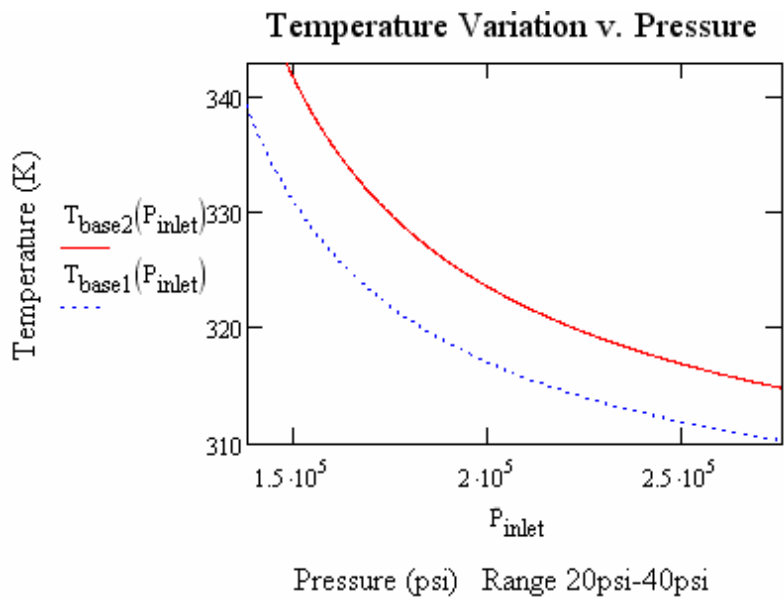


Figure 7.2.b.13: Temperature Variation vs. Pressure

If one wishes to find the pressure necessary for a given operating temperature, the following equation can be used:

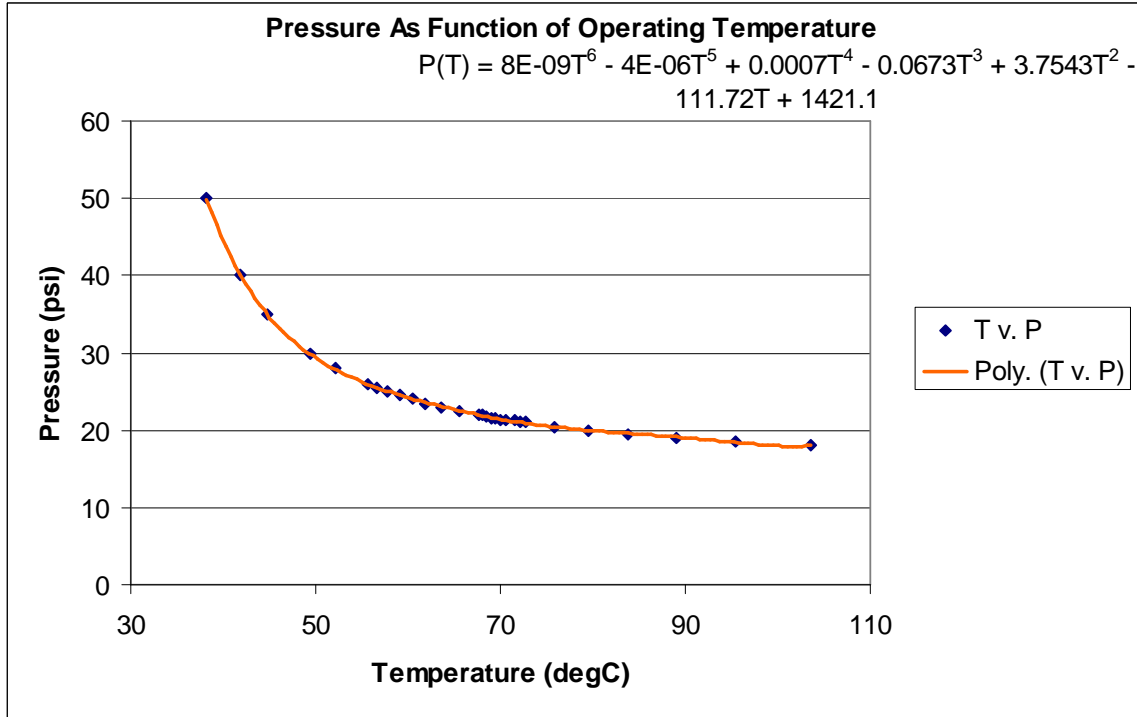


Figure 7.2.b.14: Pressure as a Function of Operating Temperature

A comparison between the temperature variation as a function of distance for the actual profile vs. the ideal profile follows:

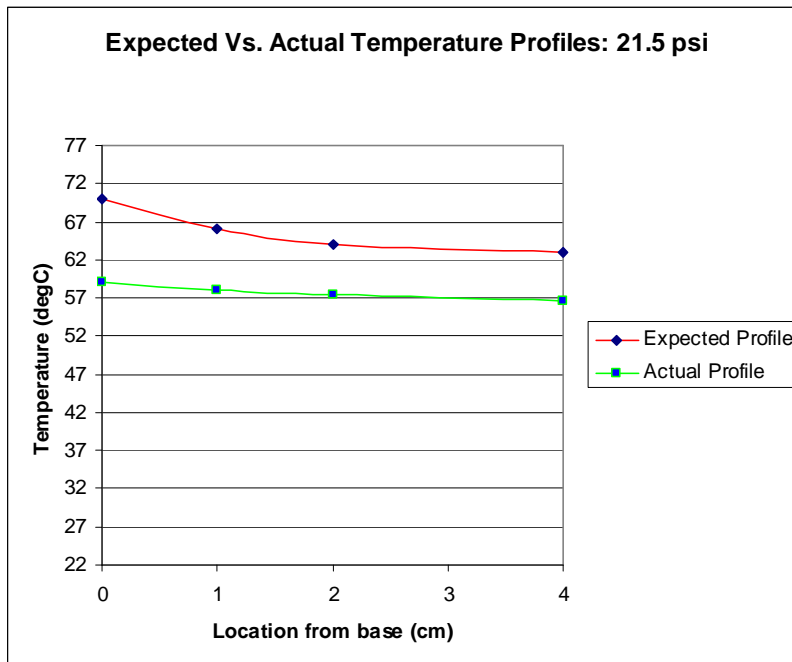


Figure 7.2.b.15: Expected and Actual Temperature Profiles

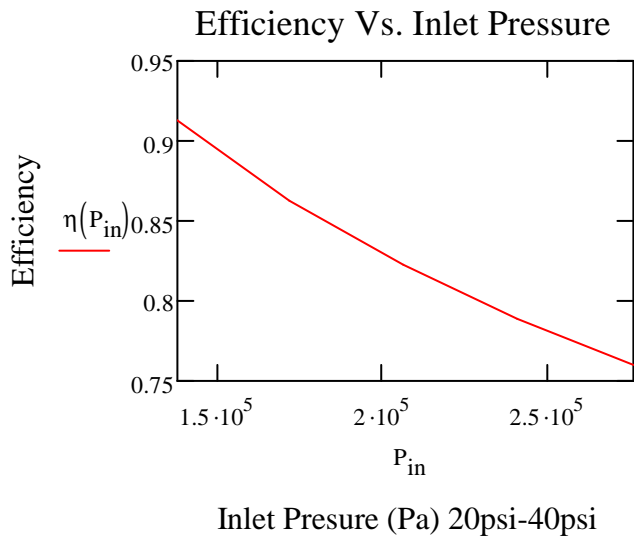
Location	T_ideal	T_actual	% Difference
0	70	59	15.7
1	66	58	12.1
2	64	57.4	10.3
4	63	56.6	10.1
			12.0

Average

Table 7.2.b.2

This plot indicates that the average temperature in the interior of the carbon foam heat exchanger matches within 12% the expected temperature profile.

Because with varying inlet pressure, the velocity of the air flowing inside the part, and hence the convective coefficient varies. It was therefore that efficiency decreases inversely proportional to pressure in a trend that follows:



The analysis clearly indicates that the flow injection system is a high performance heat dissipation alternative for high heat output electrical devices.

### Discussion

It is expected that the heat lost by the fluid injection system will be greater than that lost by the finned heat sinks from the previous experiment. The reasoning behind this is as follows. The fluid injection system allows the processor chip to be cooled by two modes of heat transfer, conduction and convection. Heat is transferred upward through the heat sink by conduction. The heat is transferred to the air traveling through the pores of the carbon foam. This occurs by convection and makes use of the large internal surface area of the foam. Once the heat has been transferred to the moving air, it travels from within the pores to the outside of the heat sink as the air is forced through the foam.

### Conclusion

It was concluded that the flow injection system is an excellent alternative when the necessity of cooling high thermal output devices arises.

# **Thermal Management**

---

---

## *Appendices*

## **Appendix B.1: Analysis of Experiment 1**

Assumptions:

5. Steady state conditions apply to the system
6. Fin geometry has constant cross section
7. Material has constant thermal conductivity
8. Heat is lost from fin tip by convection

Thermodynamic Analysis was carried out based on the following:

5. Conservation of Energy Principle: Energy can neither be created nor destroyed; it can only change forms. This law provides a sound basis for studying the relationships among various forms of energy and energy interactions.
6. First law of Thermodynamics: For all adiabatic processes between two specified states of a closed system, the net work done is the same regardless of the nature of the closed system and the details of the process. This is based on the conservation of energy principle.
7. Energy Balance: The net change (increase or decrease) in the total energy of the system during a process is equal to the difference between the total energy entering and the total energy leaving the system during that process. This balance is a result of the two preceding laws.
8. Fourier's Law of Heat Conduction: The rate of heat conduction through a plane layer is proportional to the temperature difference across the layer and the heat transfer area, but is inversely proportional to the thickness of the layer.

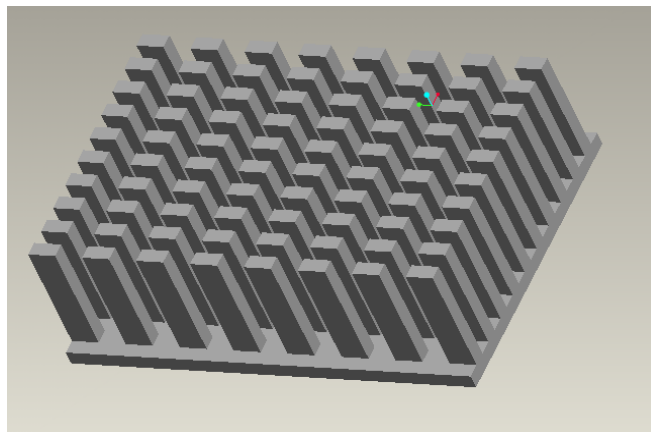


*Figure B.1.1: Model of Finned Heat Sink*

First Law of Thermodynamics:

$$\dot{Q} - \dot{W} + \sum_{in} (\dot{m} \cdot \theta) - \sum_{out} (\dot{m} \cdot \theta) = 0$$

This simplifies to:

$$Q_{in} = Q_{out}$$

$$Q_{cond\_x} = Q_{cond\_x\Delta x} + Q_{conv}$$

where

$$Q_{conv} = h(p\Delta x)(T - T_{inf})$$

Substituting and dividing by  $\Delta x$  gives:

$$\frac{Q_{cond\_x\Delta x} - Q_{cond\_x}}{\Delta x} + h \cdot p \cdot (T - T_{inf}) = 0$$

Taking the limit as  $\Delta x$  approaches 0

$$\frac{d}{dx} Q_{cond} + h \cdot p \cdot (T - T_{inf}) = 0 \quad \text{Eq. 1}$$

Fourier's Law of Heat Conduction:

$$Q_{cond} = -k \cdot A_c \cdot \frac{dT}{dx} \quad \text{Eq. 2}$$

Substitution of Eq. 2 into Eq. 1 yields:

$$\frac{d}{dx} \left( k \cdot A_c \cdot \frac{dT}{dx} \right) - h \cdot p \cdot (T - T_{inf}) = 0 \quad \text{Eq. 3}$$

For the case of constant cross section and constant thermal conductivity; Eq. 3 becomes

$$\frac{d^2}{dx^2} (\theta) - a^2 \cdot \theta = 0 \quad \text{Eq. 4}$$

where

$$a^2 = \frac{h \cdot p}{k \cdot A_c} \quad \theta = T - T_{inf}$$

Eq. 4 is a linear, homogeneous, second-order differential equation whose general solution

$$\theta(x) = C_1 \cdot e^{a \cdot x} + C_2 \cdot e^{-a \cdot x}$$

The boundary condition at the fin base is:

$$\theta(0) = \theta_b = T_b - T_{inf}$$

For the case of negligible heat loss from the fin tip, the boundary condition at the fin tip is

$$\text{For } x = L \quad \frac{d\theta}{dx} = 0$$

Applying boundary conditions to Eq. 4 yields the following relation for temperature distri

$$\frac{T(x) - T_{inf}}{T_b - T_{inf}} = \frac{\cosh(a(L - x))}{\cosh(a \cdot L)} \quad \text{Adiabatic Fin Tip}$$

Applying Fourier's Law of Heat Conduction yields:

$$Q_{\text{adiabatic\_tip}} = \sqrt{h \cdot p \cdot k \cdot A_c} \cdot (T_b - T_{inf}) \cdot \tanh(aL)$$

Heat loss from the tip is accounted for by using a corrected fin length

$$L_c = L + \frac{A_c}{p}$$

For a rectangular fin configuration, the corrected fin length is:

$$L_{c\_rect} = L + \frac{t}{2}$$

Thus, the rate of heat loss from a rectangular fin taking into consideration convection at fi

$$Q = \sqrt{h \cdot p \cdot k \cdot A_c} \cdot (T_b - T_{inf}) \cdot \tanh \left[ a \cdot \left( L + \frac{t}{2} \right) \right] \quad \text{Eq. 5}$$

**For Aluminum:**

$$\begin{aligned} L &:= 0.04 & W &:= 0.0075 & t &:= 0.005 & n &:= 78 \\ h &:= 8 & k &:= 237 & T_b &:= 333 & T_{inf} &:= 300 \\ A_c &:= W \cdot t & p &:= 2(W + t) & L_c &:= L + \frac{A_c}{p} & a &:= \sqrt{\frac{h \cdot p}{k \cdot A_c}} \\ H &:= 0.04 & B &:= 0.075 & A_b &:= H \cdot B \\ A_{fin} &:= 2(L \cdot W + L \cdot t) + W \cdot t & A_{unfin} &:= A_b - n \cdot A_c \end{aligned}$$

$$Q_{fin} := \sqrt{h \cdot p \cdot k \cdot A_c} \cdot (T_b - T_{inf}) \cdot \tanh(a \cdot L_c)$$

$$Q_{fin,max} := h \cdot A_{fin} \cdot (T_b - T_{inf}) \quad Q_{no,fin} := h \cdot A_b \cdot (T_b - T_{inf})$$

$$Q_{n,fin} := n \cdot \sqrt{h \cdot p \cdot k \cdot A_c} \cdot (T_b - T_{inf}) \cdot \tanh\left[a \cdot \left(L + \frac{t}{2}\right)\right]$$

$$Q_{unfin} := h \cdot A_{unfin} \cdot (T_b - T_{inf})$$

$$Q_{total} := Q_{n,fin} + Q_{unfin}$$

$$\eta_{fin} := \frac{Q_{fin}}{Q_{fin,max}} \quad \varepsilon_{fin} := \frac{Q_{fin}}{Q_{no,fin}} \quad \varepsilon_{overall} := \frac{Q_{total}}{Q_{no,fin}}$$

$$Q_{fin} = 0.27 \quad Q_{n,fin} = 21.587 \quad Q_{unfin} = 0.02$$

$$\varepsilon_{fin} = 0.341 \quad Q_{fin,max} = 0.274$$

$$Q_{total} = 21.607$$

$$\eta_{fin} = 0.987$$

$$\varepsilon_{overall} = 27.282$$

**For Carbon Foam:**

$$\begin{aligned}
 L &:= 0.04 & W &:= 0.0075 & t &:= 0.005 & n &:= 78 \\
 h &:= 8 & k &:= 64 & T_b &:= 333 & T_{inf} &:= 300 \\
 A_c &:= W \cdot t & p &:= 2(W + t) & L_c &:= L + \frac{A_c}{p} & a &:= \sqrt{\frac{h \cdot p}{k \cdot A_c}} \\
 H &:= 0.04 & B &:= 0.075 & A_b &:= H \cdot B \\
 A_{fin} &:= 2(L \cdot W + L \cdot t) + W \cdot t & A_{unfin} &:= A_b - n \cdot A_c
 \end{aligned}$$

$$Q_{fin} := \sqrt{h \cdot p \cdot k \cdot A_c} \cdot (T_b - T_{inf}) \cdot \tanh(a \cdot L_c)$$

$$Q_{fin,max} := h \cdot A_{fin} \cdot (T_b - T_{inf}) \quad Q_{no,fin} := h \cdot A_b \cdot (T_b - T_{inf})$$

$$Q_{n,fin} := n \cdot \sqrt{h \cdot p \cdot k \cdot A_c} \cdot (T_b - T_{inf}) \cdot \tanh\left[a \cdot \left(L + \frac{t}{2}\right)\right]$$

$$Q_{unfin} := h \cdot A_{unfin} \cdot (T_b - T_{inf})$$

$$Q_{total} := Q_{n,fin} + Q_{unfin}$$

$$\eta_{fin} := \frac{Q_{fin}}{Q_{fin,max}} \quad \varepsilon_{fin} := \frac{Q_{fin}}{Q_{no,fin}} \quad \varepsilon_{overall} := \frac{Q_{total}}{Q_{no,fin}}$$

$$Q_{fin} = 0.262 \quad Q_{n,fin} = 20.844 \quad Q_{unfin} = 0.02$$

$$\varepsilon_{fin} = 0.33 \quad Q_{fin,max} = 0.274$$

$$Q_{total} = 20.863$$

$$\eta_{fin} = 0.955$$

$$\varepsilon_{overall} = 26.343$$

The total heat lost from the aluminum heat sink is greater than the total heat lost from the carbon foam heat sink of identical dimensions. This is due to the higher thermal conductivity of aluminum. In addition, the efficiency and effectiveness of the aluminum heat sink exceeds that of the carbon foam heat sink, for the same reason.

From the calculations above, it can be observed that parameters affecting the performance of the fin design are as follows:

Thermal Conductivity (k): Fourier's Law of Heat Conduction states that heat transferred by conduction increases with thermal conductivity. An effective, efficient finned heat sink is made from a material with a high thermal conductivity. The thermal conductivity of carbon foam is less than that of aluminum, hence the decreased heat loss, efficiency and effectiveness.

Geometry: A high perimeter to cross-sectional area ratio ( $p/A_c$ ) increases the effectiveness of the heat sink. For this analysis, the heat sinks are identical. Consequently, geometry does not account for any part of the difference between the calculated values of total heat loss, efficiency and effectiveness for the two heat sinks.

Convection heat transfer coefficient (h): It is not intuitively obvious that there exists an inverse relationship between effectiveness and heat transfer coefficient. The use of fins is more easily justified when heat transfer occurs by natural convection, rather than forced convection. In this case, both heat sinks are being cooled by natural convection.

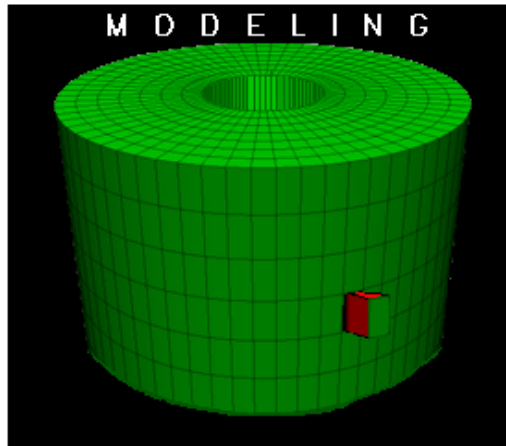
## Appendix B.2: Analysis of Experiment 2

### Assumptions used:

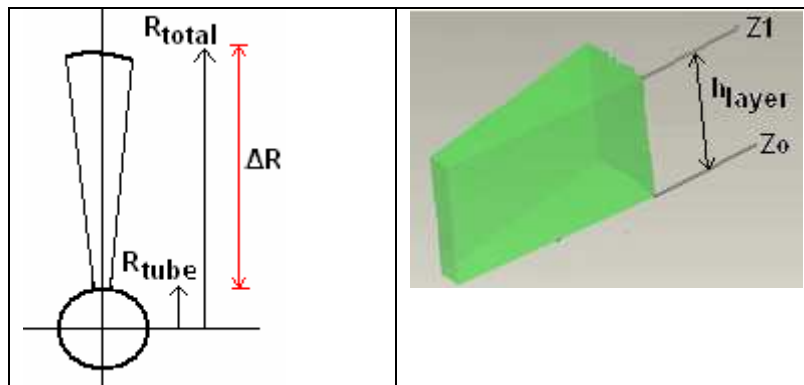
- Properties are uniform throughout the material
- Material features are uniform throughout the material
- Steady state heat conduction

### Models used:

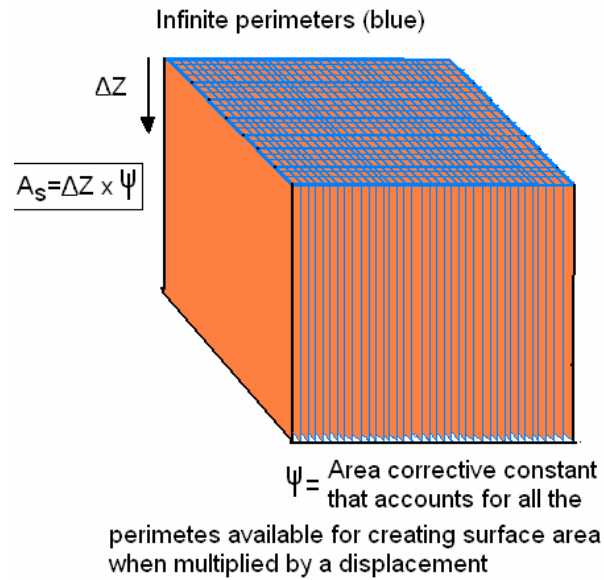
The initial model was broken into peaces in order to facilitate modeling. The heat transfer from each one of these peaces was considered, and summed to obtain the total heat transfer of the heat sink.



Integral sections were selected for the heat transfer modeling process:



A modification to the solid fin heat transfer equation had to be made to account for the increased surface area inside of the porous foam:



The above models were used to aid in the modeling of the heat transfer for the flow injection system.

#### Laws and Principles:

- Law of conservation of energy
- Fourier law of heat conduction:

$$Q = -kA \cdot \frac{dT}{dx}$$

- Law of convective heat transfer:

$$Q = h \cdot A (T_s - T_{inf})$$

#### Derivations:

Heat is to be transferred into the part by conduction from an electronic device, and dissipated by convection making use of its porous nature and high surface area to increase heat dissipation capabilities.

It was determined that the flow through a porous material could be characterized by using the Darcy's law of permeability, and that it is possible to obtain the pressure difference necessary to create a desired flow rate through the material.

$$V_{fr} = \frac{\kappa \cdot A_{ave} \cdot (P_{in} - P_{out})}{\mu \cdot (R_{tot} - R_{tube})}$$

It was also determined that a Reynolds number characteristic of porous media was also available, and that the volumetric flow rate as a function of pressure was part of this expression.

$$\text{Re}_{\text{porous}}(P_{\text{in}}) = \frac{V_{\text{fr}}(P_{\text{in}}) \cdot \rho \cdot d_{\text{pore}}}{\mu \cdot A_{\text{ave}} \cdot \phi}$$

The Nusselt Number Selected for this heat transfer analysis was also as a function of inlet pressure given that the Reynolds number term in it is expressed as a function of inlet pressure.

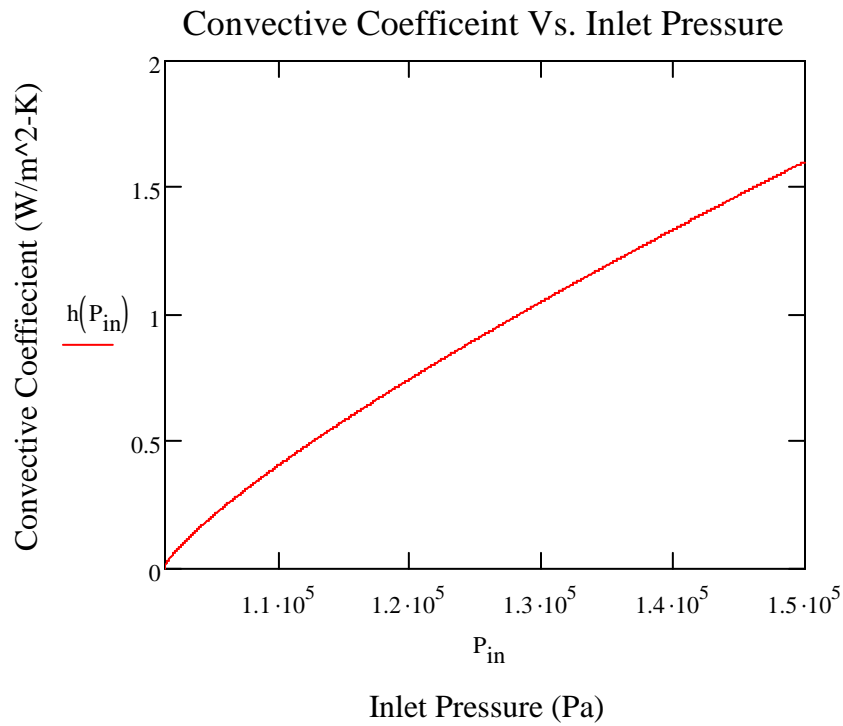
$$\text{Nu} = 0.037 \text{Re}(P_{\text{in}})^{0.8} \text{Pr}^{\frac{1}{3}}$$

By obtaining this Nusselt number expression, it was possible to determine the convective coefficient characteristic of this form of heat transfer, also as a function of inlet pressure.

$$\text{Nu}(P_{\text{in}}) = \frac{h \cdot L_c}{K_{\text{air}}}$$

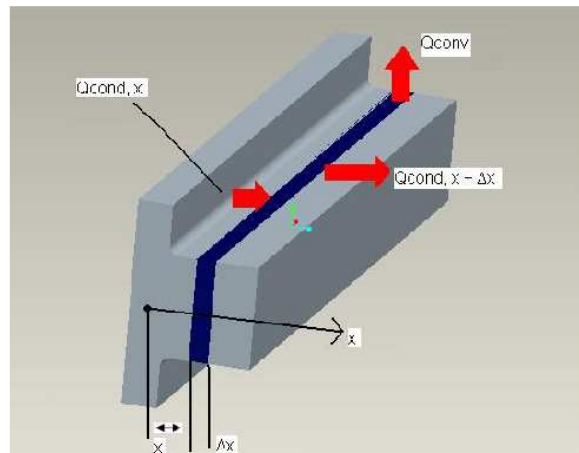
Solving for the convective coefficient, and expanding this equation, gives:

$$h_{\text{m}}(P_{\text{in}}) := \left( \frac{K_{\text{air}}}{L_c} \right) \cdot \left[ 0.037 \left[ \frac{\kappa \cdot A_{\text{ave}} \cdot |P_{\text{in}} - P_{\text{out}}|}{\mu \cdot (R_{\text{total}} - R_{\text{tube}})} \cdot \rho \cdot d_{\text{pore}} \right]^{0.8} \cdot \text{Pr}^{\frac{1}{3}} \right]$$



The equation above is represented by the plot which shows the variation of the convective coefficient with respect to pressure.

With this Expression ready, the modeling of heat transfer through a fin may be used to model heat transfer through our flow injection system if properly altered to account for the parameters that change due to the special properties of this particular material.



Assumptions:

9. Steady state conditions apply to the system
10. Geometry has constant cross section
11. Material has constant thermal conductivity
12. Heat is lost from fin tip by convection

Thermodynamic Analysis was carried out based on the following:

9. Conservation of Energy Principle: Energy can neither be created nor destroyed; it can only change forms. This law provides a sound basis for studying the relationships among various forms of energy and energy interactions.

10. Energy Balance:

$$\sum_{\text{in}} E = \sum_{\text{out}} E$$

11. First law of Thermodynamics:

$$Q_{\text{dot}} - W_{\text{dot}} + \sum_{\text{in}} (\dot{m} \cdot \theta) - \sum_{\text{out}} (\dot{m} \cdot \theta) = 0$$

12. Fourier's Law of Heat Conduction:

$$Q_{\text{cond}} = -k \cdot A_c \cdot \frac{dT}{dx}$$

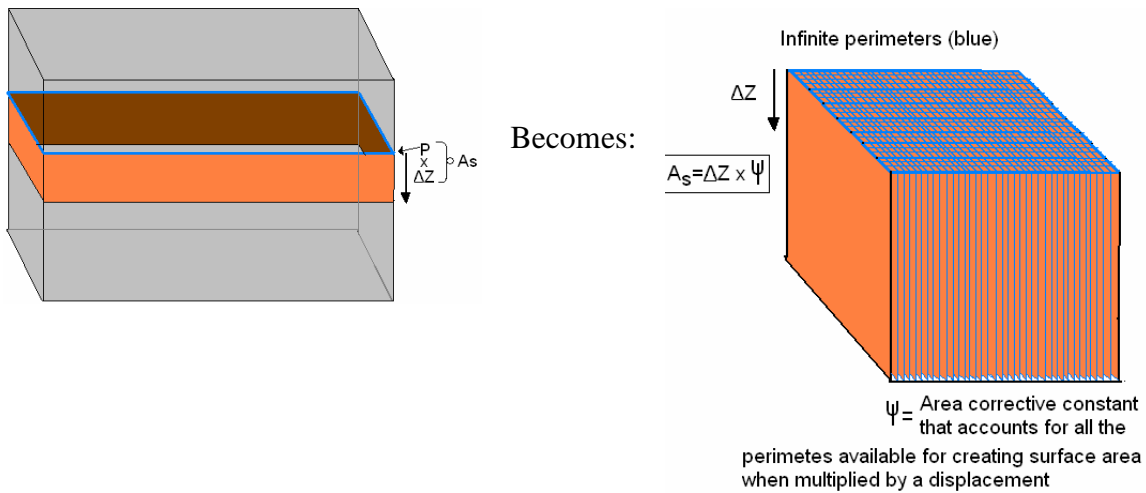
13. Heat Transfer by Convection:

$$Q_{\text{conv}} = h \cdot A_s \cdot (T - T_{\text{inf}})$$

14. Setting heat input by conduction equal to heat dissipated by convection:

$$-K_{\text{foam}} \cdot A_c \cdot \frac{dT}{dz} + h \cdot A_s \cdot (T - T_{\text{inf}}) = 0$$

Initially the expression to account for the surface area of a regular fin replaces  $A_s$  in the above equation for  $pdz$ , where  $p$  is the perimeter, and  $dz$  a displacement in differential form. Together, perimeter multiplied by length gives the surface area of the fin. The expression must be modified so that the internal surface area of the carbon foam exchanger can be accounted for in this expression.



Purpose: transformation of fin equation

$$Q_{\text{conv}} = h \cdot A_s \cdot (T - T_{\text{inf}})$$

$$-K_{\text{foam}} \cdot A_c \cdot \frac{dT}{dz} + h \cdot A_s \cdot (T - T_{\text{inf}}) = 0$$

$$-K_{\text{foam}} \cdot A_c \cdot \frac{dT}{dz} + h \cdot p \cdot dz \cdot (T - T_{\text{inf}}) = 0$$

$$A_s = \Delta Z \cdot p \quad \text{transformed into} \quad A_s = \Delta Z \cdot \psi$$

$$Q = \sqrt{h \cdot \psi \cdot k_{\text{foam}} \cdot A_c} (T_{z0} - T_{\text{flow\_in}}) \cdot \tanh(\beta \cdot 4 \cdot h_{\text{layer}})$$

Q	Total heat lost
H	Convective coefficient
$k_{\text{foam}}$	Thermal Conductivity of foam
$A_c$	Crosssectional area of part
$T_{z0}$	Base Temperature
$T_{\text{flow\_in}}$	Temperature of cooling fluid
$h_{\text{layer}}$	Length of the heat exchanger
$\psi$	Rate of change of surface area with displacement

Where

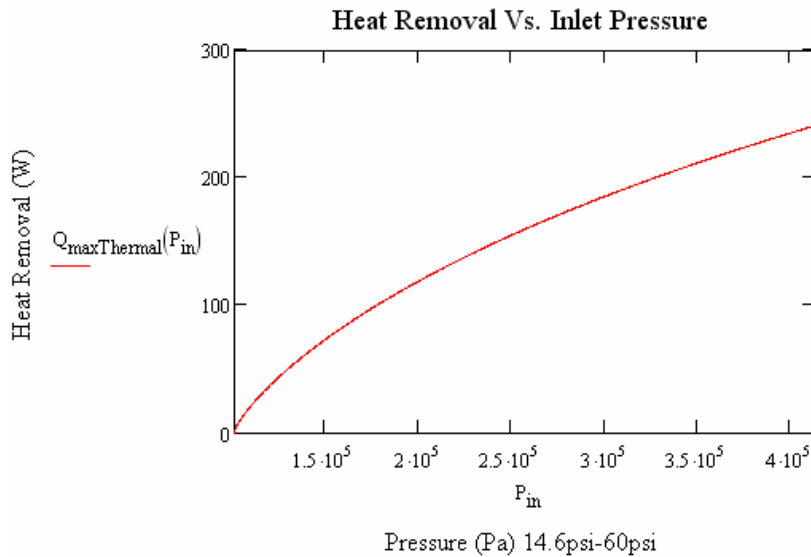
$$\beta = \sqrt{\frac{\left(\frac{K_{air}}{L_c}\right) \cdot 0.037 \cdot \left[ \frac{\kappa \cdot A_{ave} \cdot (P_{in} - P_{out})}{\mu \cdot (R_{total} - R_{tube})} \cdot \rho \cdot d_{pore} \right]^{0.8} \cdot \frac{1}{Pr^3} \cdot \psi}{k_{foam} \cdot A_c}}$$

15. Express heat dissipation as a function of inlet pressure:

$$Q(P_{in}) = \sqrt{h(P_{in}) \cdot \psi \cdot k_{foam} \cdot A_c} (T_{z0} - T_{flow\_in}) \cdot \tanh(\beta(P_{in}) \cdot 4 \cdot h_{layer})$$

In an expanded form, the parameters can be appreciated as follows:

$$Q_{TOTAL}(P_{in}) := 12 \cdot \sqrt{\frac{\left(\frac{K_{air}}{L_c}\right) \cdot 0.037 \cdot \left[ \frac{\kappa \cdot A_{ave} \cdot (|P_{in} - P_{out}|)}{\mu \cdot (R_{total} - R_{tube})} \cdot \rho \cdot d_{pore} \right]^{0.8} \cdot \frac{1}{Pr^3} \cdot \psi \cdot k_{foam} \cdot A_c (T_{z0} - T_{flow\_in}) \tanh\left[ \frac{\left(\frac{K_{air}}{L_c}\right) \cdot 0.037 \cdot \left[ \frac{\kappa \cdot A_{ave} \cdot (|P_{in} - P_{out}|)}{\mu \cdot (R_{total} - R_{tube})} \cdot \rho \cdot d_{pore} \right]^{0.8} \cdot \frac{1}{Pr^3} \cdot \psi}{k_{foam} \cdot A_c} \right] \cdot 4 \cdot h_{layer}}$$

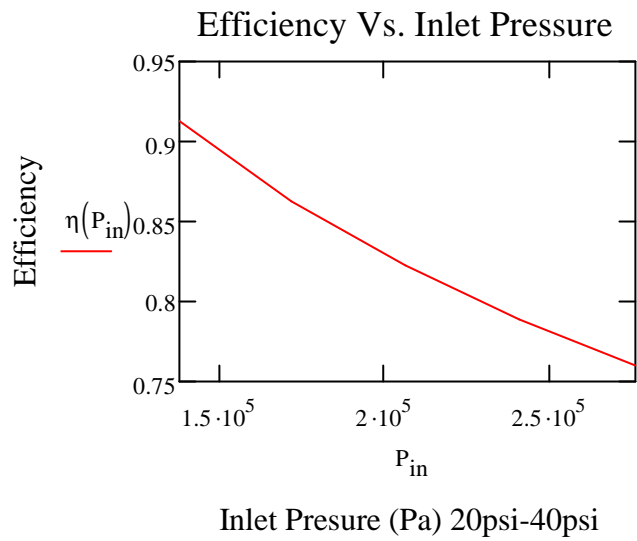


The above illustrated is the form that the heat removal with respect to inlet pressure takes.

### Calculated Values:

Actual/Ideal	Heat Dissipation	Maximum Operating Temp	Inlet Pressure
Calculated	89W	70C	21.5 psi
Experimental	68.6W	59C	21.5 psi
Error	22%	15.7%	

The efficiency was also determined to be a function of inlet pressure:



# **Thermal Management**

---

---

## *References*

## References

- Carbon Foam. 2006. Touchstone Research Laboratory. 10 Oct. 2007.  
<<http://www.carbonfoam.com/>>
- Cengel, Yunus A. and Robert H. Turner. Fundamentals of Thermal-Fluid Sciences. 2nd Ed. New York: McGraw-Hill, 2005.
- Collins, Royal E. Flow of Fluids through Porous Materials. New York: Reinhold Publishing Corporation, 1961
- Dullien, F.A.L. Porous Media Fluid Transport and Pore Structure. 2nd Ed. San Diego, California: Academic Press Inc., 1992
- Fluid Property Calculator. Industrial Refrigeration Consortium. 25 Nov 2007  
<<http://www.irc.wisc.edu/properties/>>
- Martin, Holger. Heat Exchangers. New York: Hemisphere Publishing Corporation, 1992.
- MEMS Applications. 2nd Ed. Ed. Mohamed Gad-el-Hak.. CRC Press, 2006
- Microfluidics Tutorial- A Highly Biased Primer. 8 Aug. 2004. University of Washington. 05 Oct. 2007  
<<http://faculty.washington.edu/yagerp/microfluidicstutorial/tutorialhome.htm>>
- Oosthuizen, Patrick H. and David Naylor. Introduction to Convective Heat Transfer Analysis. McGraw-Hill, 1999.
- ORNL Carbon and Graphite Foams. Oak Ridge National Laboratory. 15 Sep. 2007.  
<<http://www.ms.ornl.gov/researchgroups/CMT/FOAM/foams.htm>>
- Poco Graphite- Thermal Management Materials. Oak Ridge National Laboratory. 10 Oct 2007. <<http://www.poco.com/us/Thermal/foam.asp>>
- Science Direct- Applied Thermal Engineering: Carbon-Foam Finned Based Tubes in Air-Water Heat Exchangers. 18 Aug. 2005. The University of Western Ontario and The University of Ottawa. 25 Oct 2007. <<http://www.sciencedirect.com/science>>
- Yerkes, Kirk L. and Daniel L. Vrable. A Thermal Management Concept for the More Electric Aircraft for Power System Applications. 22 Apr. 1998. Society of Automotive Engineers. 25 Oct. 2007  
<<http://www.dtic.mil/dticasd/sbir/sttr04/m010b.pdf>>